



DAA/LANGLEY

IN-32

69640-CR  
p. 102

**USER MANUAL FOR SEMI-CIRCULAR  
COMPACT RANGE REFLECTOR CODE -- VERSION II**

**Inder J. Gupta  
Walter D. Burnside**

**The Ohio State University**

**ElectroScience Laboratory**

**Department of Electrical Engineering  
Columbus, Ohio 43212**

(NASA-CR-180550) USER MANUAL FOR  
SEMI-CIRCULAR COMPACT RANGE REFLECTOR CODE:  
VERSION 2 (Ohio State Univ.) 102 p Avail:  
NTIS HC A06/MF A01 CSCL 20N

N87-26252

Unclas  
G3/32 0069640

**Technical Report 716148-18  
Grant NSG 1613  
January 1987**

**National Aeronautics and Space Administration  
Langley Research Center  
Hampton, VA 22217**

## NOTICES

When Government drawings, specifications, or other data are used for any purpose other than in connection with a definitely related Government procurement operation, the United States Government thereby incurs no responsibility nor any obligation whatsoever, and the fact that the Government may have formulated, furnished, or in any way supplied the said drawings, specifications, or other data, is not to be regarded by implication or otherwise as in any manner licensing the holder or any other person or corporation, or conveying any rights or permission to manufacture, use, or sell any patented invention that may in any way be related thereto.

<b>REPORT DOCUMENTATION PAGE</b>	<b>1. REPORT NO.</b>	<b>2.</b>	<b>3. Recipient's Accession No.</b>
<b>4. Title and Subtitle</b> USER MANUAL FOR SEMI-CIRCULAR COMPACT RANGE REFLECTOR CODE -- VERSION II		<b>5. Report Date</b> January 1987	
<b>7. Author(s)</b> Inder J. Gupta and W.D. Burnside		<b>6.</b>	
<b>9. Performing Organization Name and Address</b> The Ohio State University ElectroScience Laboratory 1320 Kinnear Road Columbus, Ohio 43212		<b>8. Performing Organization Rept. No.</b> 716148-18	
<b>12. Sponsoring Organization Name and Address</b> National Aeronautics and Space Administration Langley Research Center Hampton, Virginia 22217		<b>10. Project/Task/Work Unit No.</b>	
<b>15. Supplementary Notes</b>		<b>11. Contract(C) or Grant(G) No</b> (C) (G) Grant NSG 1613	
<b>16. Abstract (Limit: 200 words)</b>  A computer code has been developed at The Ohio State University ElectroScience Laboratory to analyze a semi-circular paraboloidal reflector with or without a rolled edge at the top and a skirt at the bottom. The code can be used to compute the total near field of the reflector or its individual components at a given distance from the center of the paraboloid.  The code computes the fields along a radial, horizontal, vertical or axial cut at that distance. Thus, it is very effective in computing the size of the "sweet spot" for a semi-circular compact range reflector. This report describes the operation of the code. Various input and output statements are explained. Some results obtained using the computer code are presented to illustrate the code's capability as well as being samples of input/output sets.		<b>13. Type of Report &amp; Period Covered</b> Technical	
<b>17. Document Analysis a. Descriptors</b>		<b>14.</b>	
<b>b. Identifiers/Open-Ended Terms</b>			
<b>c. COSATI Field/Group</b>			
<b>18. Availability Statement</b> A. Approved for public release; distribution is unlimited		<b>19. Security Class (This Report)</b> Unclassified	<b>21. No. of Pages</b> 104
		<b>20. Security Class (This Page)</b> Unclassified	<b>22. Price</b>

## TABLE OF CONTENTS

	Page
LIST OF FIGURES	iv
I. INTRODUCTION	1
II. METHODS OF COMPUTATION	3
A. SPECULAR REFLECTION	4
B. JUNCTION DIFFRACTION	8
C. SKIRT DIFFRACTION	13
D. FEED BLOCKAGE	18
E. FEED SPILLOVER	18
F. DIFFRACTION FROM A MECHANICAL DISCONTINUITY	20
III. INPUT AND OUTPUT DATA	22
A. INPUT DATA	22
B. OUTPUT DATA	32
IV. SAMPLE RESULTS	33
V. SUMMARY	87
APPENDIX A CODE TO GENERATE THE CROSS-SECTIONAL SHAPE	89
REFERENCES	96

PRECEDING PAGE BLANK NOT FILMED

iii

PAGE ii INTENTIONALLY BLANK

## LIST OF FIGURES

Figure	Page
1(a). Paraboloid reflector with blended rolled edge at the top and skirt at the bottom and the field plane. (b). Front view of the reflector.	2
2(a). Radial cut on the paraboloid reflector. (b). Cross-sectional view of the infinite cylinder.	9
3(a). Various mechanisms contributing to the scattered field. (b). Magnetic line source illumination of an infinitely long cylinder.	11
4. A 3-dimensional wedge with smooth junction.	15
5. Flat plate used to compute feed blockage. The plate is symmetrical about the $x_a$ axis. Note that the $x_a$ - $y_a$ plane is parallel to the x-y plane.	19
6. Mechanical discontinuity in the surface. (a) step discontinuity (b) discontinuity due to angular tilt	21
7. Feed configuration with feed tilt specified by $\alpha$ .	25
8. Short magnetic dipole.	25
9. Description of the observation plane.	30
10. Cross-sectional view of the semi-circular Scientific-Atlanta reflector in the xz plane.	34
11. Cross-sectional shape of the infinitely long cylinder.	36
12. The copolarized (x) component of the scattered electric field versus vertical displacement. $Y_{CUT}=0$ , feed tilt angle= $0^\circ$ , various mechanisms included in the scattered field are: 1. specular reflection, 2. upper edge diffraction, and 3. lower edge diffraction.	39
13. Specular reflection, upper edge diffraction and the lower edge diffraction versus vertical displacement. $Y_{CUT}=0$ , feed tilt angle= $0^\circ$ .	40

Figure	Page
14. The copolarized (x) component of the scattered electric field versus vertical displacement. $Y_{CUT}=0$ , feed tilt angle= $0^\circ$ , various mechanisms included in the scattered fields are: 1. specular reflection, 2. junction diffraction, and 3. skirt diffraction.	41
15. Specular reflection, junction diffraction, and skirt diffraction versus vertical displacement. $Y_{CUT}=0$ , field tilt angle= $0^\circ$ .	44
16. Specular reflection versus vertical displacement for various feed tilt angles. $Y_{CUT}=0$ .	46
17. Specular reflection versus horizontal displacement. $X_{CUT}=8.5$ feet, feed tilt angle= $5^\circ$ .	50
18. Specular reflection versus horizontal displacement. $X_{CUT}=8.5$ feet, feed tilt angle= $10^\circ$ .	51
19. Specular reflection versus horizontal displacement. $X_{CUT}=8.5$ feet, feed tilt angle= $20^\circ$ .	52
20. Specular reflection versus horizontal displacement. $X_{CUT}=8.5$ feet, feed tilt angle= $30^\circ$ .	53
21. Feed blockage versus vertical displacement for various size feed aperture. $Y_{CUT}=0$ , feed tilt angle= $20^\circ$ .	57
22. Scattered field versus vertical displacement. $Y_{CUT}=0$ , feed tilt angle = $20^\circ$ , feed aperture = 3" x 3".	58
23. Copolarized (x) component of the scattered field versus radial displacement. $\phi=0^\circ$ , feed tilt angle= $20^\circ$ , feed aperture = 3" x 3". Various mechanisms included in the field are: 1. specular reflection, 2. junction diffraction, 3. skirt diffraction, and 4. feed blockage.	61
24. Copolarized (x) component of the scattered field versus radial displacement. $\phi=15^\circ$ , feed tilt angle= $20^\circ$ , feed aperture = 3" x 3". Various mechanisms included in the field are: 1. specular reflection, 2. junction diffraction, 3. skirt diffraction, and 4. feed blockage.	62
25. Copolarized (x) component of the scattered field versus radial displacement. $\phi=30^\circ$ , feed tilt angle= $20^\circ$ , feed aperture = 3" x 3". Various mechanisms included in the field are: 1. specular reflection, 2. junction diffraction, 3. skirt diffraction, and 4. feed blockage.	63

Figure	Page
26. Copolarized (x) component of the scattered field versus radial displacement. $\phi=45^\circ$ , feed tilt angle= $20^\circ$ , feed aperture = 3" x 3". Various mechanisms included in the field are: 1. specular reflection, 2. junction diffraction, 3. skirt diffraction, and 4. feed blockage.	64
27. Copolarized (x) component of the scattered field versus radial displacement. $\phi=60^\circ$ , feed tilt angle= $20^\circ$ , feed aperture = 3" x 3". Various mechanisms included in the field are: 1. specular reflection, 2. junction diffraction, 3. skirt diffraction, and 4. feed blockage.	65
28. Copolarized (x) component of the scattered field versus radial displacement. $\phi=75^\circ$ , feed tilt angle= $20^\circ$ , feed aperture = 3" x 3". Various mechanisms included in the field are: 1. specular reflection, 2. junction diffraction, 3. skirt diffraction, and 4. feed blockage.	66
29. Useable target zone at 2 GHz. Target distance = 36 feet, maximum ripple = 0.2 dB.	68
30. Cross-polarized (y) component of the scattered field versus radial displacement. $\phi=15^\circ$ . Various mechanisms included in the field computation are: 1. specular reflection, 2. junction diffraction, 3. skirt diffraction, and 4. feed blockage.	69
31. Cross-polarized (y) component of the scattered field versus radial displacement. $\phi=30^\circ$ . Various mechanisms included in the field computation are: 1. specular reflection, 2. junction diffraction, 3. skirt diffraction, and 4. feed blockage.	70
32. Cross-polarized (y) component of the scattered field versus radial displacement. $\phi=45^\circ$ . Various mechanisms included in the field computation are: 1. specular reflection, 2. junction diffraction, 3. skirt diffraction, and 4. feed blockage.	71
33. Cross-polarized (y) component of the scattered field versus radial displacement. $\phi=60^\circ$ . Various mechanisms included in the field computation are: 1. specular reflection, 2. junction diffraction, 3. skirt diffraction, and 4. feed blockage.	72

Figure	Page
34. Cross-polarized (y) component of the scattered field versus radial displacement. $\phi=75^\circ$ . Various mechanisms included in the field computation are: 1. specular reflection, 2. junction diffraction, 3. skirt diffraction, and 4. feed blockage.	73
35. Scattered field versus axial displacement. $\phi=0^\circ$ , radial distance = 30 feet, feed tilt angle = $20^\circ$ .	76
36. Scattered fields versus axial displacement. $\phi=60^\circ$ , radial distance = 30 feet, feed tilt angle = $20^\circ$ .	78
37. Scattered field versus radial displacement. $\phi=0^\circ$ , distance from vertex = 36 feet, mechanical discontinuity at 16 feet.	79
38. Feed pattern in $x_fz_f$ plane.	83
39. Feed spillover versus radial displacement. $\phi=0^\circ$ , distance from vertex = 36 feet. Measurement feed pattern is used. Feed tilt angle= $20^\circ$ .	84
40. Scattered field versus radial displacement. $\phi=0^\circ$ , distance from vertex = 36 feet. Measured feed pattern is used. Feed tilt angle= $20^\circ$ . Various mechanisms included are: 1. specular reflection, and 2. feed spillover.	85
A.1. Various parameters used in the code.	93
A.2. Various parameters used in the code. Mechanical discontinuity due to tilt.	94
A.3. Various parameters used in the code. Mechanical discontinuity due to displacement.	95

## I. INTRODUCTION

A computer code has been developed at The Ohio State University ElectroScience Laboratory to analyze a semi-circular paraboloid reflector antenna with a rolled edge at the top and a skirt at the bottom as shown in Figure 1. The code can be used to compute the total near field of a compact antenna range reflector or its (fields) individual components at a given distance from the center of the paraboloid. The code computes the fields along a radial, horizontal, vertical or axial cut at that distance. Thus, it is very effective in computing the size of the "sweet spot" for a semi-circular compact range. The code can also be used to compute the illumination of the walls, floor or ceiling of the room. Thus, the fields obtained using the code can be used to study the scattering from the absorber covering inside of the room. Various mechanisms included in the field computation are:

- a) Specular reflection (geometrical optics term)
- b) Junction diffraction (diffraction from the junction between the paraboloid and the rolled edge)
- c) Skirt diffraction (diffraction from the junction between the paraboloid and the skirt)
- d) Feed blockage
- e) Feed spillover, and
- f) Diffraction from a mechanical discontinuity in the reflector surface.

The user has a choice of computing these mechanisms in any combination. The three field components (x,y,z) for each mechanism as well as the total field are stored in an output file. Outside the

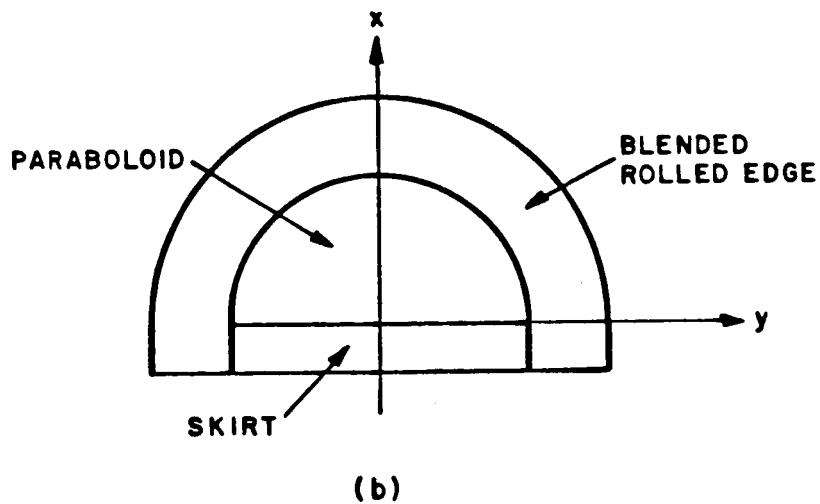
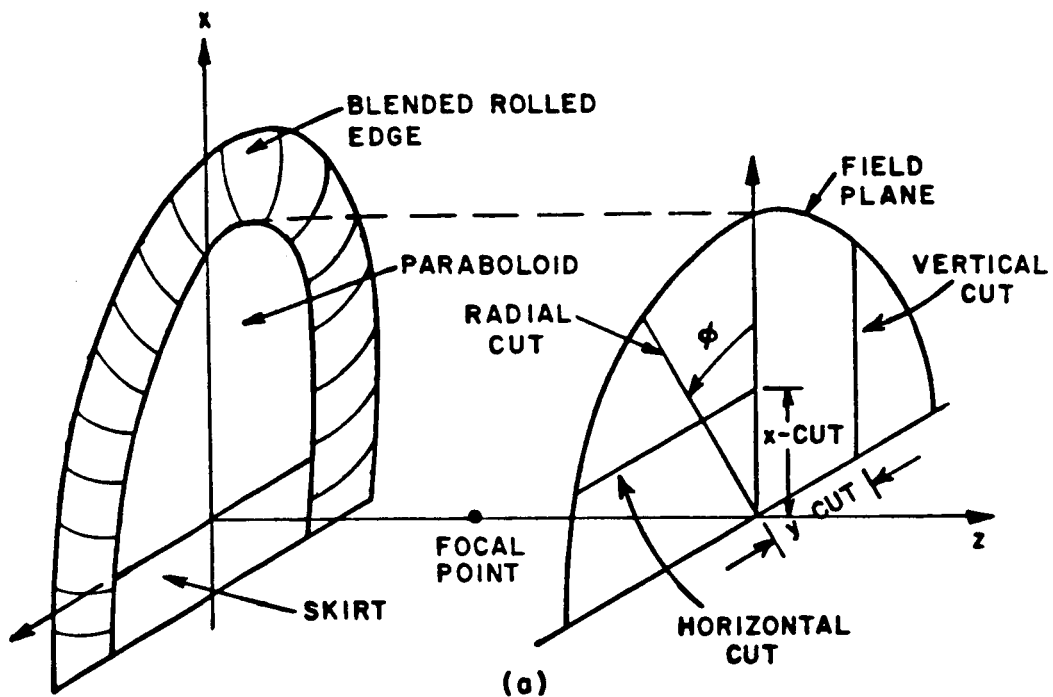


Figure 1(a). Paraboloid reflector with blended rolled edge at the top and skirt at the bottom and the field plane.  
 1(b). Front view of the reflector.

"sweet region" (semi-circular region whose radius is equal to the radius of the paraboloid), only the specular reflection is computed. The code can also be used to analyze reflectors without rolled edge and/or skirt. This report describes the operation of the code. To help the user in understanding the input data, a brief description of the method of computation of each mechanism is also given. Some results obtained using the computer code are presented to illustrate the code's capability as well as being samples of input/output sets.

A brief description of the methods of computation of the various mechanisms is given in the next section. Section III explains the input and output statements used in the code. Finally, Section IV contains various examples of the use of the code.

## **II. METHODS OF COMPUTATION**

In this section, methods of computation of the various mechanisms included in the analysis of the reflector antenna are discussed. The purpose of this documentation is to help the user in understanding the input data. Various mechanisms included in the analysis are as follows:

- a) Specular reflection
- b) Junction diffraction
- c) Skirt diffraction
- d) Feed blockage
- e) Feed spillover, and
- f) Diffraction from a mechanical discontinuity.

## A. SPECULAR REFLECTION

The code can be used to compute specular reflections both inside and outside the sweet region. Inside the sweet region, the reflected field comes from the paraboloidal section of the reflector. It is trivial to find the point of reflection on the paraboloidal section. Let  $(x_0, y_0, z_0)$  be the coordinates of the field point (observation point). Then the coordinates of the reflection point on the paraboloidal section are given by

$$\begin{aligned}x_r &= x_0 \\y_r &= y_0\end{aligned}\tag{1}$$

and

$$z_r = (x_0^2 + y_0^2)/4F$$

where  $F$  is the focal length of the paraboloid. The specular reflection at  $(x_0, y_0, z_0)$  is then given by

$$\vec{H}^r(x_0, y_0, z_0) = \{\vec{H}^i(x_r, y_r, z_r) - 2\hat{n}[\vec{H}^i(x_r, y_r, z_r) \cdot \hat{n}]\} \cdot e^{-jk(z_0 - z_r)}\tag{2}$$

where  $\vec{H}^i(x_r, y_r, z_r)$  is the incident field at the point of reflection, and  $\hat{n}$  is the unit normal to the paraboloid section at the point of reflection. Outside the sweet region, the reflected field may be due to the blended rolled edge or skirt part of the reflector. If the  $x$  coordinate of the field point is positive (see Figure 1), the point of reflection lies on the blended rolled edge; otherwise, the point of reflection lies on the skirt of the reflector. To find the point of

reflection on the rolled edge for a given field point, one needs the analytical expression defining the rolled edge. Even if the analytical expression is known, it is not trivial to find the point of reflection. To avoid this problem, discrete points on a radial cross sectional cut of the reflector surface are input to the code. Note that since for  $x > 0$  the reflector has rotational symmetry, one can choose any radial cut. This information is read from unit #17. The data file linked to unit #17 should have the following information:

1. Number of samples (NS) along the cross section
2.  $\rho$  and  $z$  coordinates of the various samples in centimeters

This file is read using the following formats:

```
Read (17,*) NS
Do 2 I=1, NS
2 Read (17,*) (Z(I), $\rho$ (I))
```

Note that the "\*" symbol indicates free format input. The spacing between the samples should be of the order of  $0.05\lambda$ , where  $\lambda$  is the wavelengths in centimeters. As written, the code can handle a maximum of 2001 samples ( $NS < 2001$ ). If the number of samples exceeds this value, the first statement in the code should be changed accordingly.

For a fixed  $z$  (radial, horizontal or vertical cut for field probing) or fixed  $\phi$  (axial cut for field probing), the code computes the radial or axial distances, respectively, at which these discrete points will reflect the signal in the 2-dimensional system. Next, for a given field point  $(x_0, y_0, z_0)$ , the corresponding reflection point  $(\rho_r, z_r)$  in

the 2-dimensional system is found from the above discrete set using linear interpolation. The principal radii of curvature of the reflected wavefront ( $\rho^r$ ) and direction of the normal ( $\hat{n}$ ) at the point of the reflection are also computed. Then in the 2-dimensional system the specularly reflected magnetic field is given by

$$\vec{H}^r(\rho_0, z_0) = [H^i(\rho_r, z_r) - 2\hat{n}\{H^i(\rho_r, z_r) \cdot \hat{n}\}] \sqrt{\frac{\rho^r}{s+\rho^r}} e^{-jks} \quad (3)$$

where  $\rho_0 = \sqrt{x_0^2 + y_0^2}$ ,  $H^i(\rho_r, z_r)$  is the incident field at the point of reflection, and  $s$  is the distance between the point of reflection and field point. Then the specularly reflected magnetic field in the 3-dimensional case is given by

$$H^r(x_0, y_0, z_0) = [H^i(x_r, y_r, z_r) - 2\hat{n}_1\{H^i(x_r, y_r, z_r) \cdot \hat{n}_1\}] \cdot \sqrt{\frac{\rho^r}{s+\rho^r}} \cdot \sqrt{\frac{\rho_r}{\rho_0}} e^{-jks} \quad (4)$$

where

$$x_r = \rho_r \cos\phi$$

$$y_r = \rho_r \sin\phi$$

$$\phi = \tan^{-1}(y_0/x_0)$$

and

$$\hat{n}_1 = n_\rho \cos\phi \hat{x} + n_\rho \sin\phi \hat{y} + n_z \hat{z} .$$

To find the point of reflection on the skirt, one proceeds as follows. First the y and z coordinate of the point of reflection are found. If  $|y_0| < R$ , where  $y_0$  is the y coordinate of the field point and R is the radius of the paraboloid, then the reflection point lies on the parabolic part of the skirt and  $y_r = y_0$  and  $z_r = y_0^2/4F$ . Otherwise, the reflection point lies on the blended rolled edge part of the skirt. To find the y and z coordinates of the reflection point in this case, one follows the same linear interpolation procedure as outlined above. In this case, for fixed  $z_0$  (radial, horizontal or vertical cut) the interpolation is done for  $y_0$ . For this reflection point, the radii of curvature of the reflected wavefront ( $\rho^r$ ) in the yz plane and normal vector ( $\hat{n}$ ) is also computed. Note that for the parabolic part of the skirt,  $\rho^r = \infty$ . Next, the x coordinate of the reflection point is found. Since the skirt part of the reflector is a finite cylinder with its axis aligned with the x axis, the x coordinate of the point of reflection is given by

$$x_r = x_0 \frac{(z_s - z_r)n_z + (y_s - y_r)n_y}{(z_0 + z_s - 2z_r)n_z + (y_0 + y_s - 2y_r)n_y} \quad (6)$$

where  $(x_s, y_s, z_s)$  is the source (feed) location and  $\hat{n} = n_x \hat{x} + n_y \hat{y} + n_z \hat{z}$ .

The specularly reflected magnetic field is then given by

$$\vec{H}^r(x_0, y_0, z_0) \cong [\vec{H}^i(x_r, y_r, z_r) - 2\hat{n}\{\vec{H}^i(x_r, y_r, z_r) \cdot \hat{n}\}] \sqrt{\frac{\rho^r}{\rho^r + s}} \sqrt{\frac{s'}{s' + s}} e^{-jks} \quad (7)$$

where  $s$  is the distance between the point of reflection and the field point, and  $s'$  is the distance between the source and the reflection point.

## B. JUNCTION DIFFRACTION

The junction between the paraboloid and a rolled edge is a higher order discontinuity in that at least the slope is continuous. For a blended rolled edge, the junction is continuous to even higher order derivatives. Since closed form solution for the fields diffracted from such junctions are not available, a new technique [1] has been developed to find the diffracted field from the junction. In this new technique, the first step is to reduce the three-dimensional problem to a two-dimensional one; i.e., the reflector is replaced by an infinitely long cylinder of the same cross section as that of a radial cut through the reflector as shown in Figure 2(a). This radial cut contains the point of diffraction. The skirt part of this cylinder is then replaced with a parabolic cylinder with the same focal length as the paraboloidal section. A cross section view of the cylinder is shown in Figure 2(b). Note that the cross section of the cylinder is independent of which radial cut is taken in that the reflector has rotational symmetry. The total field scattered by this cylindrical reflector with a rolled edge is found using physical optics. Since it is a two-dimensional problem, one has to do a contour integration to compute the total field. Thus, physical optics integration can be carried out quite efficiently. The total field obtained using the PO integration contains contributions

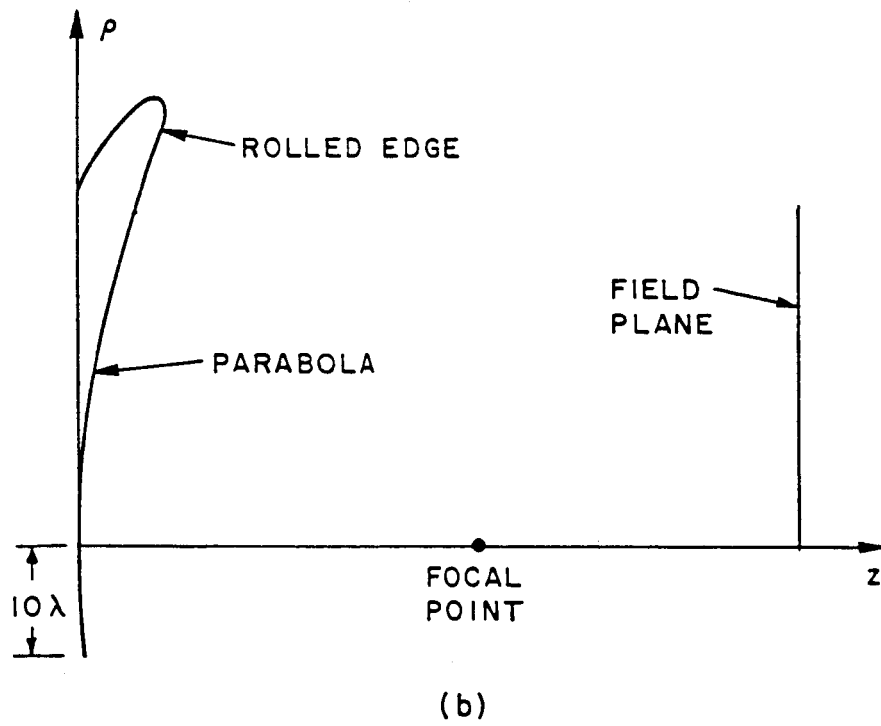
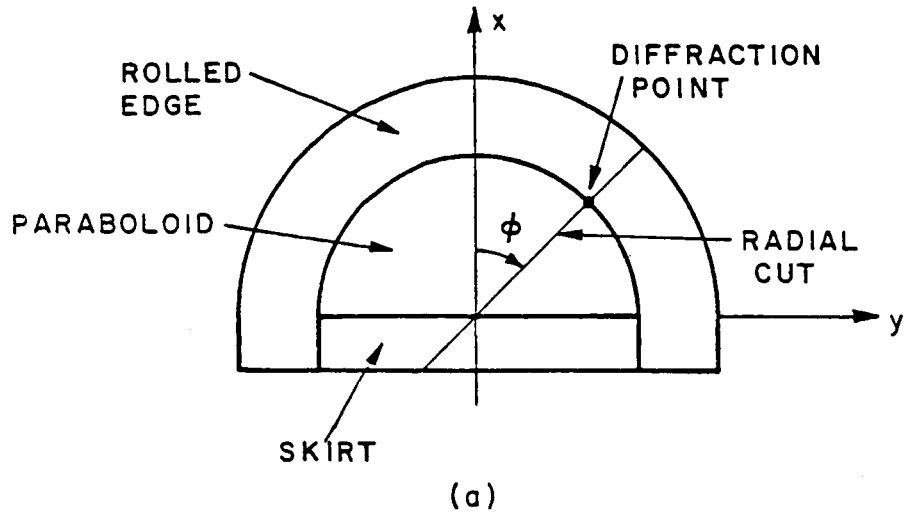


Figure 2(a). Radial cut on the paraboloid reflector.

(b). Cross-sectional view of the infinite cylinder.

from four different mechanisms as shown in Figure 3(a). These mechanisms are as follows:

1. Stationary point contribution (specular reflected field)
2. Two end point contributions, and
3. Diffracted field from the junction.

The stationary point contribution and the end point contributions from the cylinder are known. For example, assuming that the cylinder is illuminated by a magnetic line source (see Figure 3(b)), the PO scattered magnetic field is given by

$$\vec{H}^S = c \int_0^{\ell} (\vec{J}_{po} \times \hat{s}) \frac{e^{-jks}}{\sqrt{s}} d\ell \quad (8)$$

where  $c$  is a constant,  $\hat{s}$  is the unit vector in the observation direction, and  $\vec{J}_{po}$  is the physical optics current which is given by

$$\vec{J}_{po} = 2 \hat{n} \times \vec{H}^i \quad (9)$$

The  $\phi$  component of  $\vec{H}^S$  is

$$H_{\phi}^S = c \int_0^{\ell} \hat{\phi} \cdot (\vec{J}_{po} \times \hat{s}) \frac{e^{-jks}}{\sqrt{s}} d\ell = c \int_0^{\ell} F e^{jk\phi} d\ell \quad (10)$$

where

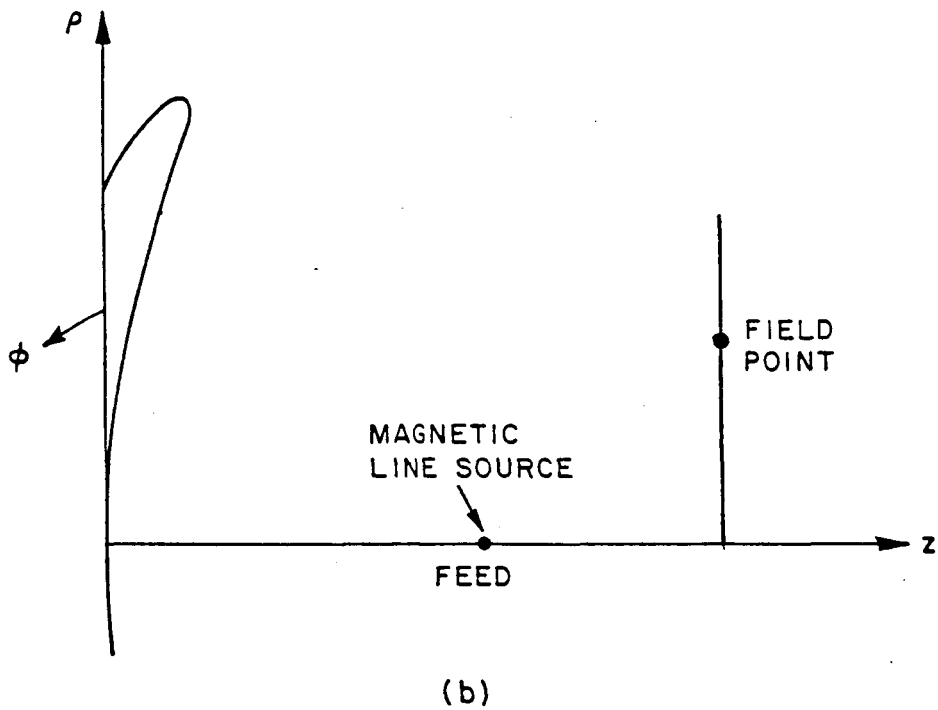
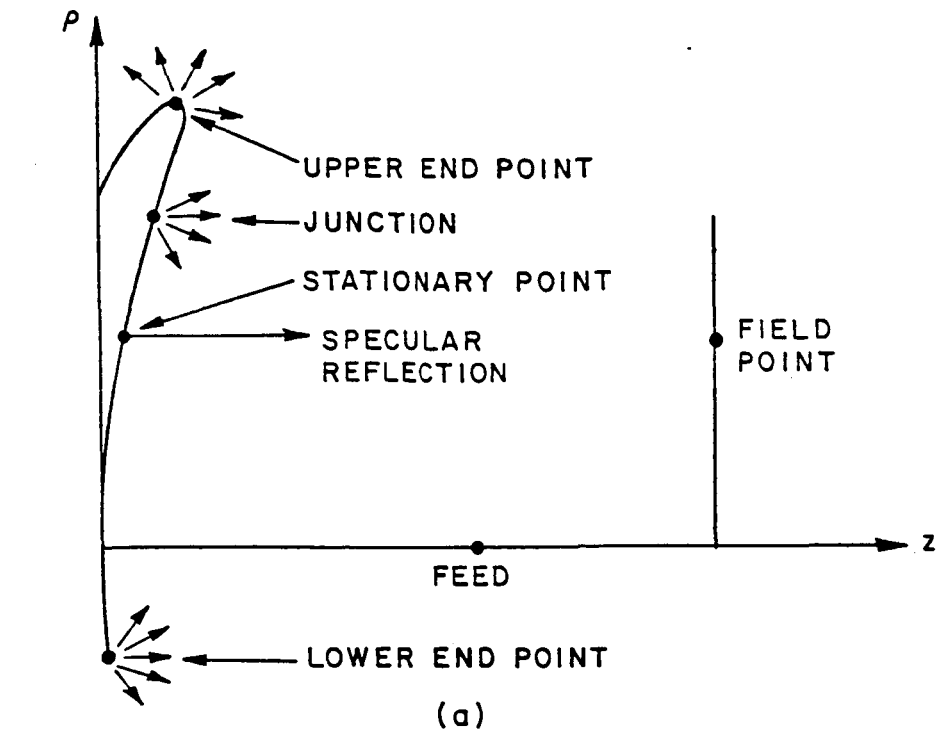


Figure 3(a). Various mechanisms contributing to the scattered field.

(b). Magnetic line source illumination of an infinitely long cylinder.

$$\frac{\hat{\phi} \cdot (\vec{J}_{PO} \times \hat{s})}{\sqrt{s}} = F e^{jk\tilde{\phi}} \quad (11)$$

$$\text{and } \phi = \tilde{\phi} - s \quad (12)$$

Then the end point contributions [2] are given by

$$H_{\phi}^e = c \sum_{n=0}^{\infty} \frac{(-1)^n F_n}{jk\phi'} e^{-jk\phi} \Big|_0^{\ell} \quad (13)$$

$$\text{where } F_n = \frac{d}{d\ell} \frac{F_{n-1}}{jk\phi'} \text{ and } F_0 = F. \quad (14,15)$$

The first two terms of the infinite series give a good approximation to the end point contribution. In (13), the end points are assumed to be far from the stationary point. This condition is easily met by the upper end point. However, the same may not be true for the lower end point. To meet this requirement, the skirt should be replaced by a parabolic section of dimension at least 10 wavelengths as shown in Figure 3(b). The focal length of the parabolic section is equal to that of the original reflector.

The stationary point contribution and the end point contributions are subtracted from the PO scattered field. This leaves the diffracted field which comes from the junction between the parabola and the rolled edge. This is a two-dimensional diffracted field, which means that an appropriate spread factor must be applied to this field in order to

obtain the desired three-dimensional diffracted field. One needs to input the cross-sectional shape of the cylinder to carry out the physical optics integration. This information is read from unit #17. In fact, the cross-sectional shape used in the calculation of the junction diffraction term is also used to compute the specular reflection from the rolled edge. Thus, the data file linked to unit #17 should have the same information as before.

The code can also be used to analyze reflectors without any rolled edge. In this case, the junction diffraction term is replaced with the edge diffraction from the rim of the reflector. The Geometrical Theory of Diffraction (GTD) [3] is used to compute the edge diffraction.

### C. SKIRT DIFFRACTION

The diffraction by the junction between the lower end of the paraboloid and the skirt is computed using GTD diffraction coefficients. Since this is a smooth junction, the diffracted fields will be due to the continuity in the reflected fields. The diffracted field from a smooth junction (see Figure 4) is given by [4]

$$\begin{bmatrix} E_B^d \\ E_\phi^d \end{bmatrix} = \begin{bmatrix} -D_s & 0 \\ 0 & -D_h \end{bmatrix} \begin{bmatrix} E_{\beta'}^i \\ E_{\phi'}^i \end{bmatrix} \sqrt{\frac{\rho}{(s+\rho)s}} e^{-jks} \quad (16)$$

where

$$D_{\frac{s}{h}}(\phi, \phi', \beta_0) = \pm \frac{e^{-j\pi/4}}{2\sqrt{2\pi k} \sin\beta_0} \tan\left(\frac{\phi+\phi'}{2}\right) \cdot$$

$$\{F[kL^{r_0}_a(\phi+\phi')] - F[kL^{r_n}_a(\phi+\phi')]\} \quad (17)$$

$$L^{r_0} = \frac{s(\rho_e^{r_0+s}) \rho_1^{r_0} \rho_2^{r_0}}{\rho_e^r (\rho_1^{r_0+s}) (\rho_2^{r_0+s})} \sin^2\beta_0 \quad (18)$$

$$L^{r_n} = \frac{s(\rho_e^{r_n+s}) \rho_1^{r_n} \rho_2^{r_n}}{\rho_e^r (\rho_1^{r_n+s}) (\rho_2^{r_n+s})} \sin^2\beta_0 \quad (19)$$

$$a(\phi+\phi') = 2\cos^2\left(\frac{\phi+\phi'}{2}\right) \quad (20)$$

$$\frac{1}{\rho_e^r} = \frac{1}{\rho_e^i} - \frac{2(\hat{n} \cdot \hat{n}_e)(\hat{s}' \cdot \hat{n})}{a_e \sin^2\beta_0} \quad (21)$$

$$\frac{1}{\rho} = \frac{1}{\rho_e^i} - \frac{\hat{n}_e \cdot (\hat{s}' - \hat{s})}{a_e \sin^2\beta_0} \quad (22)$$

$$\frac{1}{\rho_1^{r_{0,n}}} = \frac{1}{\rho_1^i} + \frac{2}{a_e \cos\theta_i}, \text{ and} \quad (23)$$

$$\frac{1}{\rho_2^{r_{0,n}}} = \frac{1}{\rho_2^i} + \frac{2 \cos\theta_i}{a_{0,n}} \quad (24)$$

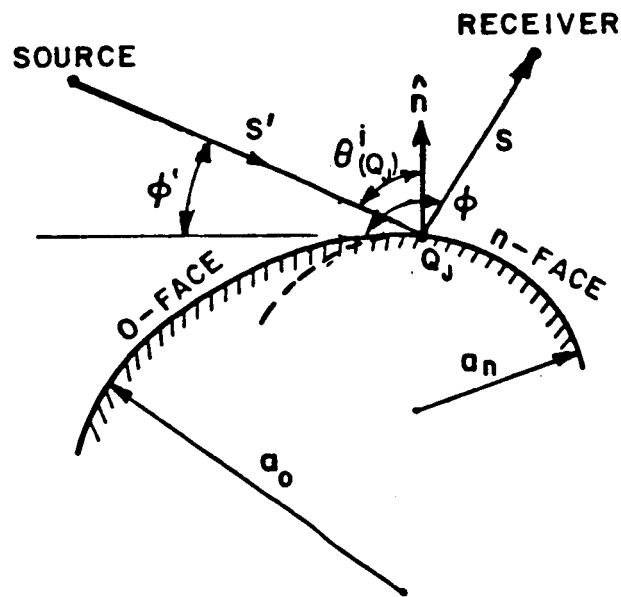
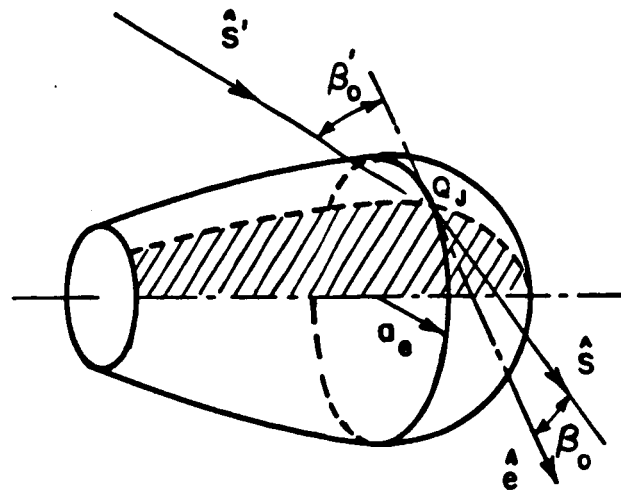


Figure 4. A 3-dimensional wedge with smooth junction.

The various parameters used in Equations (16) - (24) are defined as follows:

$\rho_1^i, \rho_1^r$  = the principal radii of curvature of the (incident, reflected) wavefront at  $Q_j$  in the plane of incidence

$\rho_2^i, \rho_2^r$  = the principal radii of curvature of the (incident, reflected) wavefront at  $Q_j$  in the transverse plane

$a_e$  = the radius of curvature of the edge at  $Q_j$

$\hat{n}$  = the unit normal to the surface at  $Q_j$

$\hat{n}_e$  = the unit normal to the edge at  $Q_j$  directed away from the center of edge curvature

$\hat{s}'$  = the unit vector in the incident ray direction at  $Q_j$

$\hat{s}$  = the unit vector in the diffracted ray direction at  $Q_j$

$\hat{e}$  = the unit tangent to the edge at  $Q_j$

$\beta_0$  = the angle between the incident and edge tangent directions such that

$$\cos \beta_0 = \hat{e} \cdot \hat{s}' \quad (25)$$

$\hat{\phi}', \hat{\phi}$  = the unit vectors in the plane perpendicular to the edge at  $Q_j$

$$\hat{\beta}' = \hat{s}' \times \hat{\phi}' \quad (26)$$

$$\hat{\beta} = \hat{s} \times \hat{\phi} \quad (27)$$

and

$\rho_e^i$  = the radius of curvature of the incident wavefront  
at  $Q_j$  in the plane containing  $\hat{e}$  and  $\hat{s}'$ .

For the paraboloid-skirt junction, assuming the skirt to be the 0-face and the feed is at the focus, one obtains

$$\begin{aligned} \rho_e^r &= \rho_1^{r_0, n} = \infty \\ \rho_2^r &= \infty, \text{ and} \\ \rho_2^o &= \rho_2^i \end{aligned} \quad (28)$$

Thus, the distance parameters are given by

$$L^{r_0} = \frac{s \rho_2^{r_0}}{(\rho_2^{r_0} + s)} \sin^2 \beta_0, \text{ and} \quad (29)$$

$$L^{r_n} = s \quad (30)$$

Knowing the coordinates of the observation point  $(x_0, y_0, z_0)$ , one can find the point of diffraction on the edge. The law of diffraction will be satisfied at the point of diffraction. Once the point of diffraction is found, one can compute the incident field  $(E_{\beta'}^i, E_{\phi'}^i)$  at that point. The angles  $(\beta_0, \phi$  and  $\phi')$  can also be found. Knowing  $\rho_1^i$  and  $\rho_2^i$ , one can compute  $\rho$ ,  $L^{r_0}$ ,  $L^{r_n}$  and then using (3), the diffracted fields can be calculated. Note that  $\phi' = 90^\circ$  in this case.

As pointed out before, the code can also be used to analyze the reflector without any skirt. In this case, the skirt diffraction term is replaced with edge diffraction from the lower end of the paraboloid. Again GTD is used to compute this edge diffraction term.

#### **D. FEED BLOCKAGE**

The feed blockage is computed using a physical optics integration technique. The feed aperture is assumed to be a flat plate located at a distance  $Z_a$  from the center of the paraboloid. The flat plate is defined by the coordinates of its corners. The number of corners and their coordinates are input parameters. The plate is assumed to be symmetrical about the  $x_a$  axis as shown in Figure 5. The field incident on the flat plate is assumed to be uniform and equal to the specular reflected field at  $(0,0,Z_a)$ . For small plates, the surface integration is replaced by a contour integration along the periphery of the plate [5]. For large plates, the plate is subdivided into rectangular patches as shown in Figure 5(b). As written, the maximum number of rectangular segments is equal to 625. The corners of the flat plate are numbered in a clockwise fashion as shown in Figure 5(b).

#### **E. FEED SPILLOVER**

To compute the feed spillover, the feed pattern should be known. The code computes the feed spillover only if the measured feed pattern is input to the code. The measured feed pattern is read by the code from unit #19. The format of the data to be stored on unit #19 is

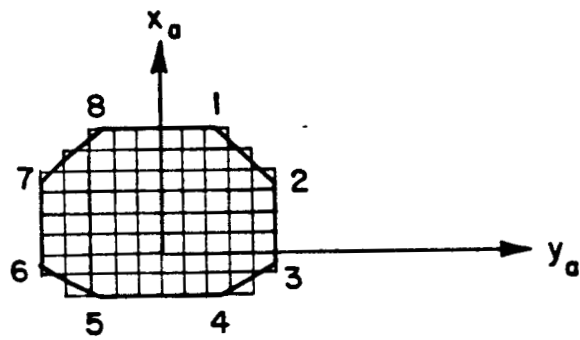
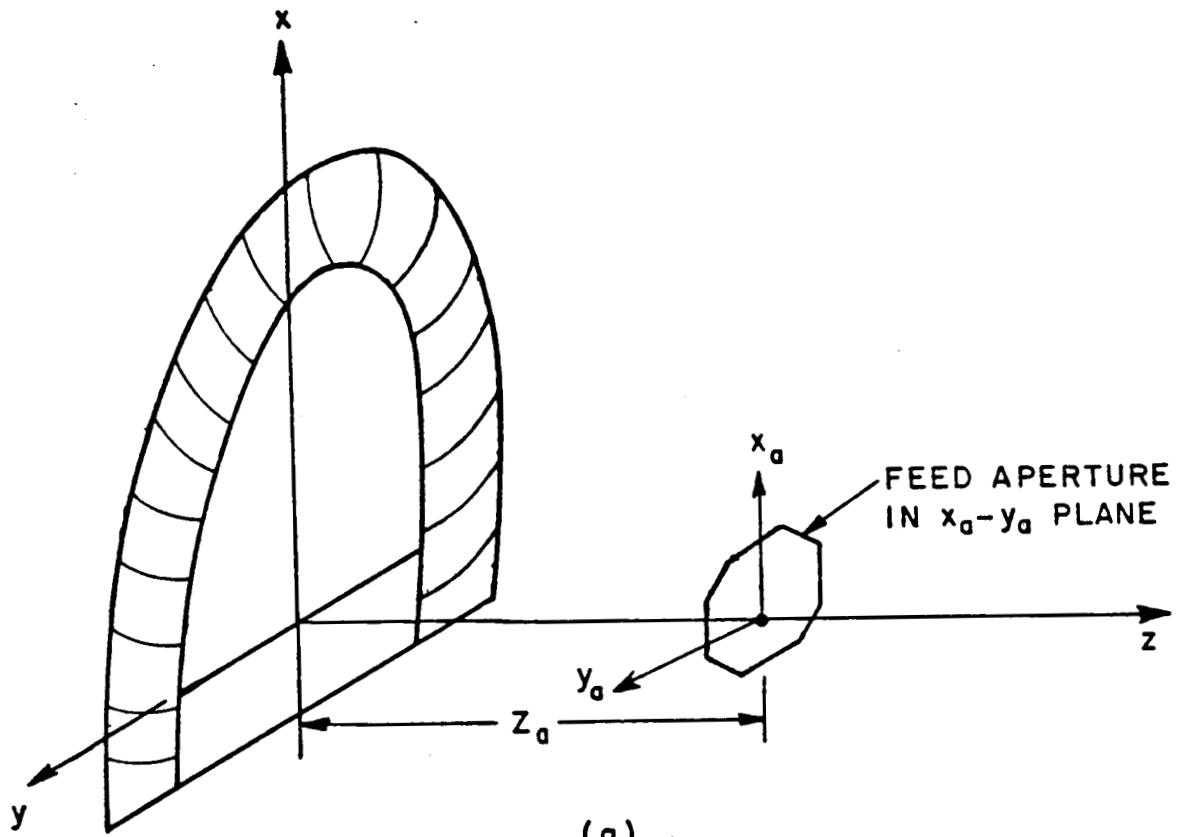
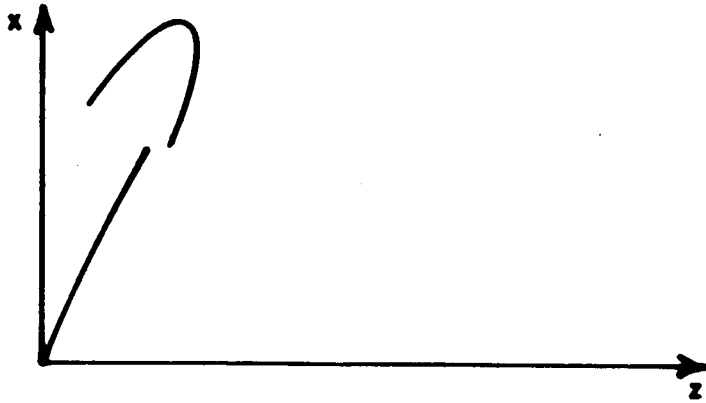


Figure 5. Flat plate used to compute feed blockage. The plate is symmetrical about the  $x_a$  axis. Note that the  $x_a$ - $y_a$  plane is parallel to the  $x$ - $y$  plane.

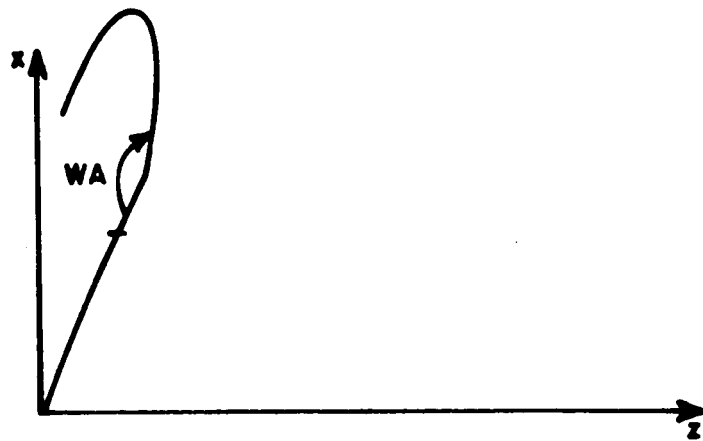
discussed in the next section, where various input/output statements used in the code are explained.

#### **F. DIFFRACTION FROM A MECHANICAL DISCONTINUITY**

The code can also be used to compute the diffraction from a mechanical discontinuity [6] in the surface of the reflector. The mechanical discontinuity results from misalignment of the two sections of the reflector and can be in the form of a step and/or an angular tilt (see Figure 6) and is assumed to be circularly symmetrical. The physical optics (PO) method described in [6] is used to compute the diffraction from the mechanical discontinuity; i.e., first the scattered fields from a perfect surface (no mechanical discontinuity) are computed and then the fields from the imperfect surface are computed. The scattered fields of the perfect surface are then subtracted from the scattered fields of the imperfect surface to isolate the diffraction from the surface discontinuity. The code uses the same approach as used for computing the junction diffraction to compute these scattered fields. In fact, the total scattered field from the perfect surface are computed while computing the junction diffraction and are stored on unit #30 for future use. Thus, one should run the junction diffraction option before computing the diffracted fields from the surface discontinuity. However, if one wants to study the effect of various discontinuities, the junction diffraction option needs to be run only once in the beginning. The code saves the data stored on unit #30.



(a)



(b)

Figure 6. Mechanical discontinuity in the surface.  
(a) step discontinuity  
(b) discontinuity due to angular tilt

To compute the total PO scattered fields from the imperfect surface, one needs to input the cross-sectional shape of the imperfect surface to the code. This geometrical shape is read from unit #18. The data file linked to unit #18 has the same information as the data file linked to unit #17 except that it is for the imperfect surface.

By subtracting the scattered fields of the perfect surface from those of the imperfect surface, one obtains the 2-dimensional diffracted fields from the mechanical discontinuity. An appropriate spread factor must be applied to this field in order to obtain the desired 3-dimensional diffracted fields. One needs the coordinates of the surface discontinuity to compute the spread factor. This is an input parameter and is equal to the radial distance of the mechanical discontinuity from the axis of the reflector.

A brief description of the various input and output statements used in the code is given next.

### **III. INPUT AND OUTPUT DATA**

#### **A. INPUT DATA**

The code is written to accept the input data on an interactive basis in free format; i.e., a statement will appear on the user's terminal explaining what input is needed. The statements are self explanatory and are listed below.

1. Input the frequency of operation in GHz.
2. Input the focal length of the reflector in feet.
3. Input the radius of the parabolic section in feet.

4. Is there a rolled edge on top? If yes, type 1.
5. Is there a skirt at the bottom? If yes, type 1.
6. Is the feed to be simulated? If yes, type 1.
- 6a. Input the magnitude of the magnetic dipoles along x and y axes.
- 6b. Input the magnitude of the electric dipoles along x and y axes.
7. Input the feed tilt angle in degrees.
8. Input the type of cut (IFCUT) along which near field data is to be computed.
- 9a. Input PHI (degrees) for the field cut.
- 9b. Input y-cut (feet) for the field cut.
- 9c. Input x-cut (feet) for the field cut.
10. Input the distance of the field cut from the vertex of the reflector in feet.
11. Input the start point and end point for field probing (in feet).
12. Input the distance between field points in feet.
13. Do you want GO term? If yes, type 1.
14. Do you want junction diffraction? If yes, type 1.  
Or, Do you want diffraction from top edge? If yes, type 1.
- 14a. Will you be studying the diffraction due to a mechanical discontinuity? If yes, type 1.
15. Do you want skirt diffraction? If yes, type 1.  
Or, Do you want diffraction from lower edge? If yes, type 1.
16. Do you want feed blockage? If yes, type 1.
- 16a. Input the z location of the feed structure in feet.
- 16b. Input the number of corners in the flat plate used to simulate the feed structure.

- 16c. Input the coordinates (in inches) of the corners of the plate.
- 17. Do you want feed spillover? If yes, type 1.
- 18. Do you want diffraction from the mechanical discontinuity? If yes, type 1.
- 18a. Input the radial distance of the mechanical discontinuity from the axis of the reflector in feet.
- 19. Do you want electric field as the output? If yes, type 1.

Statement 1 defines the frequency of operation. Statements 2 and 3 define the focal length and radius of the parabolic section. Statements 4 and 5 are used to tell the code whether the reflector has a rolled edge at the top and a skirt at the bottom or not. Statement 6 defines the type of feed to be used in the analysis. The code is written for the case where measured feed pattern data can be used. If the measured feed pattern data is not available, the code can simulate the fields of the feed. The fields are simulated using four short dipoles (two magnetic dipoles and two electric dipoles). Two dipoles are oriented along  $x_f$  (if dipoles are oriented along negative  $x_f$ , the magnitude of the dipoles will be negative) and the other two are oriented along  $y_f$  (see Figure 7). The dipole magnitudes are their magnetic field strength at a unit distance. For example, for a magnetic dipole oriented as shown in Figure 8, the magnetic field is given by

$$\vec{H} = -\hat{\theta} H_m \sin\theta \frac{e^{-jkR}}{R} \quad (31)$$

where  $H_m$  is input to the program and  $R$  is the distance of the observation point from the dipole in centimeters. Similarly, for an

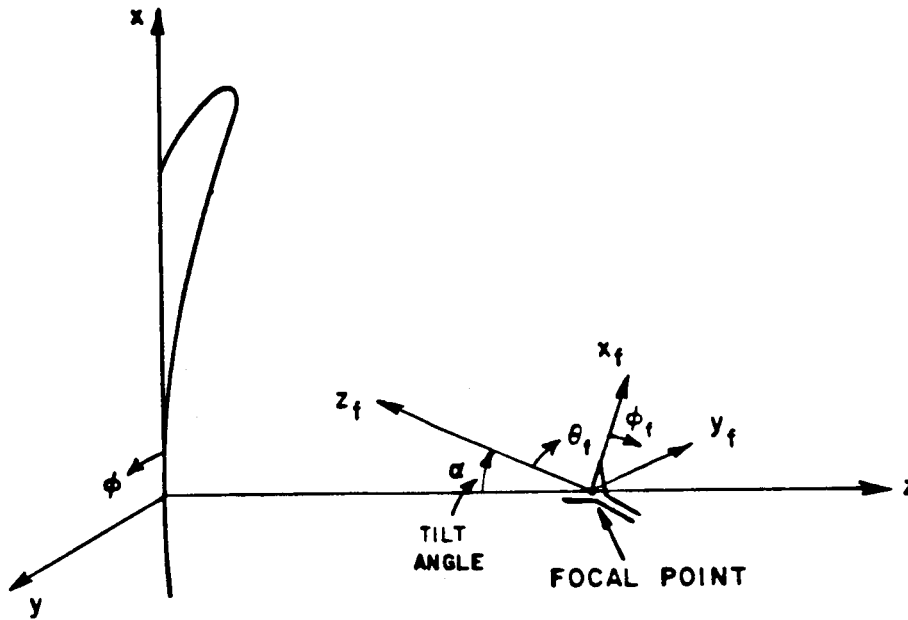


Figure 7. Feed configuration with feed tilt specified by  $\alpha$ .

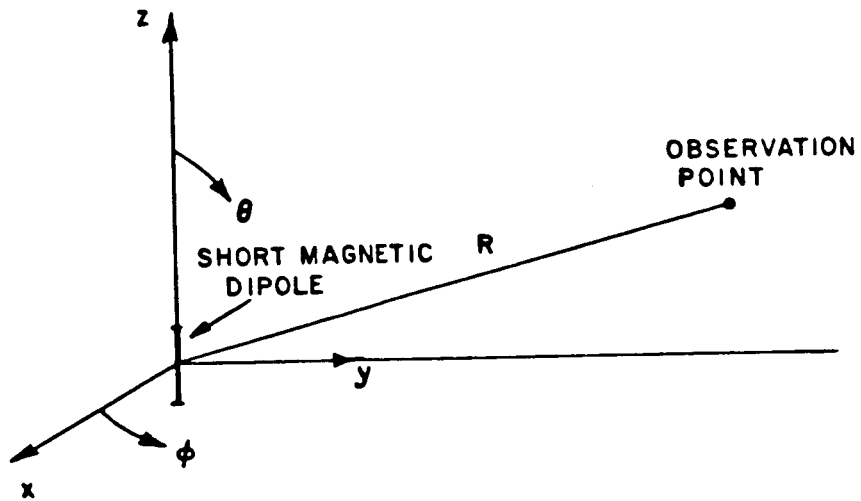


Figure 8. Short magnetic dipole.

electric dipole oriented along the z axis, the magnetic field is given by

$$\vec{H} = -\hat{\phi} H_e \sin\theta \frac{e^{-jkR}}{R} \quad (32)$$

where  $H_e$  is the input to the program. The magnitude of the various dipoles are defined in statements 6a and 6b.

If the measured feed pattern data is used, statements 6a and 6b are skipped and the measured data is read from unit #19. The data file linked to unit #19 should have the following information:

- a) The input data is in dB or volts/meter.
- b) The feed polarization.
- c) The feed is symmetrical about  $y_f$  axis (see Figure 7) or not.
- d) The number of cuts (NPHCUT) along which the feed data is input and the number of points along each  $\phi$  cut (NPOINT).
- e)  $\phi$  value (FPHI) for each  $\phi$  cut.
- f)  $\theta$  value and the feed amplitude for each point along various  $\phi$  cuts.

This file is read using the following format.

```
Read (19,*) IFDB
Read (19,*) IFPOL
Read (19,*) IYSYM
Read (19,*) NPHCUT, NPOINT
  Do 10 I=1, NPHCUT
    Read (19,*) FPHI(I)
    Do 2 J=1, NPOINT
      2 Read (19,*) FTHETA(I,J), FAMP(I,J)
    10 Continue.
```

Integer variable (IFDB) is used to tell the code whether the measured data is in dB or not. If the measured data is in dB, IFDB=1; otherwise, the measured data is assumed to be in volts/meter.

Integer variable (IFPOL) is used to tell the code the feed polarization. For a vertical polarized field (electric field along  $\hat{\theta}_f$ ), IFPOL=1. Otherwise, the feed is assumed to be horizontally polarized (electric field along  $\hat{\phi}_f$ ).

Integer variable IYSYM is used to tell the code whether the feed pattern is symmetrical about the  $y_f$  axis or not. If the feed is symmetrical about the  $y_f$  axis, IYSYM=1. The feed pattern is always assumed to be symmetrical about  $x_f$  axis.

Integer variable (NPHCUT) defines the number of input feed pattern cuts. The code is written for a maximum of 19 cuts. Each input pattern corresponds to a constant  $\phi_f$  cut in the feed coordinate system. A circular symmetric feed pattern is obtained if NPHCUT=1. Integer variable NPOINT defines the number of feed points to be read for each input  $\phi_f$  plane pattern cut. The code is written for a maximum of 37 points.

FPHI(I) defines the  $\phi_f$  value of the  $I^{\text{th}}$  pattern cut in degrees. These values must be input in monotonic order, i.e.,  $FPHI(I+1) > FPHI(I)$ . Note that for IYSYM=1,  $0 < FPHI(I) < 90^\circ$  and for IYSYM $\neq$ 1,  $0 < FPHI(I) < 180^\circ$ .

FTHETA(I,J) defines the  $\theta_f$  angle for  $J^{\text{th}}$  point of the  $I^{\text{th}}$  cut in degrees. These values should also be in monotonic order, and FTHETA(I,1) should be zero for all I. Note that  $0 < FTHETA(I,J) < 180^\circ$ .

FAMP(I,J) defines the feed pattern value (in dB if LFDB=1) at the J<sup>th</sup> point of the I<sup>th</sup> cut. The code reads the measured feed pattern and then uses cubic splines for interpolation along each  $\phi_f$  cut. Linear interpolation is done in the other direction. If the measured feed pattern is used, the following statements appear on the user's terminal.

1. Measured feed pattern is being read from unit #19.
2. The feed polarization is horizontal (vertical).

The phase center of the feed is assumed to be at the focus of the reflector. The feed may be tilted as shown in Figure 7. The tilt angle of the feed is defined in statement 7.

As stated in the Introduction, the code can be used to compute the probed near field of the reflector along various cuts. The type of cut is defined in statement 8. IFCUT is set equal to 1,2,3 or 4 for radial, vertical, horizontal or axial cuts, respectively. A radial cut is a cut in a plane parallel to the xy plane at a distance  $z_0$  from the vertex of the reflector for a given  $\phi$  (see Figure 9). A vertical cut is parallel to the x axis at a distance  $z_0$  from the vertex of the reflector along the z axis for a fixed y(YCUT). Similarly, a horizontal cut is a cut parallel to y axis at a distance  $z_0$  from the vertex of the reflector along the z axis for a fixed x(XCUT). An axial cut is parallel to the z axis at a radial distance  $\rho_0$  from the axis of the reflector for fixed  $\phi$ . These parameters are read in statements 9 and 10. For example, if IFCUT=1, statements 9a and 10 will appear on the user's terminal. If

IFCUT=2, statements 9b and 10 will appear on the user's terminal. If IFCUT=3, statements 9c and 10 will appear on the user's terminal. Finally for IFCUT=4, statements 9a and 10 will appear on the user's terminal. The code is set to compute the scattered fields for  $y > 0$ ; i.e.,  $\phi > 0^\circ$ . The performance for  $\phi < 0^\circ$  will be the same as for  $\phi > 0^\circ$ . In the case of axial cut  $0^\circ < \phi < 90^\circ$ .

The region in which the near field is to be probed and the spacing between the probed points is defined in statements 11 and 12. Presently, the code is set to compute scattered fields at a maximum of 201 points. If more than 201 points are needed, one should change statement 2 in the code accordingly; i.e., NFP should be set equal to the number of field points plus ten. The spacing between the samples should be selected such that within the sweet region, the field is computed at least at 45 points.

Statements 13-18 define the various mechanisms to be computed. Note that one can choose any combination of mechanisms, and when the junction diffraction mechanism is selected, statement 14a will appear on the user's terminal. If the user wants to compute the diffraction due to a mechanical discontinuity, appropriate action should be taken. In that case, the code writes the total P0 scattered field from the perfect surface on unit #30. This data is read automatically when diffracted fields from the mechanical discontinuity are computed. Note that one needs to run this option only once to study the effect of a mechanical discontinuity.

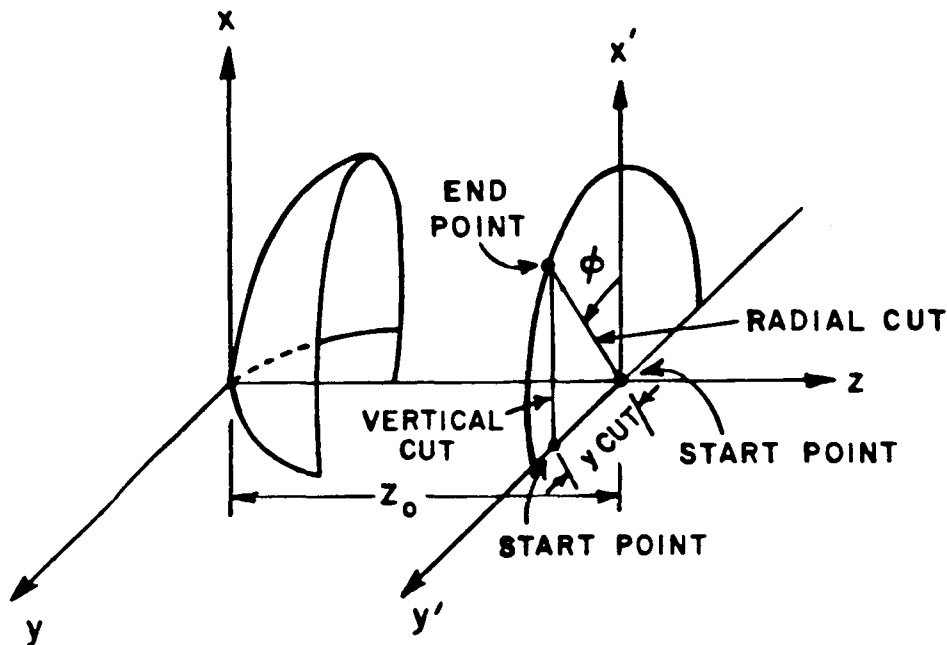


Figure 9. Description of the observation plane.

For computing the feed blockage, the code requires information about the feed structure. As pointed out in the last section, the feed aperture is assumed to be a flat plate whose normal is aligned with the axis of the reflector. The flat plate is defined by the coordinates of its corners. If the feed aperture is circular, it should be approximated by a polygon. The geometry of the flat plate is read through statements 16a-16c. The  $z$  location of the feed structure is the distance along the  $z$  axis from the vertex of the paraboloid. Statement 16b defines the number of corners in the flat plate. As written, the maximum number of corners permitted in the code is ten. Statement 16c

defines the coordinates of the corners of the plate. As discussed in Section II, the corners are numbered according to a clockwise convention with the first corner along the positive x direction or in the first quadrant with the smallest distance from the x axis. Note that the plate is assumed to be symmetrical about the x axis.

If the diffraction from a mechanical discontinuity is desired, then the radial distance of the mechanical discontinuity from the axis of the reflector should be input to the code. This information is supplied in statement 18a. The code is written to analyze a mechanical discontinuity in the rolled edge. Thus, the radial distance of the mechanical discontinuity should be larger than or equal to the radius of the parabolic section, and there should be a rolled edge on the top to study the effect of a mechanical discontinuity.

Statement 19 defines the output. The code computes both electric and magnetic fields but only one is stored as an output file. The output field chosen by the user is defined by statement 19.

Finally, one needs to input the cross-sectional shape of the cylinder to compute junction diffraction. This information should be input on unit #17 and is automatically read by the code. The format of this data was given in the last section. One also needs the cross-section of the reflector to compute specular reflection from the rolled edge. This information should also be input on unit #17. In fact, one can use the same data file to compute the junction diffraction and specular reflection terms. If no rolled edge is added to the reflector, then this information is not needed.

If one wishes to study the effect of a mechanical discontinuity in the surface of the reflector, one should input the cross-sectional shape of the appropriate cylinder. This information should be input on unit #18 and is automatically read by the code. The format of this data is the same as that of the file linked to unit #17.

## B. OUTPUT DATA

The code stores the field due to each mechanism as well as the total field in terms of separate output files. As chosen by the user, all three components (x,y,z) of either the electric or the magnetic field are stored. The specular reflected field is stored on unit #20, the junction diffraction on unit #21, the skirt diffraction on unit #22, the feed blockage on unit #23, diffraction from a mechanical discontinuity on unit #24, the feed spillover on unit #25, and the total field on unit #26. The fields are stored for various distances from the center of the reflector using the following format:

```
WRITE(IUNIT,100) DIS(I),FX(I), FY(I), FZ(I)
100 FORMAT (7E 16.6)
```

where IUNIT=20, 21, 22, 23, 24, 25 or 26; FX(I), FY(I) and FZ(I) are the x,y and z components of the field at the I<sup>th</sup> probing point, and DIS(I) is the radial, vertical, horizontal or axial distance (in feet) of the I<sup>th</sup> probing point.

Some sample results obtained using this code are given in the next section.

#### IV. SAMPLE RESULTS

In this section, some results obtained using this computer code are presented to illustrate the code's capability as well as being samples of input/output sets. Scientific-Atlanta's new 15 foot reflector antenna (model 5753) with a blended rolled edge is used for illustration. The focal length of the reflector is 24 feet, and the frequency of operation is 2 GHz. Figure 10 shows a cross-sectional view (in the xz plane) of the reflector. Note that the reflector has a blended rolled edge at the top and a skirt at the bottom. The semi major axis of the elliptical section used as the rolled edge is 3.2808 feet, and its semi minor axis is 1.3123 feet. The two sections (elliptical and parabolic) are blended using a cosine blending function (see Appendix A).

The code is used to compute the field scattered by the reflector along various cuts at a distance of 36.0 feet from the center of the reflector. As pointed out in the last section, one needs the cross-sectional shape of the infinitely long cylinders to compute the junction diffraction, specular reflection and diffraction from the mechanical discontinuity. This cross-sectional shape was obtained using the computer code "SURFACE", which is described in Appendix A. This code (SURFACE) reads the input data from unit #70. The input data file assigned to unit #70 contained the following information:

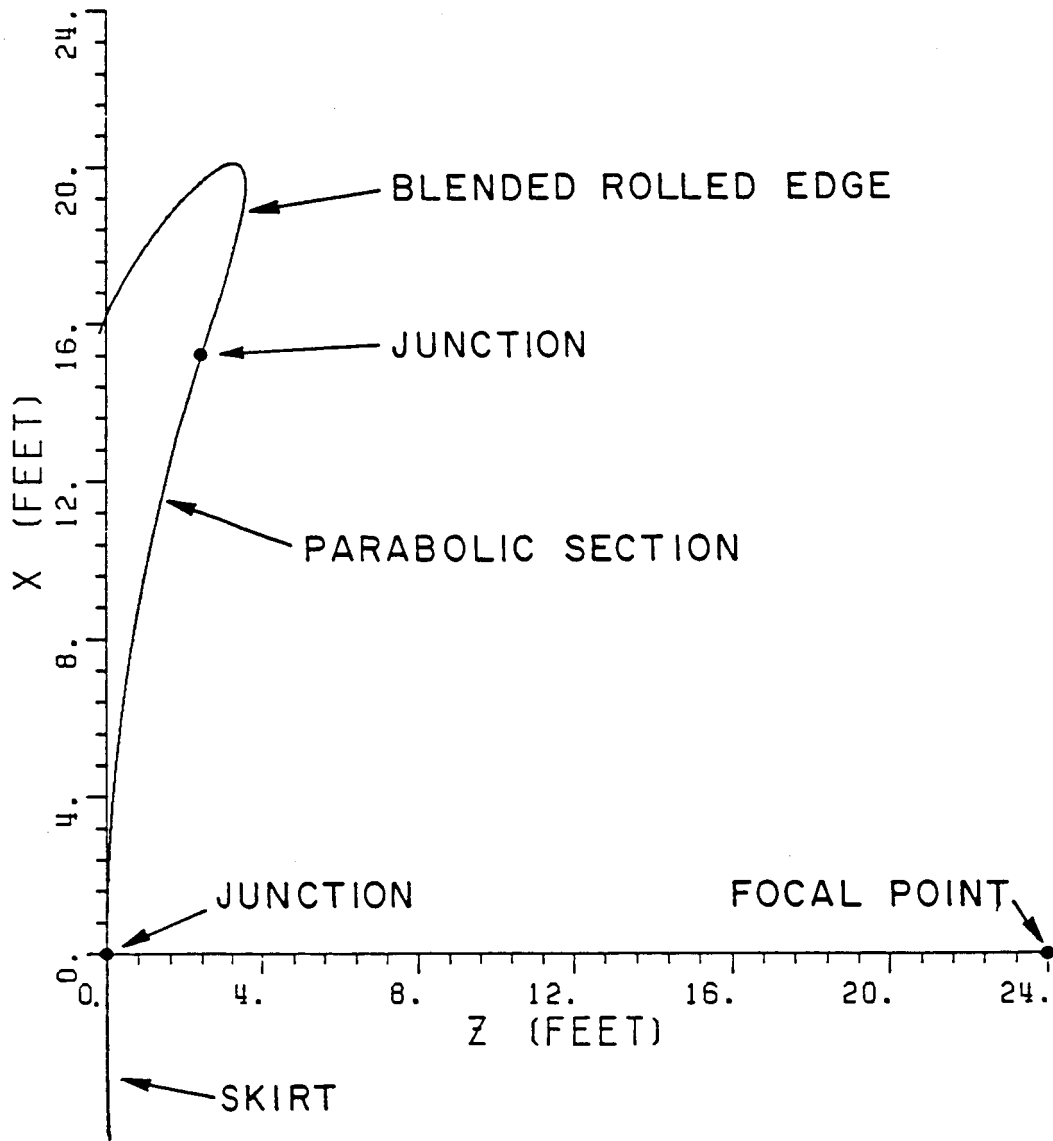


Figure 10. Cross-sectional view of the semi-circular Scientific-Atlanta reflector in the xz plane.

2.  
24.  
15.  
-5.  
4  
13.1233  
180.  
3.2808, 1.3123  
0.05  
0 or 1  
16.  
179.5  
0.,0.

Figure 11 shows the cross-sectional shape obtained using the computer code. Note that the cross-sectional shape is similar to the cross-section of the reflector (see Figure 10) except that the skirt is replaced by a parabolic section. The length of the parabolic section is 5 feet which is roughly equal to 10 wavelengths at 2 GHz. The scattered fields along a vertical cut with  $y\text{-cut}=0$  for various reflectors (with or without rolled edge and/or skirt) is computed first. The scattered electric field is plotted here.

Figure 12 shows the copolarized (x) component<sup>†</sup> of the scattered electric field along the vertical cut at a distance of 36 feet from the center of the reflector when the feed is a vertically polarized Huygen source<sup>††</sup> (one short electrical dipole oriented along the  $x_f$  axis (see Figure 7) and another short magnetic dipole oriented along the  $y_f$  axis). The tilt angle of the feed is zero. In the results presented in Figure

---

† The cross-polarized (y) component in this cut is negligible.

†† A Huygen source is chosen because it provides approximately uniform illumination of the reflector and for no tilt the cross-polarized component of the scattered fields will be zero.

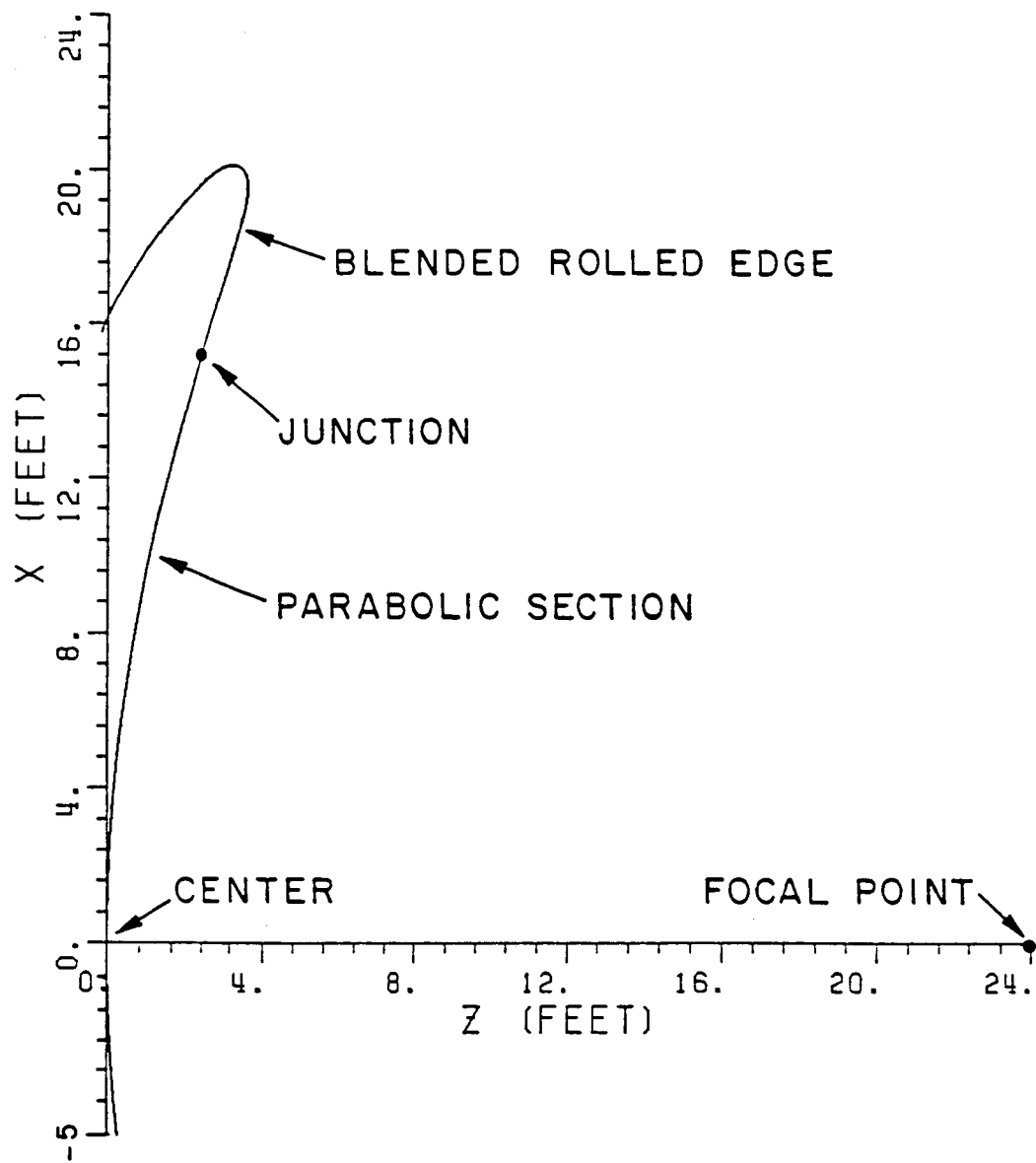


Figure 11. Cross-sectional shape of the infinitely long cylinder.

12, the reflector is assumed to have no rolled edge at the top and no skirt at the bottom. The various mechanisms included in the field computation are specular reflection, upper edge diffraction and lower edge diffraction. The input data to the code is given below which was input on an interactive basis:

INPUT THE FREQUENCY OF OPERATION IN GHz  
2.  
INPUT THE FOCAL LENGTH OF THE REFLECTOR IN FEET  
24.  
INPUT THE RADIUS OF THE PARABOLIC SECTION IN FEET  
15.  
IS THERE A ROLLED EDGE ON TOP? IF YES, TYPE 1  
0  
IS THERE A SKIRT AT THE BOTTOM? IF YES, TYPE 1  
0  
IS THE FEED TO BE SIMULATED? IF YES, TYPE 1  
1  
INPUT THE MAGNITUDE OF THE MAGNETIC DIPOLES ALONG X AND Y AXES.  
0.,1.  
INPUT THE MAGNITUDE OF THE ELECTRIC DIPOLES ALONG X AND Y AXES.  
1.,0.  
INPUT THE FEED TILT ANGLE IN DEGREES  
0.  
INPUT THE TYPE OF CUT(IFCUT) ALONG WHICH PROBED NEAR FIELD DATA IS TO BE COMPUTED  
2  
INPUT THE Y-CUT (feet) FOR THE FIELD CUT  
0.  
INPUT THE DISTANCE OF THE FIELD CUT FROM THE VERTEX OF THE REFLECTOR IN FEET  
36.  
INPUT THE START POINT AND END POINT FOR FIELD PROBING  
0.,15.  
INPUT THE DISTANCE BETWEEN FIELD POINTS IN FEET  
0.1  
DO YOU WANT GO TERM? IF YES, TYPE 1  
1  
DO YOU WANT DIFFRACTION FROM TOP EDGE? IF YES, TYPE 1  
1  
DO YOU WANT DIFFRACTION FROM LOWER EDGE? IF YES, TYPE 1  
1  
DO YOU WANT FEED BLOCKAGE? IF YES, TYPE 1  
0

DO YOU WANT FEED SPILLOVER? IF YES, TYPE 1

0

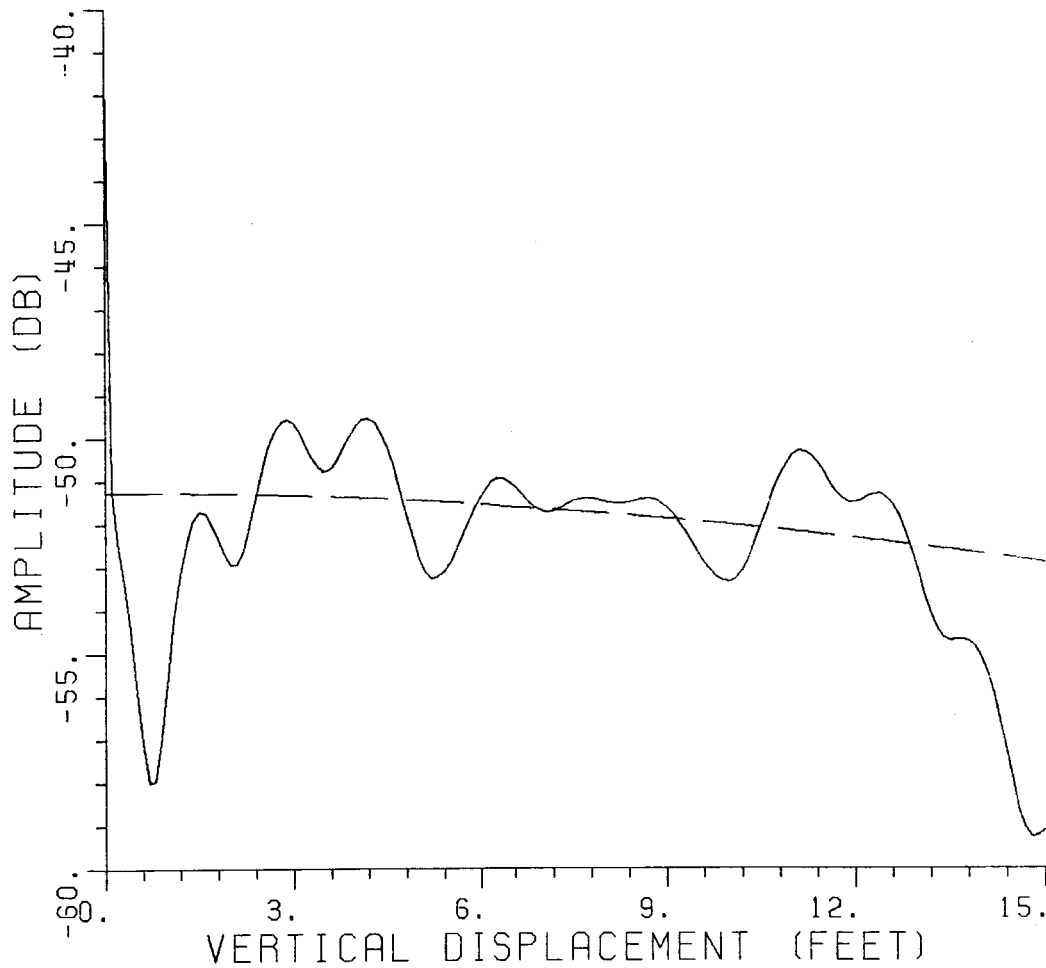
DO YOU WANT DIFFRACTION FROM THE MECHANICAL DISCONTINUITY? IF YES,  
TYPE 1

0

DO YOU WANT ELECTRIC FIELD AS THE OUTPUT? IF YES, TYPE 1

1

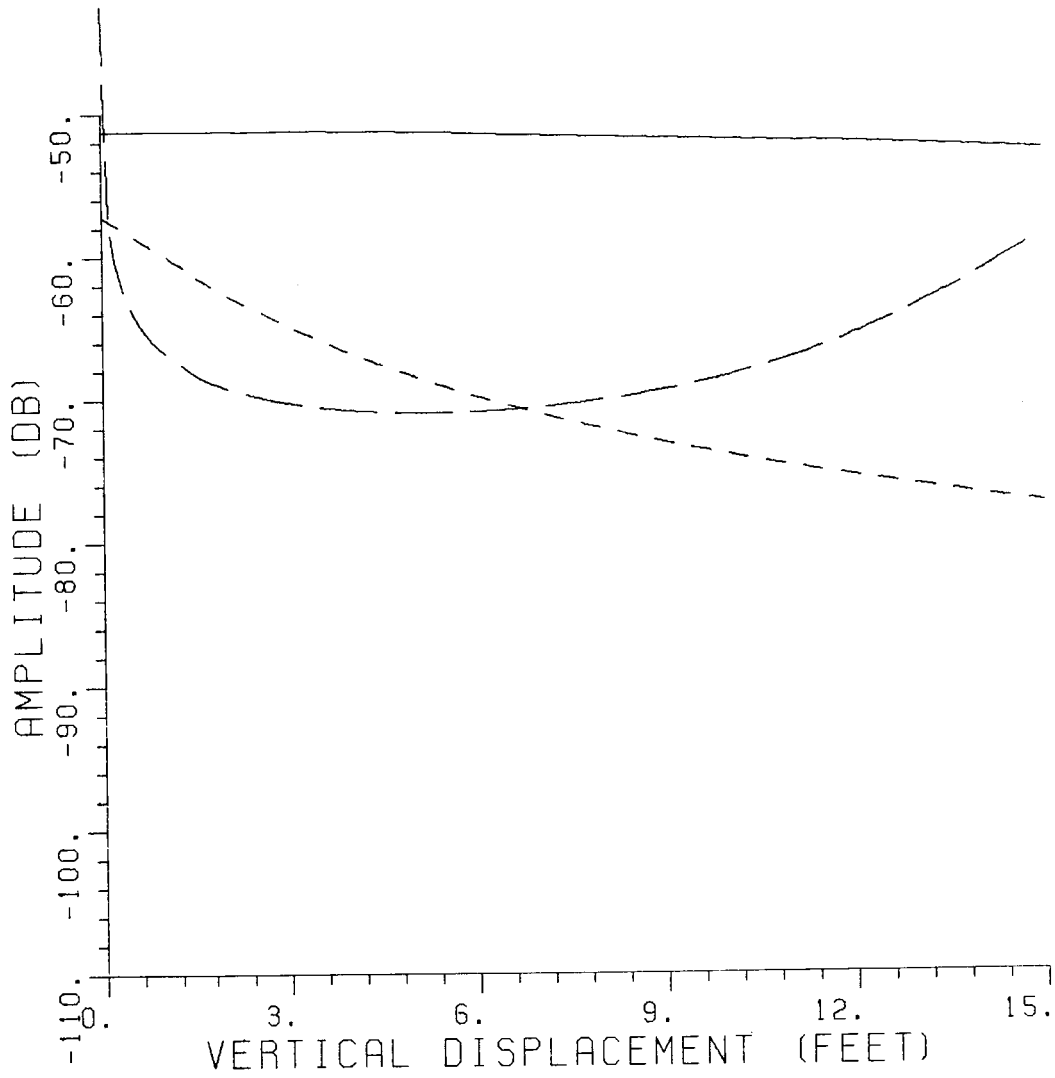
In Figure 12, the amplitude of the scattered electric field is plotted versus the vertical displacement. The specularly reflected component alone (dashed curve) is also shown in the figure. The plots in Figure 12 were obtained by using the output on units #20 and #26. Note that the total scattered field oscillates around the specularly reflected field. These oscillations are due to diffraction from the rim of the paraboloid. The ripple size of the oscillations for vertical displacements between 3 feet and 13 feet is more than 2 dB. Thus, the diffracted fields are quite strong which is further verified by the results shown in Figure 13, where the diffraction from the rim of the paraboloid is plotted. The diffracted fields from the top edge (circular section) as well as the bottom edge of the rim are plotted. The specular reflection term is also shown in the figure. Each term is plotted relative to the same level so that results can be compared. Note that the diffracted fields are quite strong. The diffraction from the top edge is dominant near the upper edge of the paraboloid (vertical displacement equal to 15 feet); whereas, the lower edge diffraction is dominant for small vertical displacements. To reduce these diffracted fields, one should add a skirt at the bottom of the paraboloid and a blended rolled edge on the top of the paraboloid.



\_\_\_\_\_ total field  
 - - - - - specular reflection

Figure 12. The copolarized (x) component of the scattered electric field versus vertical displacement. YCUT=0, feed tilt angle=0°, various mechanisms included in the scattered field are:

1. specular reflection
2. upper edge diffraction
3. lower edge diffraction



\_\_\_\_\_ specular reflection  
 - - - - - upper edge diffraction  
 - . - . - . lower edge diffraction

Figure 13. Specular reflection, upper edge diffraction and the lower edge diffraction versus vertical displacement. YCUT=0, feed tilt angle=0°.

Figure 14 shows the magnitude of the scattered electric field when a skirt and a blended rolled edge, respectively, are added to the bottom and top part of the paraboloid. The cross-section of the reflector now is similar to the one shown in Figure 10. The various mechanisms included in the field computation are: specular reflection, junction diffraction and skirt diffraction. All other parameters are the same as before. The input data set to the code is as follows:

```
INPUT THE FREQUENCY OF OPERATION IN GHz
2.
INPUT THE FOCAL LENGTH OF THE REFLECTOR IN FEET
24.
INPUT THE RADIUS OF THE PARABOLIC SECTION IN FEET
15.
IS THERE A ROLLED EDGE ON TOP? IF YES, TYPE 1
1
IS THERE A SKIRT AT THE BOTTOM? IF YES, TYPE 1
1
IS THE FEED TO BE SIMULATED? IF YES, TYPE 1
1
INPUT THE MAGNITUDE OF THE MAGNETIC DIPOLES ALONG X AND Y AXES.
0.,1.
INPUT THE MAGNITUDE OF THE ELECTRIC DIPOLES ALONG X AND Y AXES.
1.,0.
INPUT THE FEED TILT ANGLE IN DEGREES
0.
INPUT THE TYPE OF CUT(IFCUT) ALONG WHICH PROBED NEAR FIELD DATA IS TO
BE COMPUTED
2
INPUT THE Y-CUT (feet) FOR THE FIELD CUT
0.
INPUT THE DISTANCE OF THE FIELD CUT FROM THE VERTEX OF THE REFLECTOR IN
FEET
36.
INPUT THE START POINT AND END POINT FOR FIELD PROBING
0.,15.
INPUT THE DISTANCE BETWEEN FIELD POINTS IN FEET
0.1
DO YOU WANT GO TERM? IF YES, TYPE 1
1
DO YOU WANT JUNCTION DIFFRACTION? IF YES, TYPE 1
1
```

WILL YOU BE STUDYING THE DIFFRACTION DUE TO MECHANICAL DISCONTINUITY?  
IF YES, TYPE 1

0

DO YOU WANT SKIRT DIFFRACTION? IF YES, TYPE 1

1

DO YOU WANT FEED BLOCKAGE? IF YES, TYPE 1

0

DO YOU WANT FEED SPILLOVER? IF YES, TYPE 1

0

DO YOU WANT DIFFRACTION FROM THE MECHANICAL DISCONTINUITY? IF YES,  
TYPE 1

0

DO YOU WANT ELECTRIC FIELD AS THE OUTPUT? IF YES, TYPE 1

1

In Figure 14, the specularly reflected component alone is also shown (dashed curve). Again the total scattered field oscillates around the specularly reflected component. As point out before, these oscillations are due to junction and skirt diffractions. The ripple size of the oscillations for vertical displacements between 3.5 feet and 13.5 feet is, however, less than 0.2 dB. Thus, the diffracted fields in this region are quite small which is further verified by the results shown in Figure 15 where the junction diffraction and the skirt diffraction are plotted individually versus the vertical displacement. The specular reflection term is also shown. Note that for vertical displacements between 3.5 feet and 13.5 feet the diffracted fields are at least 30 dB below the specularly reflected field. Again, as expected, the skirt diffraction is dominant for small vertical displacements; whereas, the junction diffraction is dominant near the upper edge of the paraboloid (vertical displacement equal to 15 feet).

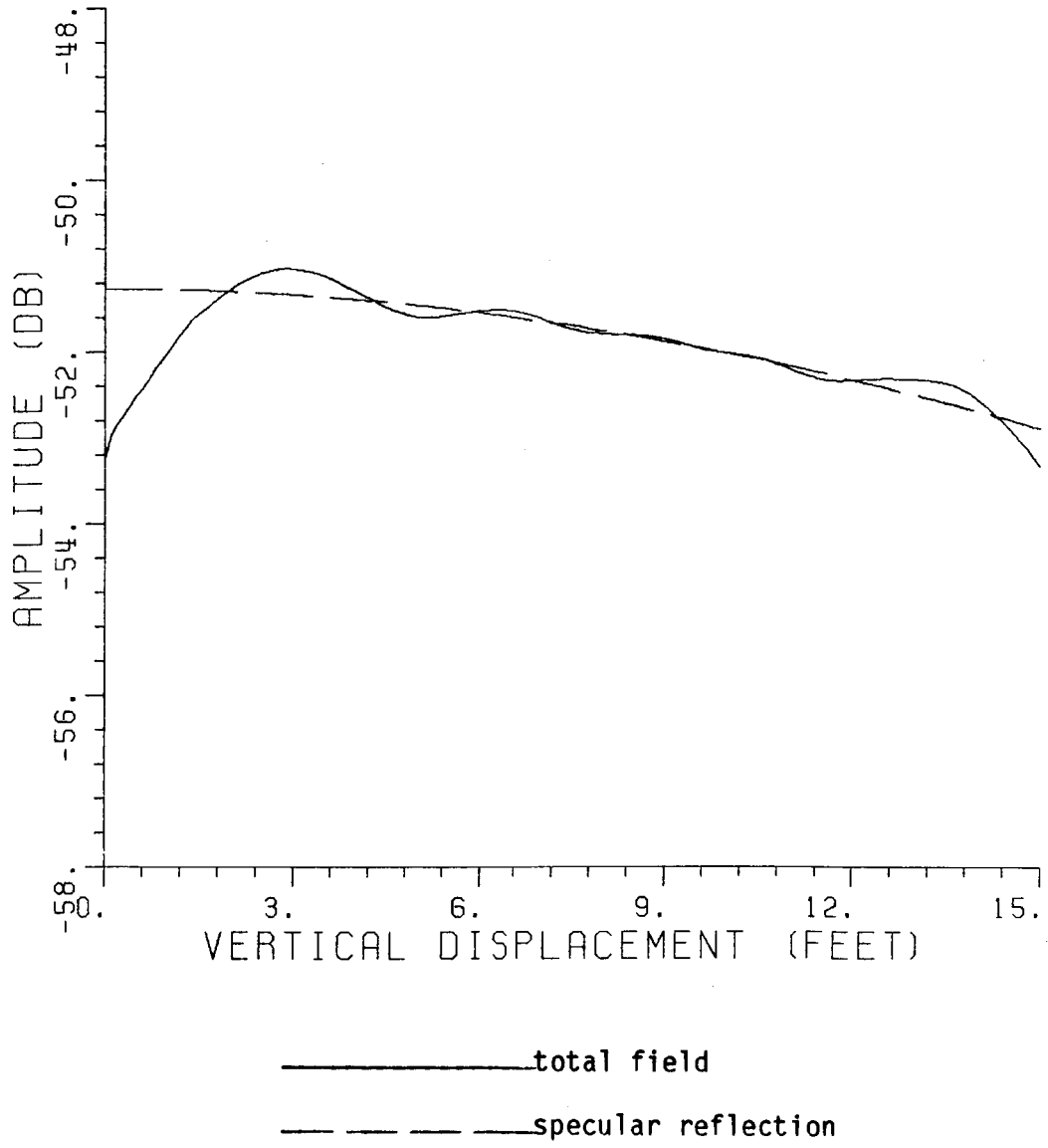
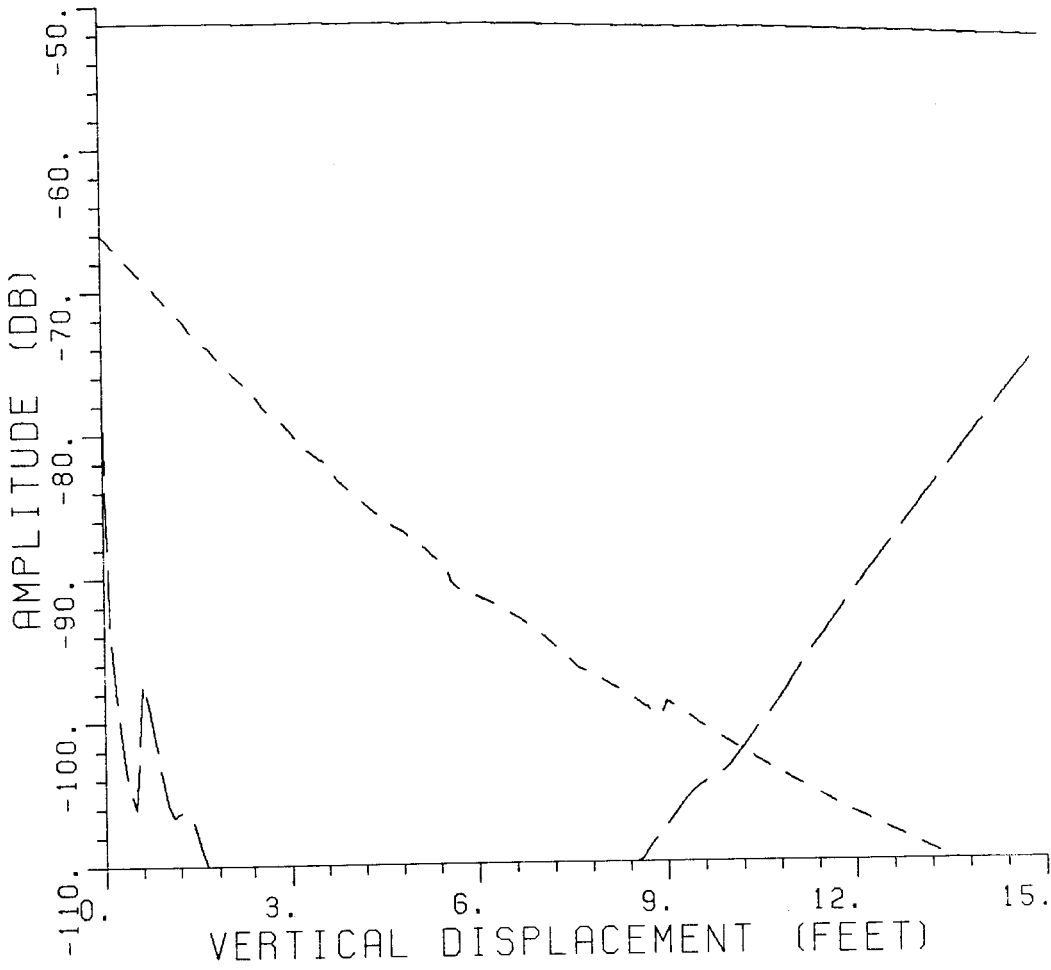


Figure 14. The copolarized (x) component of the scattered electric field versus vertical displacement.  $Y_{CUT}=0$ , feed tilt angle= $0^\circ$ , various mechanisms included in the scattered fields are

1. specular reflection
2. junction diffraction
3. skirt diffraction

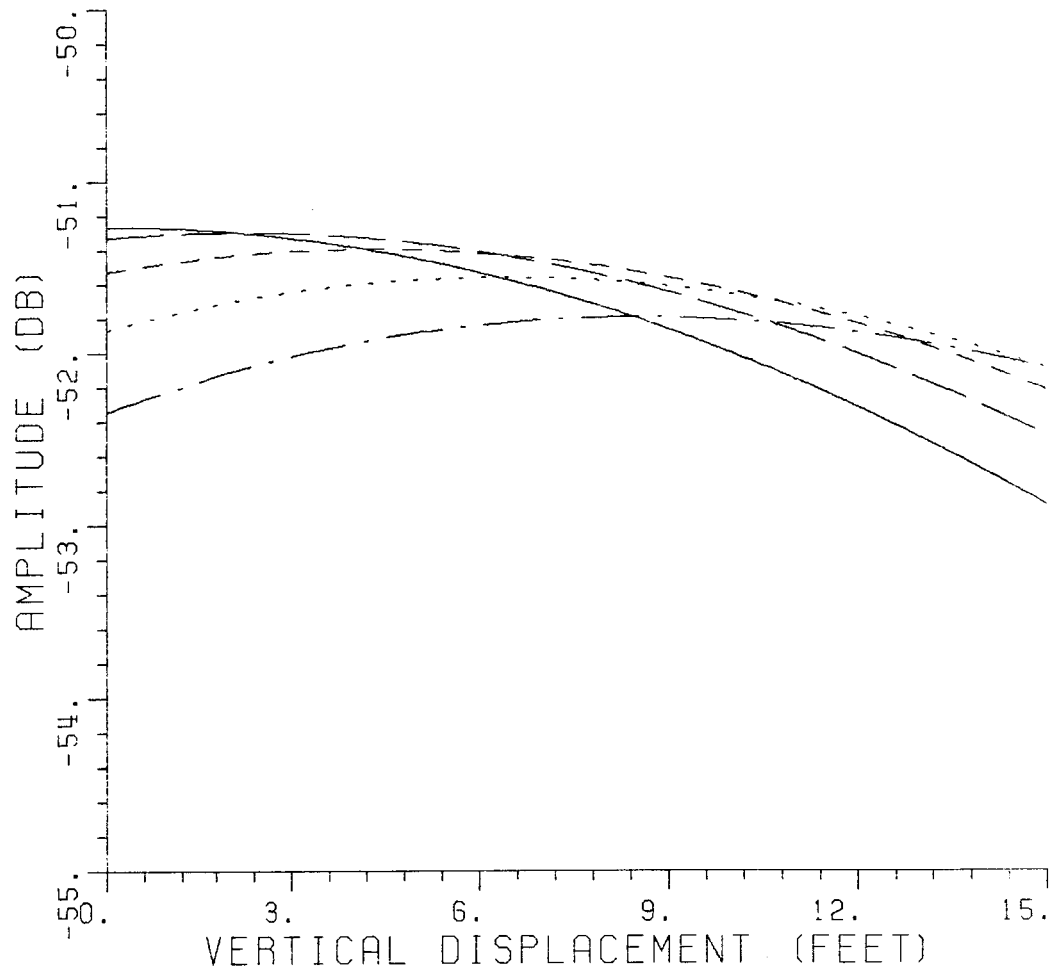


\_\_\_\_\_ specular reflection  
 - - - - - junction diffraction  
 - . - . - skirt diffraction

Figure 15. Specular reflection, junction diffraction, and skirt diffraction versus vertical displacement. YCUT=0, field tilt angle=0°.

From the plots in Figure 14, one observes that the scattered field magnitude decreases with an increase in the vertical displacement. The drop in the scattered field is approximately 1.6 dB, which may not meet the specifications for RCS measurements. The drop in the scattered field is due to the taper in the specularly reflected field. This taper results because of the following factors: A Huygen source with no tilt has its pattern maximum at the vertex of the reflector. Its field drops as one moves away from the vertex of the reflector. Second, the distance between the point of reflection and the feed increases with an increase in the vertical displacement. Thus, the incident field on the reflector decreases with an increase in the vertical displacement. The decrease in the incident field results in a taper in the reflected field. One way to decrease the field taper is to tilt the feed such that its pattern maximum is near the upper edge of the paraboloid (vertical displacement equal to 15 feet). In this case, the drop in the incident field near the reflector edge due to the increase in the distance from the feed will be compensated by the increase in the radiation intensity. Thus, the specular reflected field will be more uniform. The feed should be tilted such that the reflected field is maximum near the center of the target zone and tapers off on either side of the center of the target zone.

Figure 16 shows the specularly reflected component of the scattered field in the vertical cut for various feed tilt angles. Note that initially the taper in the reflected field decreases with an increase in the feed tilt angle. After a certain value of the feed tilt angle the



\_\_\_\_\_ 0° feed tilt angle  
 \_\_\_\_\_ 10° feed tilt angle  
 \_\_\_\_\_ 20° feed tilt angle  
 - - - - - 30° feed tilt angle  
 - . - . - . 40° feed tilt angle

Figure 16. Specular reflection versus vertical displacement for various feed tilt angles. YCUT=0.

taper again starts increasing. Now, the reflected field increases with an increase in the vertical displacement. For feed tilt angles of  $20^\circ$  and  $30^\circ$ , the reflected field is maximum for vertical displacements between 6 and 8 feet and the maximum taper in the field is less than 0.8 dB. Thus, one should choose the feed tilt angle in this range. A typical input data set used to obtain the plots in Figure 16 is given below.

```
INPUT THE FREQUENCY OF OPERATION IN GHz
2.
INPUT THE FOCAL LENGTH OF THE REFLECTOR IN FEET
24.
INPUT THE RADIUS OF THE PARABOLIC SECTION IN FEET
15.
IS THERE A ROLLED EDGE ON TOP? IF YES, TYPE 1
1
IS THERE A SKIRT AT THE BOTTOM? IF YES, TYPE 1
1
IS THE FEED TO BE SIMULATED? IF YES, TYPE 1
1
INPUT THE MAGNITUDE OF THE MAGNETIC DIPOLES ALONG X AND Y AXES.
0.,1.
INPUT THE MAGNITUDE OF THE ELECTRIC DIPOLES ALONG X AND Y AXES.
1.,0.
INPUT THE FEED TILT ANGLE IN DEGREES
20.
INPUT THE TYPE OF CUT(IFCUT) ALONG WHICH PROBED NEAR FIELD DATA IS TO
BE COMPUTED
2
INPUT Y-CUT (feet) FOR THE FIELD CUT
0.
INPUT THE DISTANCE OF THE FIELD CUT FROM THE VERTEX OF THE REFLECTOR IN
FEET
36.
INPUT THE START POINT AND END POINT FOR FIELD PROBING
0.,15.
INPUT THE DISTANCE BETWEEN FIELD POINTS IN FEET
0.1
DO YOU WANT GO TERM? IF YES, TYPE 1
1
DO YOU WANT JUNCTION DIFFRACTION? IF YES, TYPE 1
0
```

DO YOU WANT SKIRT DIFFRACTION? IF YES, TYPE 1  
0  
DO YOU WANT FEED BLOCKAGE? IF YES, TYPE 1  
0  
DO YOU WANT FEED SPILLOVER? IF YES, TYPE 1  
0  
DO YOU WANT DIFFRACTION FROM THE MECHANICAL DISCONTINUITY?  
IF YES, TYPE 1  
0  
DO YOU WANT ELECTRIC FIELD AS THE OUTPUT? IF YES, TYPE 1  
1

Another parameter which is affected by the feed tilt angle is the cross-polarization which is studied next to select the proper feed tilt angle. Since the cross-polarization is zero in the vertical cut (YCUT=0), a horizontal cut at the center of the target zone<sup>†</sup> (XCUT=8.5 feet) is chosen to study the effect of feed tilt angle on cross-polarization. Figures 17-20 show the copolarized and cross-polarized component of the specularly reflected field in the horizontal cut versus horizontal displacement for various feed tilt angles. All other parameters are the same as before. A typical input data set used to generate these plots is as follows:

INPUT THE FREQUENCY OF OPERATION IN GHz  
2.  
INPUT THE FOCAL LENGTH OF THE REFLECTOR IN FEET  
24.  
INPUT THE RADIUS OF THE PARABOLIC SECTION IN FEET  
15.  
IS THERE A ROLLED EDGE ON TOP? IF YES, TYPE 1  
1  
IS THERE A SKIRT AT THE BOTTOM? IF YES, TYPE 1  
1

---

<sup>†</sup> The center is chosen to be the mid point between 3.5 feet and 13.5 feet.

IS THE FEED TO BE SIMULATED? IF YES, TYPE 1  
 1  
 INPUT THE MAGNITUDE OF THE MAGNETIC DIPOLES ALONG X AND Y AXES.  
 0.,1.  
 INPUT THE MAGNITUDE OF THE ELECTRIC DIPOLES ALONG X AND Y AXES.  
 1.,0.  
 INPUT THE FEED TILT ANGLE IN DEGREES  
 30.  
 INPUT THE TYPE OF CUT(IFCUT) ALONG WHICH PROBED NEAR FIELD DATA IS TO  
 BE COMPUTED  
 3  
 INPUT X-CUT (feet) FOR THE FIELD CUT  
 8.5  
 INPUT THE DISTANCE OF THE FIELD CUT FROM THE VERTEX OF THE REFLECTOR IN  
 FEET  
 36.  
 INPUT THE START POINT AND END POINT FOR FIELD PROBING  
 0.,15.  
 INPUT THE DISTANCE BETWEEN FIELD POINTS IN FEET  
 0.1  
 DO YOU WANT GO TERM? IF YES, TYPE 1  
 1  
 DO YOU WANT JUNCTION DIFFRACTION? IF YES, TYPE 1  
 0  
 DO YOU WANT SKIRT DIFFRACTION? IF YES, TYPE 1  
 0  
 DO YOU WANT FEED BLOCKAGE? IF YES, TYPE 1  
 0  
 DO YOU WANT FEED SPILLOVER? IF YES, TYPE 1  
 0  
 DO YOU WANT DIFFRACTION FROM THE MECHANICAL DISCONTINUITY? IF YES,  
 TYPE 1  
 0  
 DO YOU WANT ELECTRIC FIELD AS THE OUTPUT? IF YES, TYPE 1  
 1

From the plots in Figures 17-20, it is clear that the cross-polarized component of the scattered field increases with an increase in the feed tilt angle. Even for feed tilt angles as small as 5°, the cross-polarized component is within 40 dB of the copolarized component. Thus, the feed tilt angle should be kept as small as possible. On the other hand, one needs to tilt the feed to control the

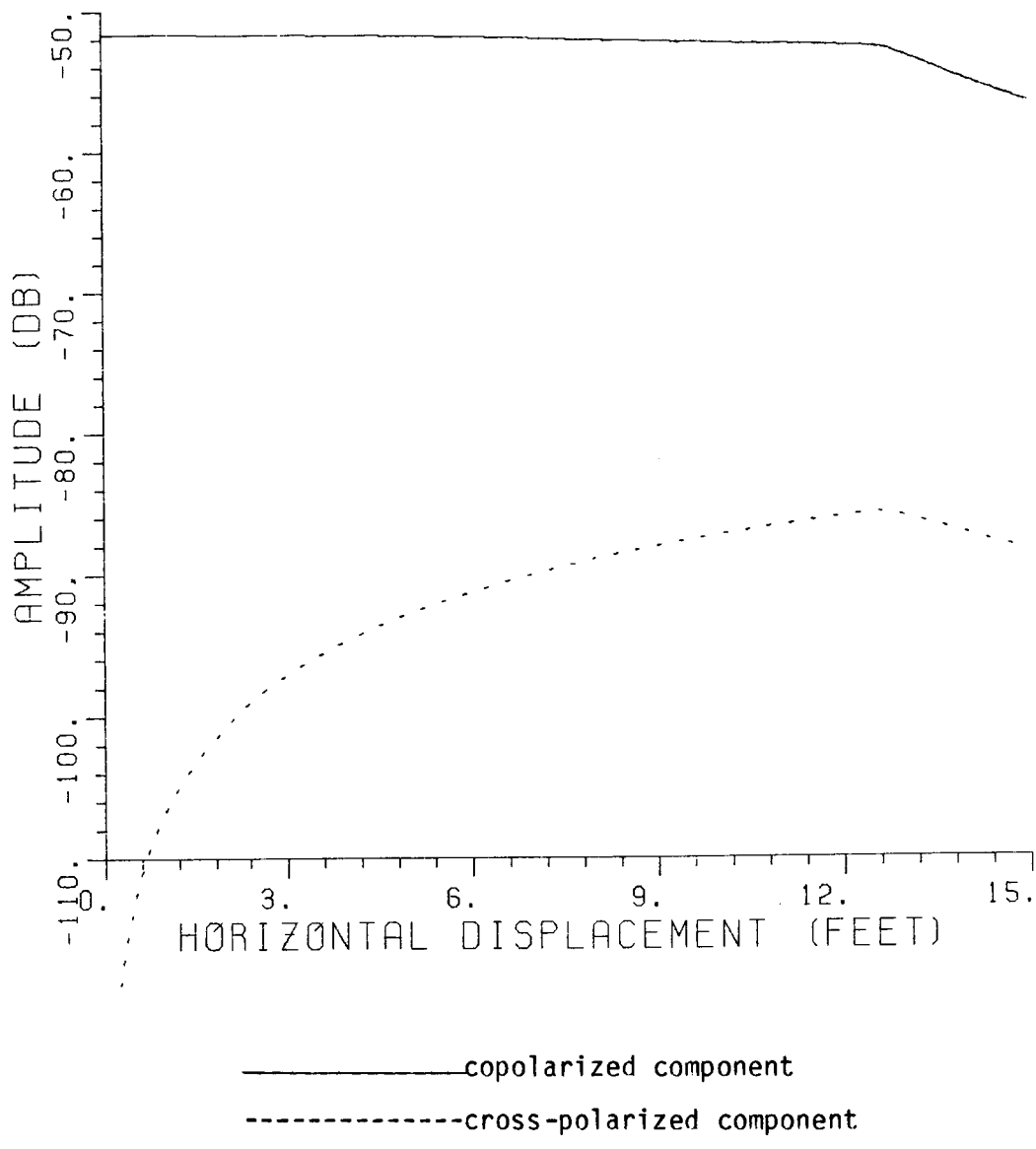


Figure 17. Specular reflection versus horizontal displacement. XCUT=8.5 feet, feed tilt angle=5°.

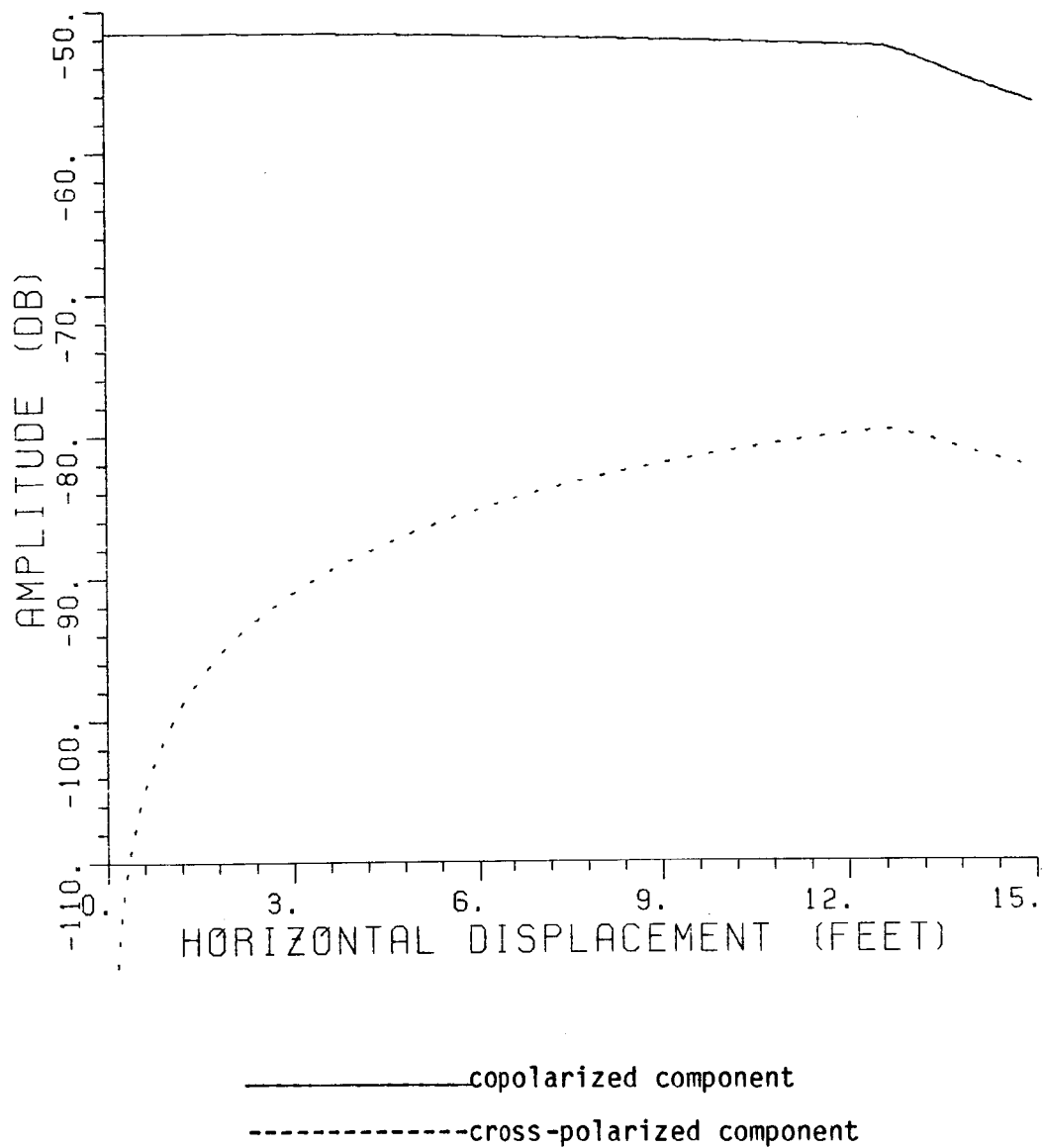


Figure 18. Specular reflection versus horizontal displacement.  
 XCUT=8.5 feet, feed tilt angle=10°.

ORIGINAL PAGE IS  
OF POOR QUALITY

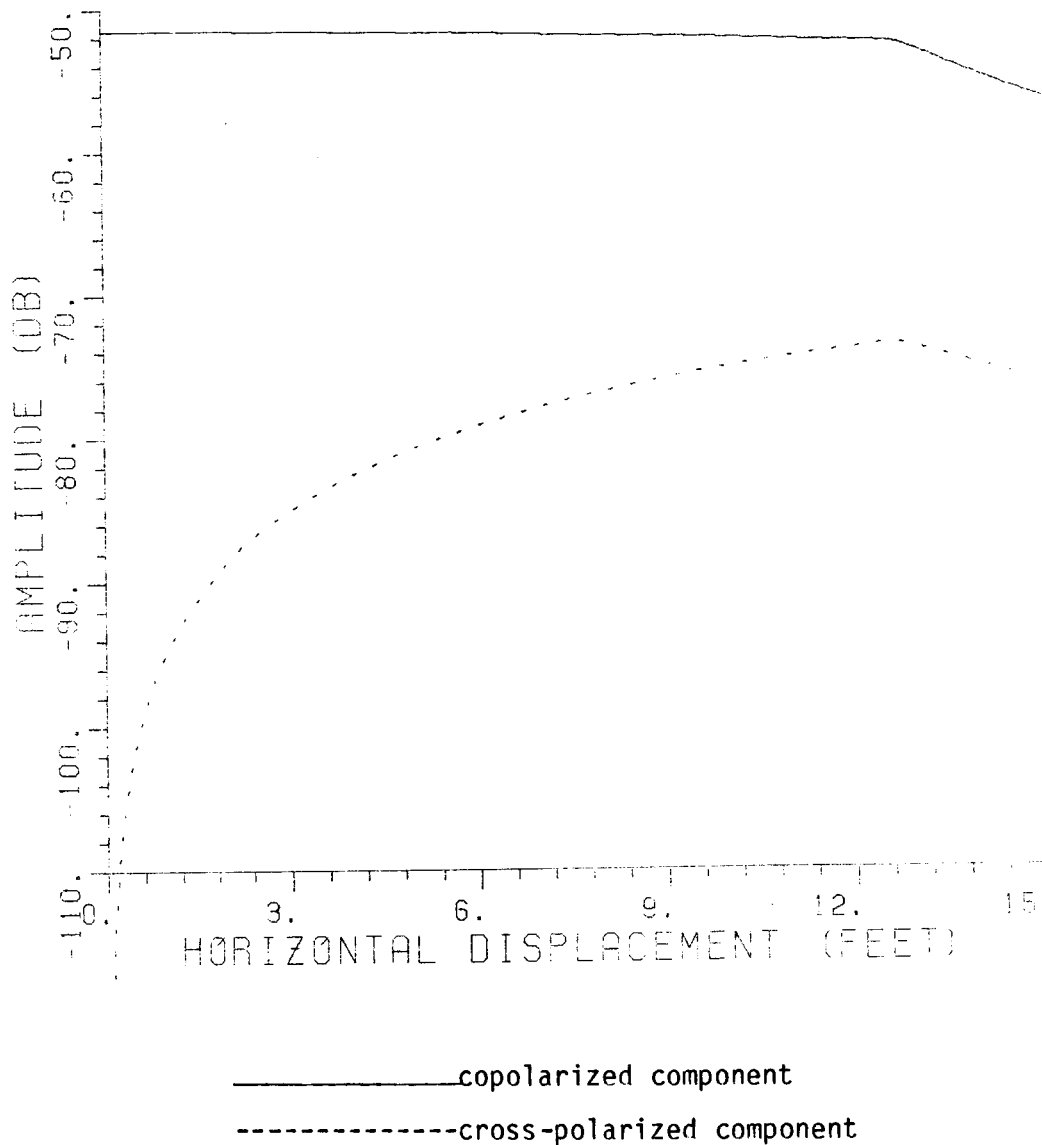
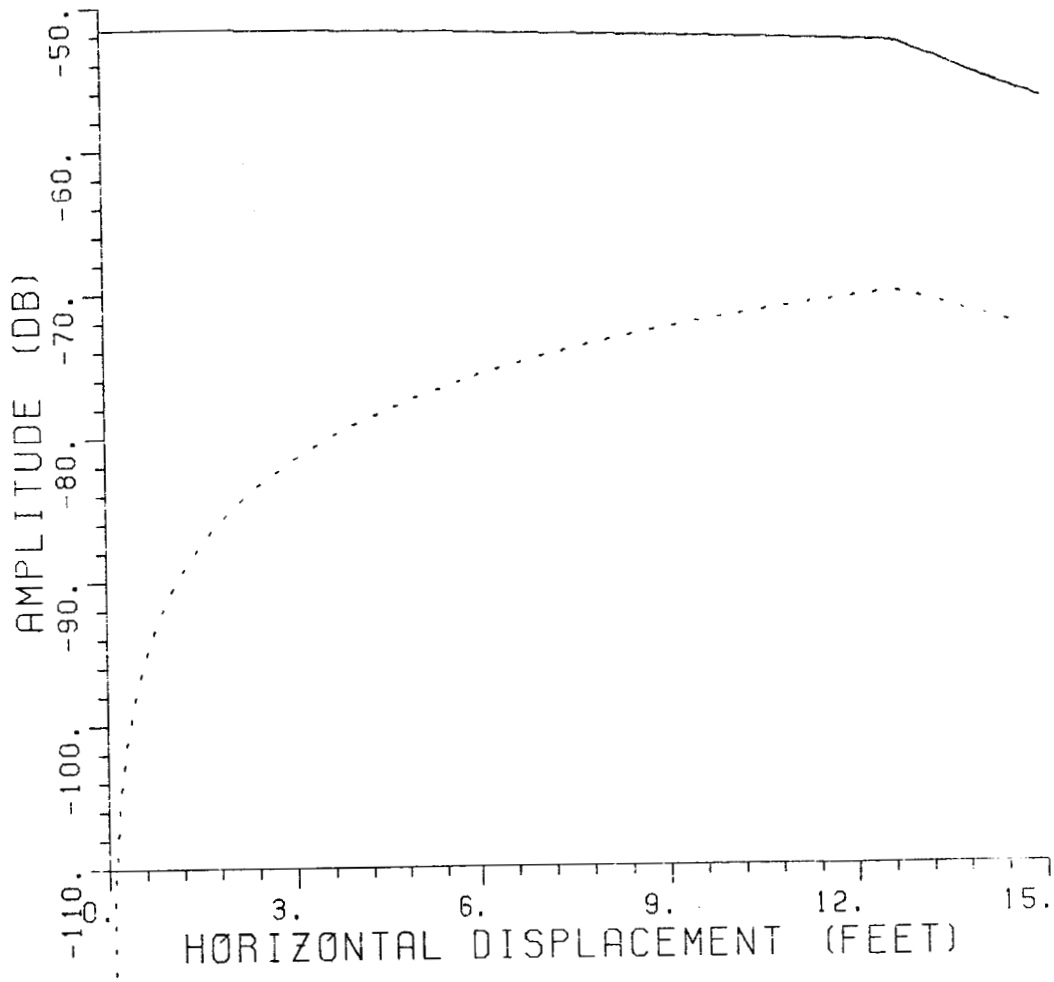


Figure 19. Specular reflection versus horizontal displacement.  
XCUT=8.5 feet, feed tilt angle=20°.



\_\_\_\_\_ copolarized component  
 - - - - - cross-polarized component

Figure 20. Specular reflection versus horizontal displacement.  
 XCUT=8.5 feet, feed tilt angle=30°.

taper in the scattered field. Thus, the tilt angle of the feed is an important parameter and should be carefully selected. In the rest of the study, a feed tilt angle of  $20^\circ$  will be used. For this tilt angle the taper in the scattered field is less than 0.8 dB and the cross-polarized scattered fields are 20 dB below the copolarized scattered fields. In Figures 17-20, the drop in the reflected field amplitude for large (more than 12.4 feet) horizontal displacements is due to the reason that the field point is outside the sweet region, and thus, the reflected field emanates from the rolled edge.

In the above discussion, the feed blockage was not included in the scattered field computation. The feed blockage also affects the field in the target zone. Therefore, to complete the discussion, the feed blockage is computed next.

Figure 21 shows the scattered electric field due to the feed blockage in the vertical cut ( $YCUT=0$ ) for various size feed apertures versus vertical displacement. The feed aperture is assumed to be a flat square plate. The feed is a Huygen source tilted at  $20^\circ$ . Since in this cut the cross-polarization is zero, only the copolarized scattered field is plotted. A typical input data set used to obtain the plots in Figure 21 is given below:

INPUT THE FREQUENCY OF OPERATION IN GHz  
 2.  
 INPUT THE FOCAL LENGTH OF THE REFLECTOR IN FEET  
 24.  
 INPUT THE RADIUS OF THE PARABOLIC SECTION IN FEET  
 15.  
 IS THERE A ROLLED EDGE ON TOP? IF YES, TYPE 1  
 1  
 IS THERE A SKIRT AT THE BOTTOM? IF YES, TYPE 1  
 1  
 IS THE FEED TO BE SIMULATED? IF YES, TYPE 1  
 1  
 INPUT THE MAGNITUDE OF THE MAGNETIC DIPOLES ALONG X AND Y AXES.  
 0.,1.  
 INPUT THE MAGNITUDE OF THE ELECTRIC DIPOLES ALONG X AND Y AXES.  
 1.,0.  
 INPUT THE FEED TILT ANGLE IN DEGREES  
 20.  
 INPUT THE TYPE OF CUT(IFCUT) ALONG WHICH PROBED NERAR FIELD DATA IS TO  
 BE COMPUTED  
 2  
 INPUT Y-CUT (feet) FOR THE FIELD CUT  
 0.  
 INPUT THE DISTANCE OF THE FIELD CUT FROM THE VERTEX OF THE REFLECTOR IN  
 FEET  
 36.  
 INPUT THE START POINT AND END POINT FOR FIELD PROBING  
 0.,15.  
 INPUT THE DISTANCE BETWEEN FIELD POINTS IN FEET  
 0.1  
 DO YOU WANT GO TERM? IF YES, TYPE 1  
 1  
 DO YOU WANT JUNCTION DIFFRACTION? IF YES, TYPE 1  
 0  
 DO YOU WANT SKIRT DIFFRACTION? IF YES, TYPE 1  
 0  
 DO YOU WANT FEED BLOCKAGE? IF YES, TYPE 1  
 1  
 INPUT THE Z LOCATION OF THE FEED STRUCTURE IN FEET  
 24.  
 INPUT THE NUMBER OF CORNERS IN THE FLAT PLATE USED TO SIMULATE THE FEED  
 STRUCTURE  
 4  
 INPUT THE COORDINATES (IN INCHES) OF THE CORNERS OF THE PLATE  
 6.,6.,-6.,6.,-6.,-6.,6.,-6.  
 DO YOU WANT FEED SPILLOVER? IF YES, TYPE 1  
 0

DO YOU WANT DIFFRACTION FROM THE MECHANICAL DISCONTINUITY? IF YES,  
TYPE 1

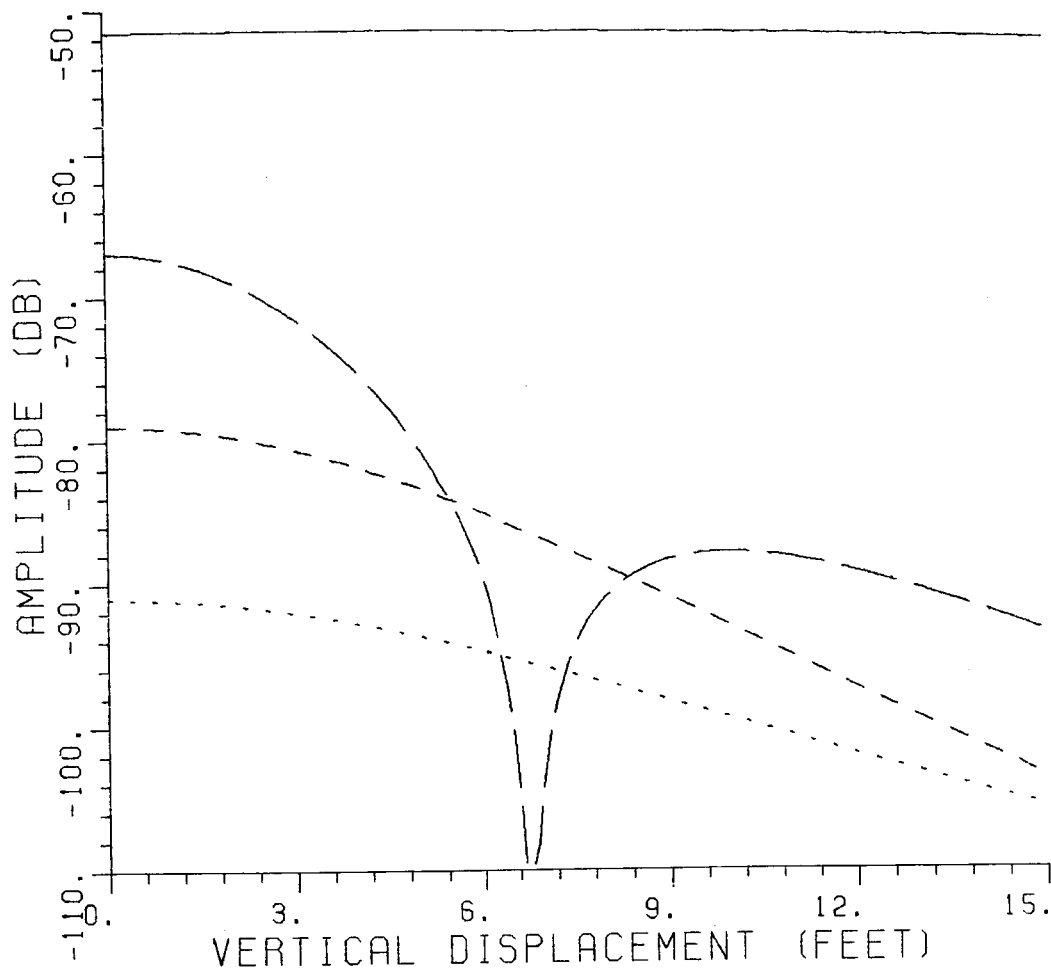
0

DO YOU WANT ELECTRIC FIELD AS THE OUTPUT? IF YES, TYPE 1

1

The specular reflected field is also shown in the figure.

Comparing the feed blockage with the specularly reflected field, one can see that for 12" x 12" ( $2\lambda \times 2\lambda$ ) feed aperture, the scattered field due to aperture blockage is quite large (within 15 dB of the specular reflection). Thus, these scattered fields will cause large oscillations in the fields in the target zone. The scattered field due to aperture blockage decreases with the size of the feed aperture. For 6" x 6" feed aperture, the scattered fields are within 26 dB of the specular reflection. Thus, if one requires the feed blockage to be at least 35 dB below the reflected field (to keep the ripple size below 0.2 dB), the feed aperture should be less than 6" x 6". Therefore, in the rest of the study, the feed aperture is chosen to be 3" x 3" ( $\frac{\lambda}{2} \times \frac{\lambda}{2}$ ). For this feed aperture size, the feed blockage in the sweet region is at least 40 dB below the reflected field. Thus, the ripple size of the oscillations due to aperture blockage will be less than 0.2 dB. The same can be seen in Figure 22, where the vector sum of the specular reflection and feed blockage is plotted for various vertical displacement in the vertical cut. The specular reflection alone is also shown in the figure. Note that the ripple size of oscillations in the total field is quite small (less than 0.2 dB) for all values of the vertical displacement. Next, the useable target zone for the reflector system is computed when the



\_\_\_\_\_ specular reflection  
 \_\_\_\_\_ 12" x 12" plate  
 \_\_\_\_\_ 6" x 6" plate  
 \_\_\_\_\_ 3" x 3" plate

Figure 21. Feed blockage versus vertical displacement for various size feed aperture.  $Y_{CUT}=0.$ , feed tilt angle= $20^\circ$ .

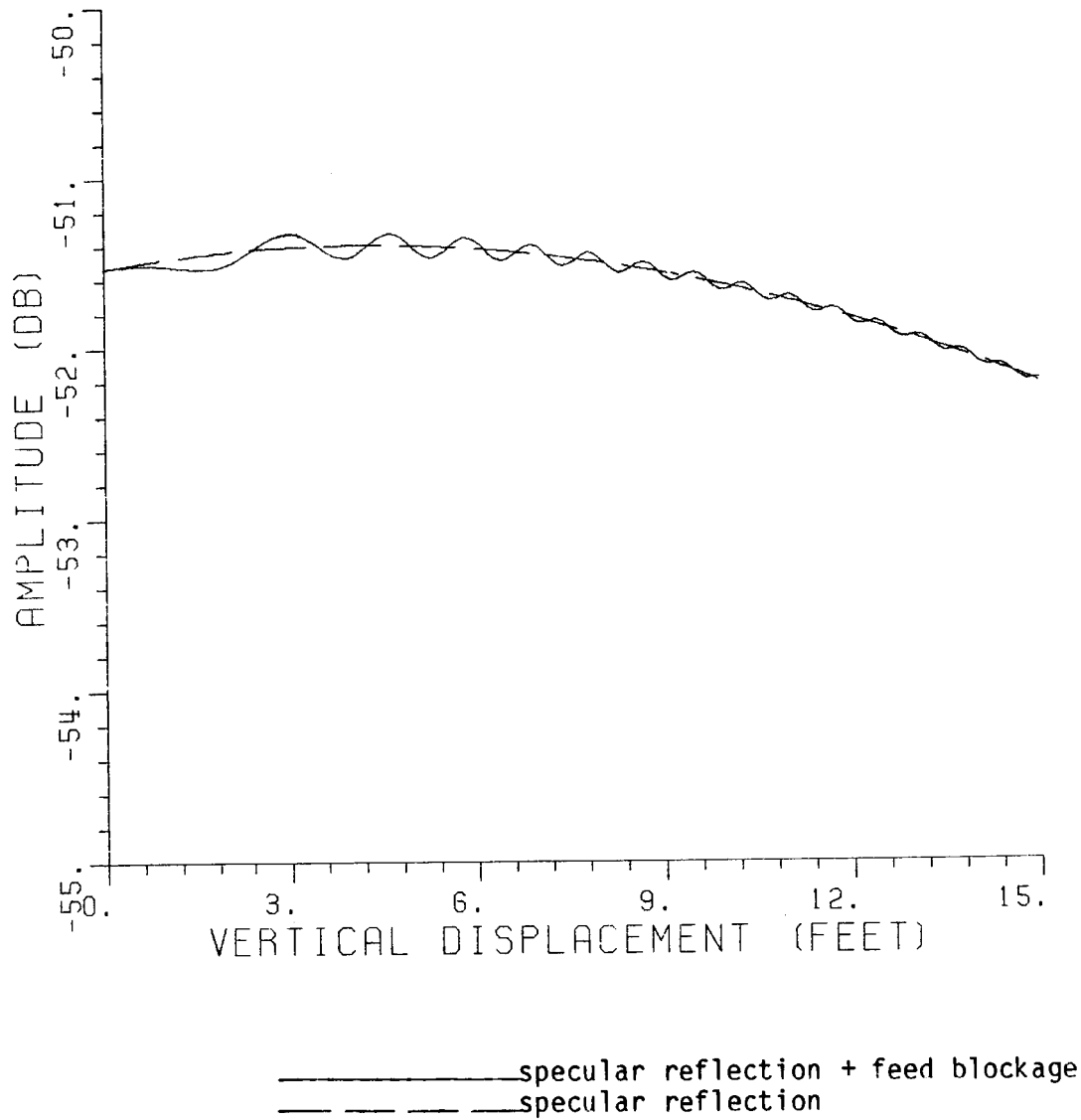


Figure 22. Scattered field versus vertical displacement.  $Y_{CUT}=0$ , feed tilt angle =  $20^\circ$ , feed aperture = 3" x 3".

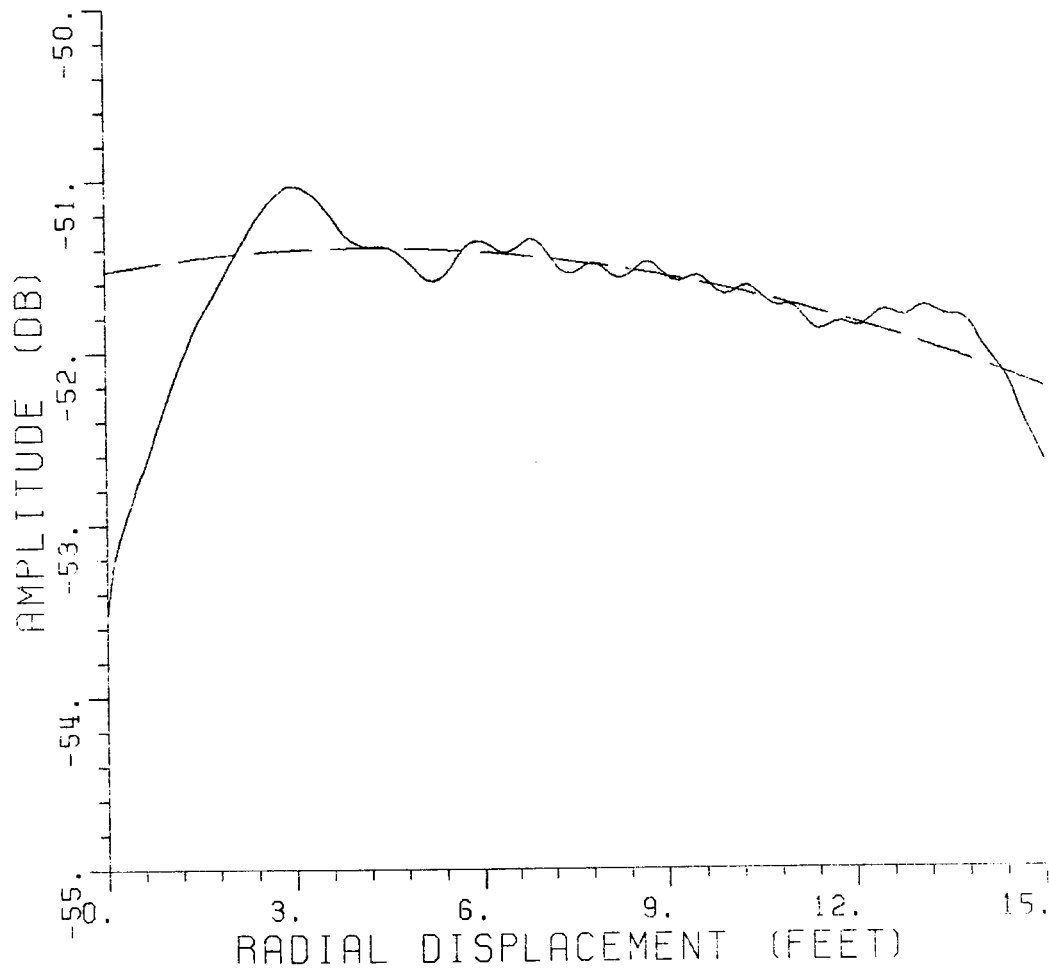
ripple requirement is 0.2 dB. To compute the useable target zone, the total scattered field is calculated along various radial cuts. Only positive values of  $\phi$  are considered. For the negative values of  $\phi$ , the performance will be the same as for the corresponding positive values of  $\phi$ .

Figure 23 shows the scattered electric field along  $0^\circ$  radial cut ( $\phi=0^\circ$ ). Various mechanisms included in the field computation are: specular reflection, junction diffraction, skirt diffraction and aperture blockage. The feed is a Huygen source tilted by  $20^\circ$ . The feed aperture is assumed to be a 3" x 3" flat plate. Since the cross-polarization is zero in this cut, only the copolarized component of the scattered field is plotted. The specular reflection term alone is also plotted in the figure (dashed curve). Note that for radial displacements between 3.5 feet and 13 feet, the taper in the reflected field is less than 0.5 dB, and in this region, the ripple size of the oscillations in the total field is less than 0.2 dB. Thus, the reflector provides a large useable target area in the vertical dimension. The input data set used in the example is given below.

```
INPUT THE FREQUENCY OF OPERATION IN GHz
2.
INPUT THE FOCAL LENGTH OF THE REFLECTOR IN FEET
24.
INPUT THE RADIUS OF THE PARABOLIC SECTION IN FEET
15.
IS THERE A ROLLED EDGE ON TOP? IF YES, TYPE 1
1
IS THERE A SKIRT AT THE BOTTOM? IF YES, TYPE 1
1
IS THE FEED TO BE SIMULATED? IF YES, TYPE 1
1
```

INPUT THE MAGNITUDE OF THE MAGNETIC DIPOLES ALONG X AND Y AXES.  
 0.,1.  
 INPUT THE MAGNITUDE OF THE ELECTRIC DIPOLES ALONG X AND Y AXES.  
 1.,0.  
 INPUT THE FEED TILT ANGLE IN DEGREES  
 20.  
 INPUT THE TYPE OF CUT(IFCUT) ALONG WHICH PROBED NEAR FIELD DATA IS TO  
 BE COMPUTED  
 1  
 INPUT PHI (degrees) FOR THE FIELD CUT  
 0.  
 INPUT THE DISTANCE OF THE FIELD CUT FROM THE VERTEX OF THE REFLECTOR IN  
 FEET  
 36.  
 INPUT THE START POINT AND END POINT FOR FIELD PROBING  
 0.,15.  
 INPUT THE DISTANCE BETWEEN FIELD POINTS IN FEET  
 0.1  
 DO YOU WANT GO TERM? IF YES, TYPE 1  
 1  
 DO YOU WANT JUNCTION DIFFRACTION? IF YES, TYPE 1  
 1  
 WILL YOU BE STUDYING THE DIFFRACTION DUE TO MECHANICAL DISCONTINUITY?  
 IF YES, TYPE 1  
 0  
 DO YOU WANT SKIRT DIFFRACTION? IF YES, TYPE 1  
 1  
 DO YOU WANT FEED BLOCKAGE? IF YES, TYPE 1  
 1  
 INPUT THE Z LOCATION OF THE FEED STRUCTURE IN FEET  
 24.  
 INPUT THE NUMBER OF CORNERS IN THE FLAT PLATE USED TO SIMULATE THE  
 FEED STRUCTURE  
 4  
 INPUT THE COORDINATES (IN INCHES) OF THE CORNERS OF THE PLATE  
 1.5,1.5,-1.5,1.5,-1.5,-1.5,1.5,-1.5  
 DO YOU WANT FEED SPILLOVER? IF YES, TYPE 1  
 0  
 DO YOU WANT DIFFRACTION FROM THE MECHANICAL DISCONTINUITY?  
 IF YES, TYPE 1  
 0  
 DO YOU WANT ELECTRIC FIELD AS THE OUTPUT? IF YES, TYPE 1  
 1

Figures 24-28 show the copolarized (x) component of the scattered  
 electric field for radial cuts of 15°, 30°, 45°, 60° and 75°,  
 respectively. All other parameters are the same as before. The



————— total scattered field  
 - - - - - specular reflection

Figure 23. Copolarized (x) component of the scattered field versus radial displacement.  $\phi=0^\circ$ , feed tilt angle= $20^\circ$ , feed aperture = 3" x 3". Various mechanisms included in the field are:

1. specular reflection
2. junction diffraction
3. skirt diffraction
4. feed blockage

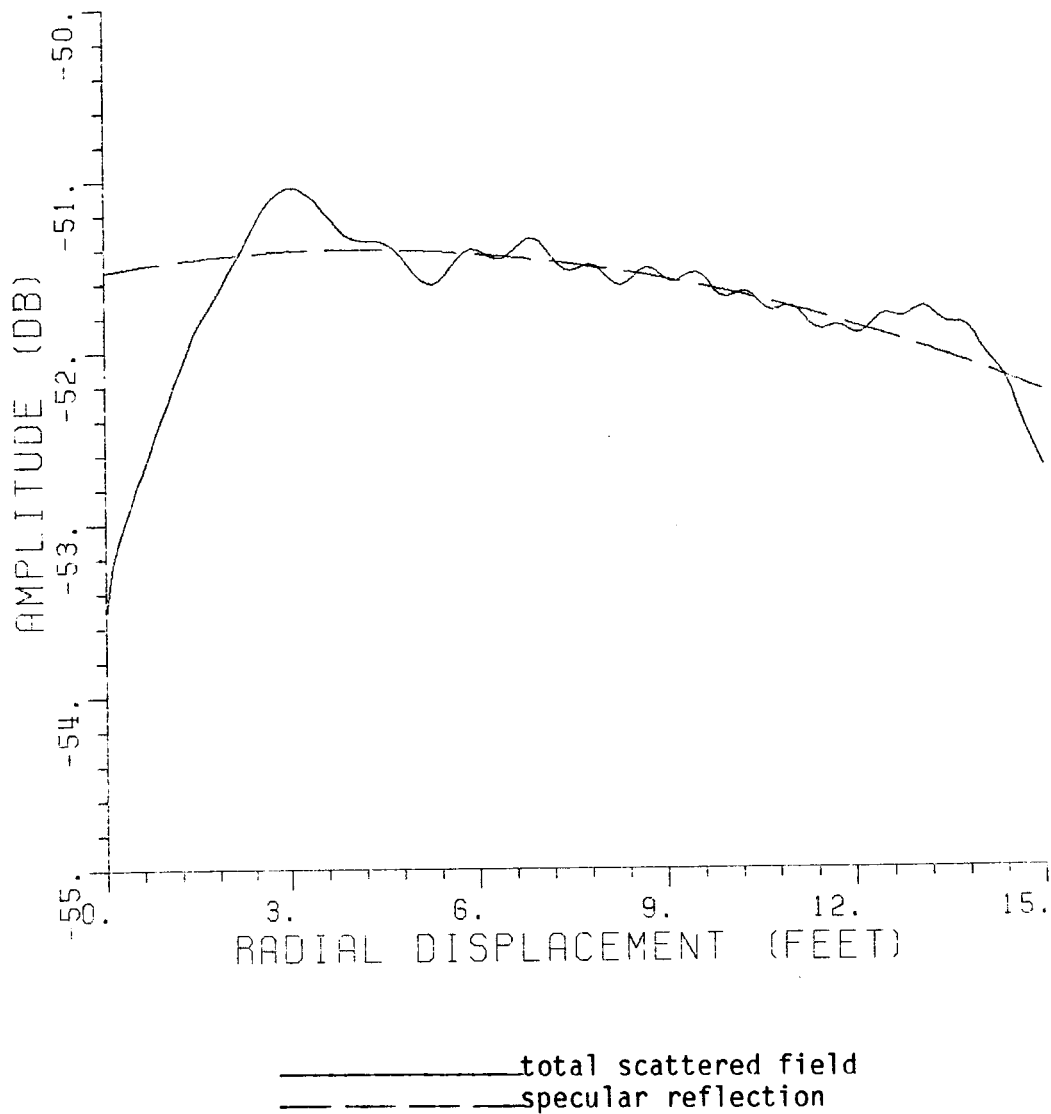


Figure 24. Copolarized (x) component of the scattered field versus radial displacement.  $\phi=15^\circ$ , feed tilt angle= $20^\circ$ , feed aperture = 3" x 3". Various mechanisms included in the field are:

1. specular reflection
2. junction diffraction
3. skirt diffraction
4. feed blockage

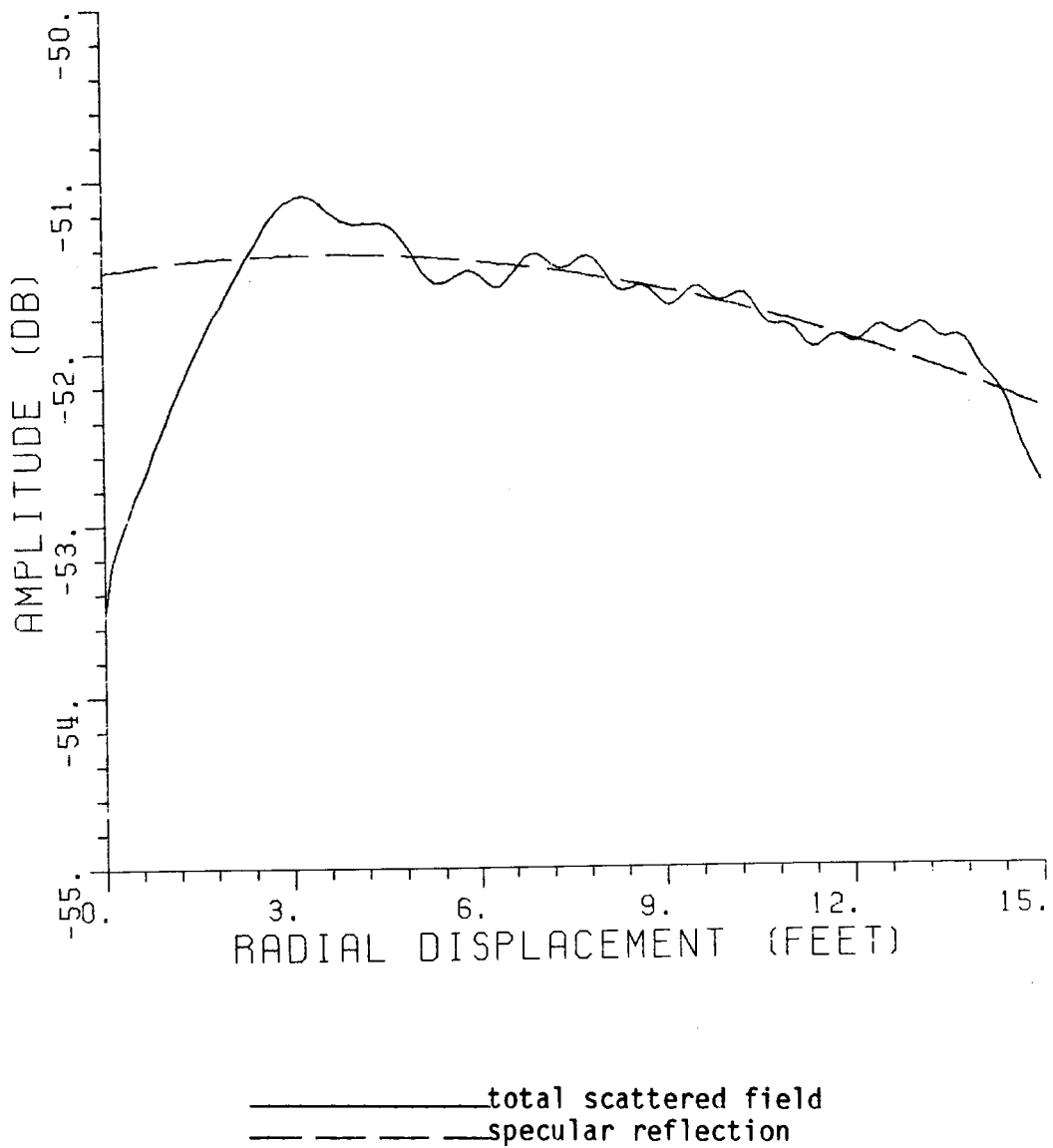


Figure 25. Copolarized (x) component of the scattered field versus radial displacement.  $\phi=30^\circ$ , feed tilt angle= $20^\circ$ , feed aperture = 3" x 3". Various mechanisms included in the field are:

1. specular reflection
2. junction diffraction
3. skirt diffraction
4. feed blockage

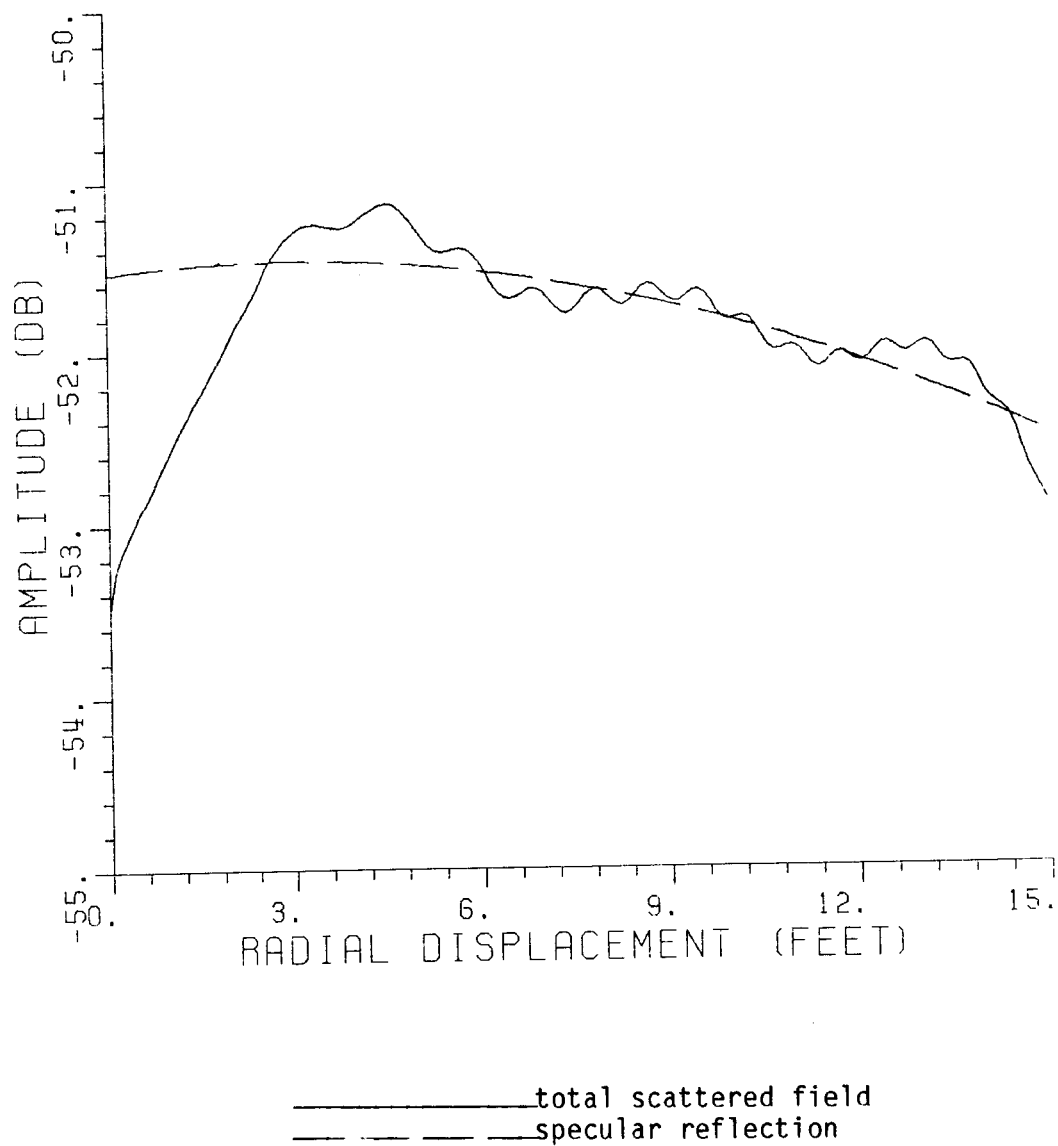


Figure 26. Copolarized (x) component of the scattered field versus radial displacement.  $\phi=45^\circ$ , feed tilt angle= $20^\circ$ , feed aperture = 3" x 3". Various mechanisms included in the field are:

1. specular reflection
2. junction diffraction
3. skirt diffraction
4. feed blockage

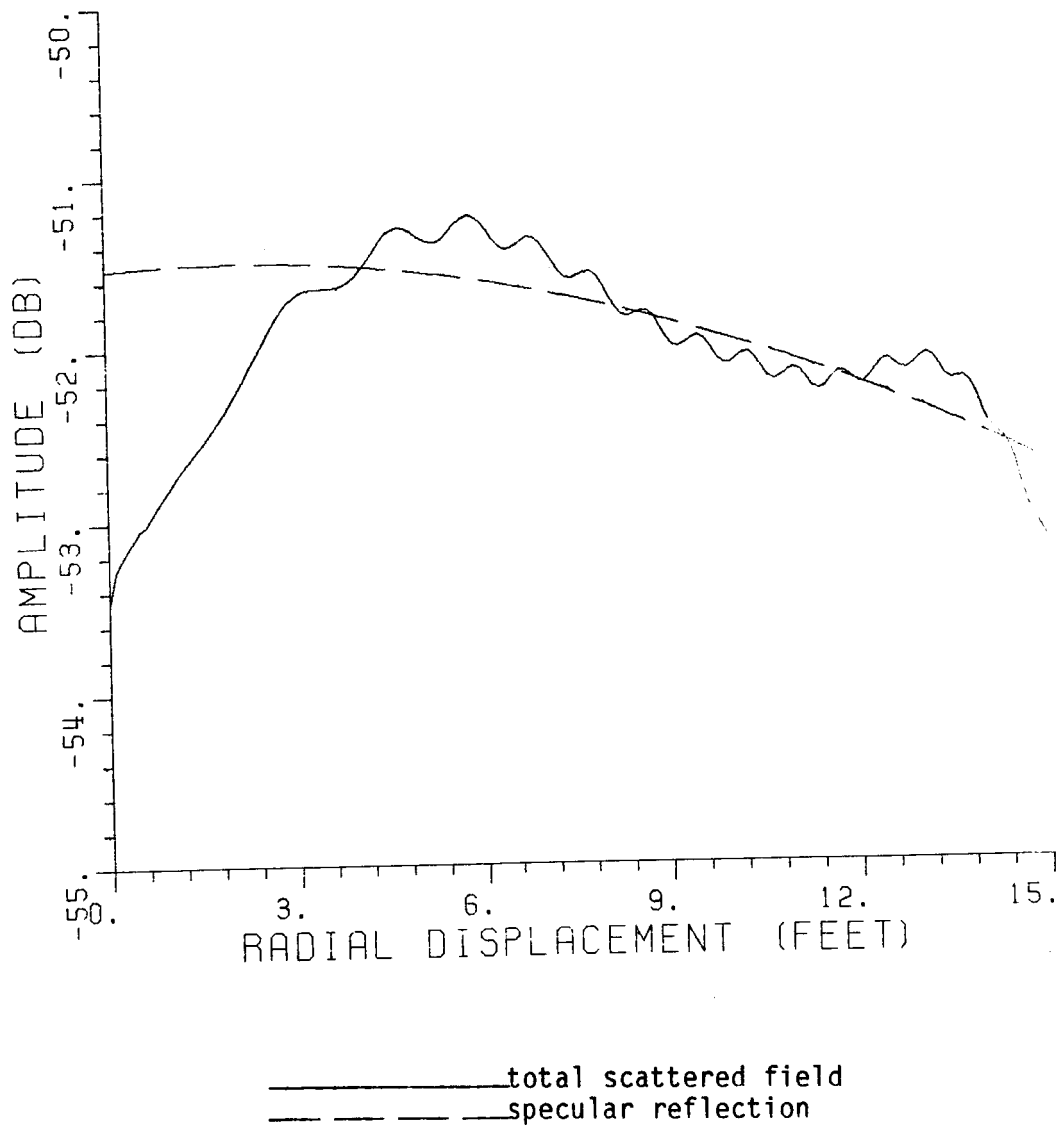
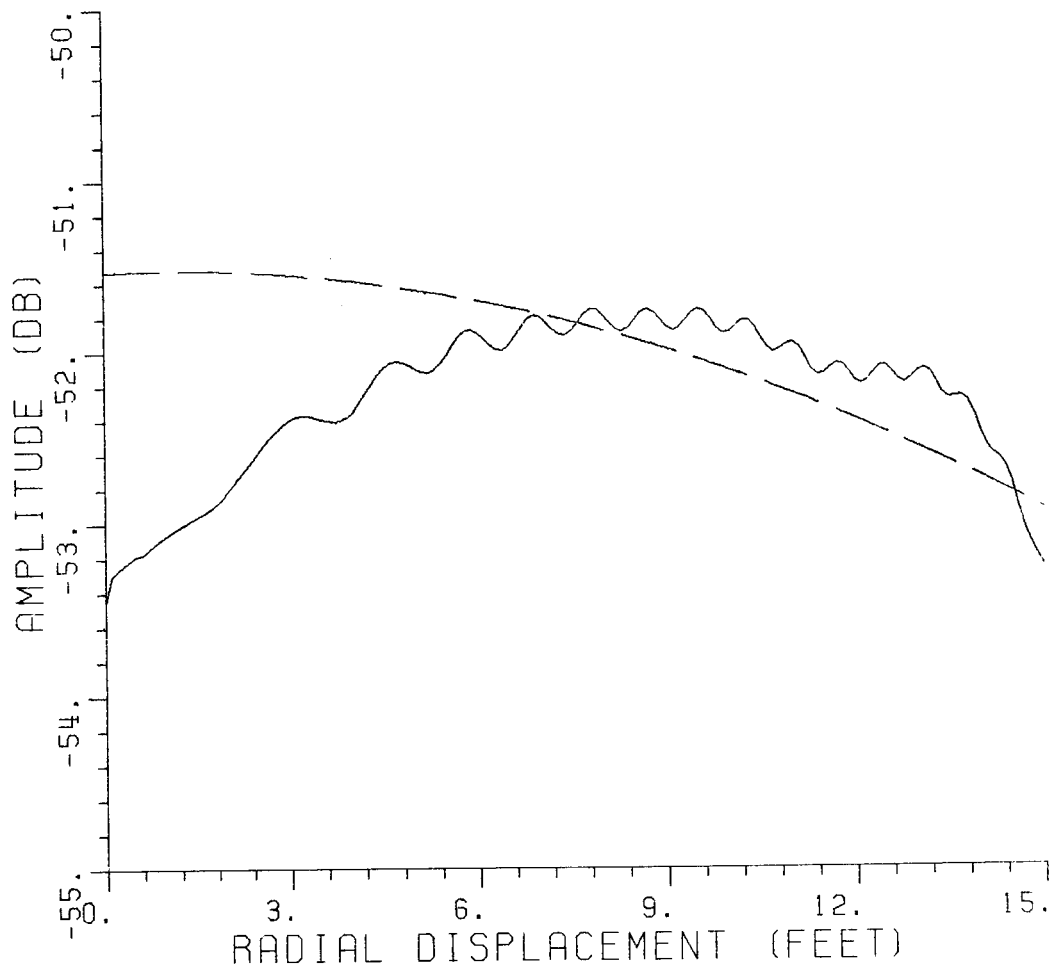


Figure 27. Copolarized (x) component of the scattered field versus radial displacement.  $\phi=60^\circ$ , feed tilt angle= $20^\circ$ , feed aperture = 3" x 3". Various mechanisms included in the field are:

1. specular reflection
2. junction diffraction
3. skirt diffraction
4. feed blockage



—————total scattered field  
 - - - - -specular reflection

Figure 28. Copolarized (x) component of the scattered field versus radial displacement.  $\phi=75^\circ$ , feed tilt angle= $20^\circ$ , feed aperture = 3" x 3". Various mechanisms included in the field are:

1. specular reflection
2. junction diffraction
3. skirt diffraction
4. feed blockage

specularly reflected component is also shown in the figures. An important observation to be made from the plots in Figures 24-28 is that the region in which the ripple size of the oscillations in the total scattered field is less than 0.2 dB decreases with an increase in the radial cut angle ( $\phi$ ). For example, for the 45° radial cut (see Figure 26), the radial displacement for which the ripple size is less than 0.2 dB lies between 5 feet and 13 feet while for the 60° radial cut (see Figure 27), the radial displacements lie between 7.2 feet and 13 feet. For the 0° radial cut, the radial displacement for which the ripple size is less than 0.2 dB lies between 3.5 feet and 13 feet. Thus, the useable target zone near the axis of the reflector has decreased. The reason for this is that as  $\phi$  increases, the observation point moves closer to the skirt of the reflector, and thus the skirt diffraction becomes a dominant component of the fields in the target zone and limits the size of the useable target zone. One can use the data in Figures 23-28 to define the useable target zone which looks as shown in Figure 29. Note that the size of the useable target zone is quite large. From the plots in Figures 23-28, one can see that the taper in the scattered field in the useable target zone defined in Figure 29 is less than 0.8 dB.

Figures 30-34 show the cross-polarization ( $y$ ) along various radial cuts. The specular reflection component of the cross-polarized scattered fields is also shown in the figures. Note that the specular reflection is the main contributor to the cross-polarization. The cross-polarization is at least 22 dB below the copolarization in the useable target zone.

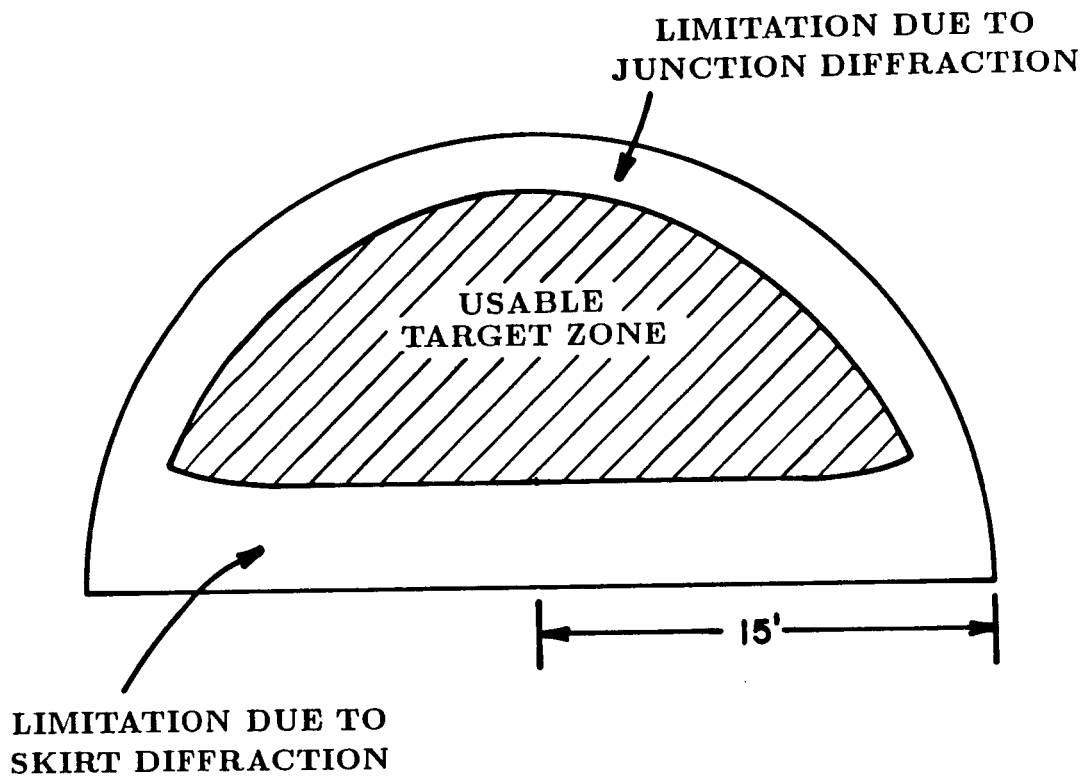


Figure 29. Useable target zone at 2 GHz. Target distance = 36 feet, maximum ripple = 0.2 dB.

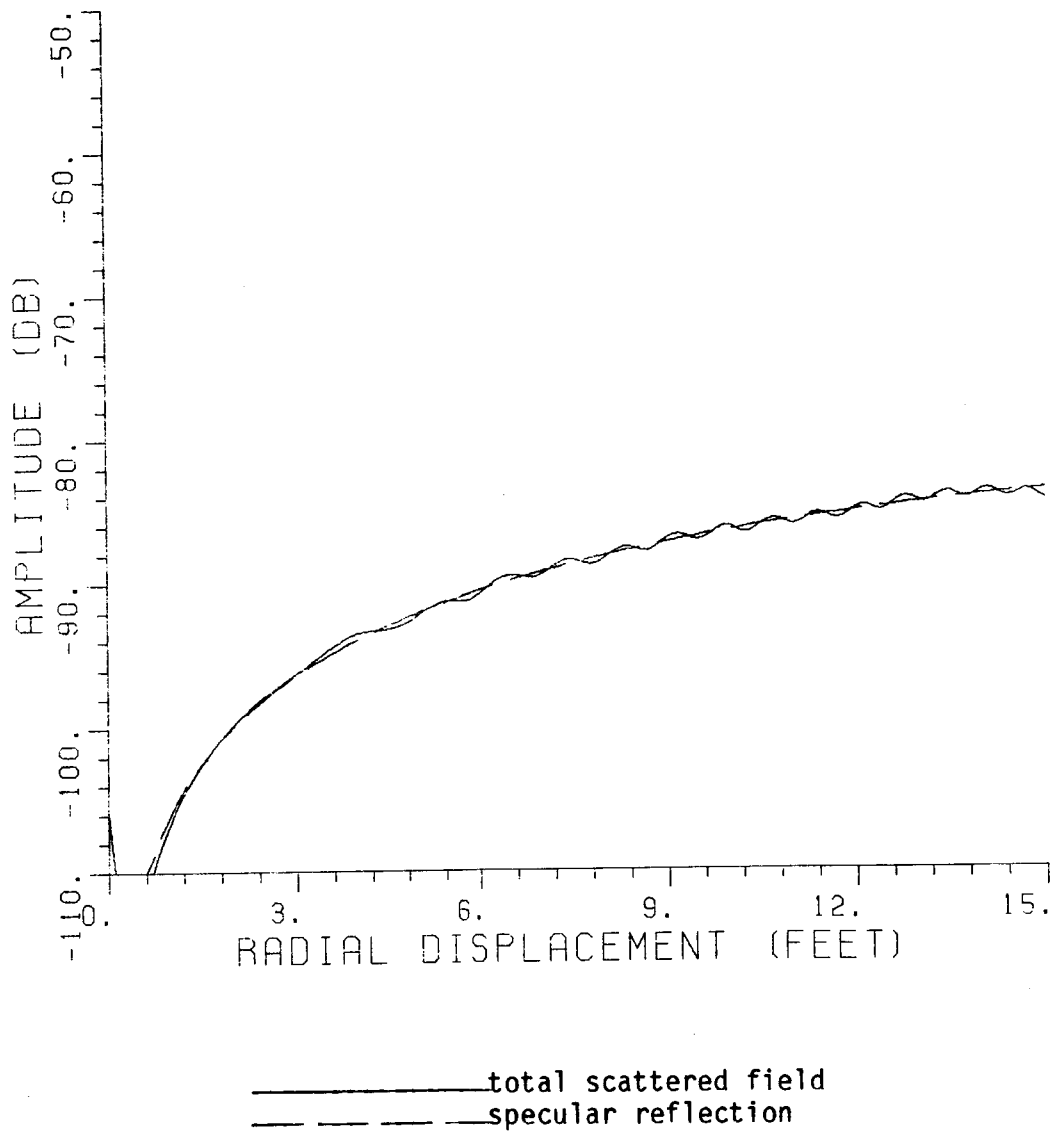


Figure 30. Cross-polarized (y) component of the scattered field versus radial displacement.  $\phi=15^\circ$ . Various mechanisms included in the field computation are:

1. specular reflection
2. junction diffraction
3. skirt diffraction
4. feed blockage

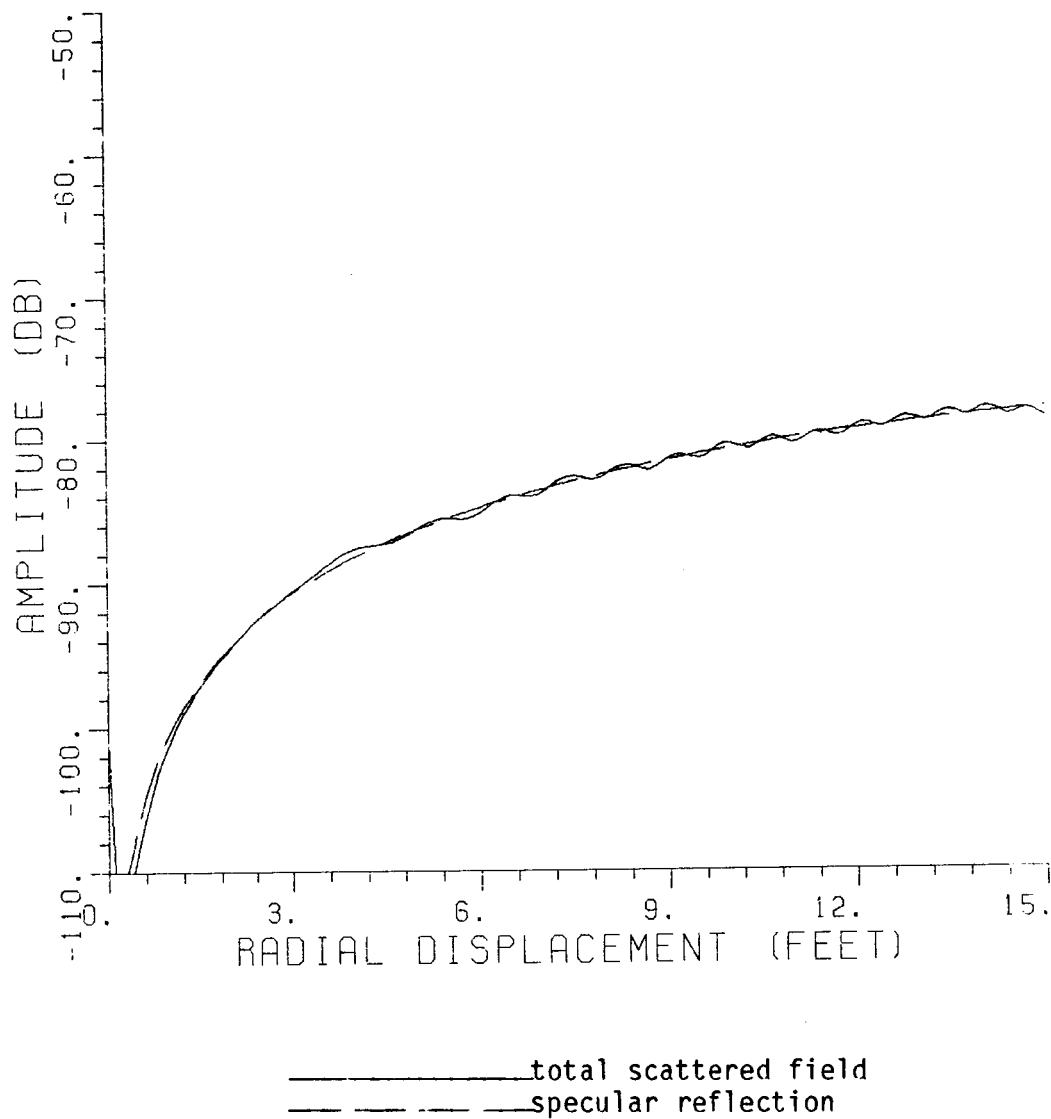


Figure 31. Cross-polarized (y) component of the scattered field versus radial displacement.  $\phi=30^\circ$ . Various mechanisms included in the field computation are:

1. specular reflection
2. junction diffraction
3. skirt diffraction
4. feed blockage

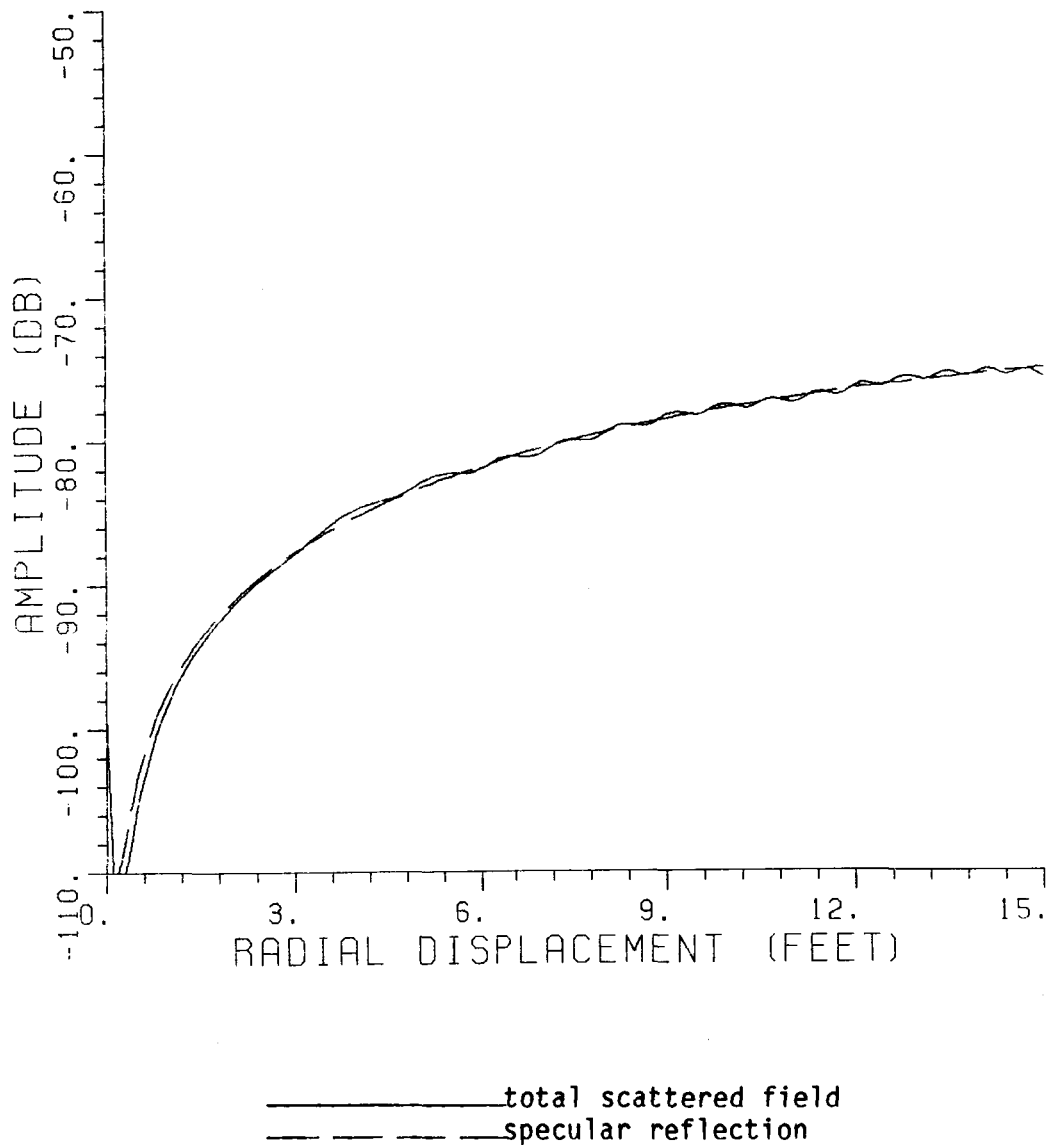


Figure 32. Cross-polarized (y) component of the scattered field versus radial displacement.  $\phi=45^\circ$ . Various mechanisms included in the field computation are:

1. specular reflection
2. junction diffraction
3. skirt diffraction
4. feed blockage

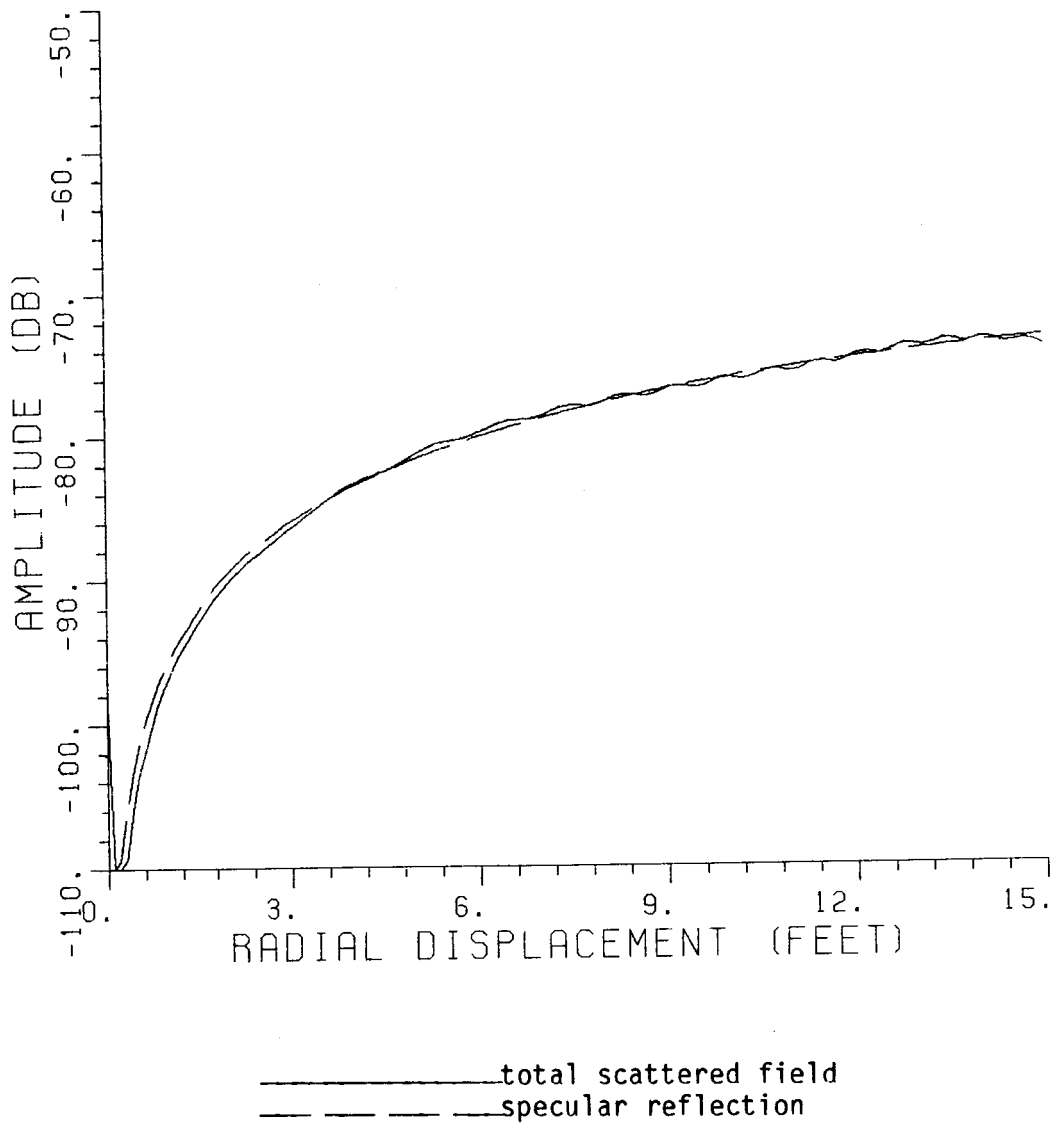


Figure 33. Cross-polarized (y) component of the scattered field versus radial displacement.  $\phi=60^\circ$ . Various mechanisms included in the field computation are:

1. specular reflection
2. junction diffraction
3. skirt diffraction
4. feed blockage

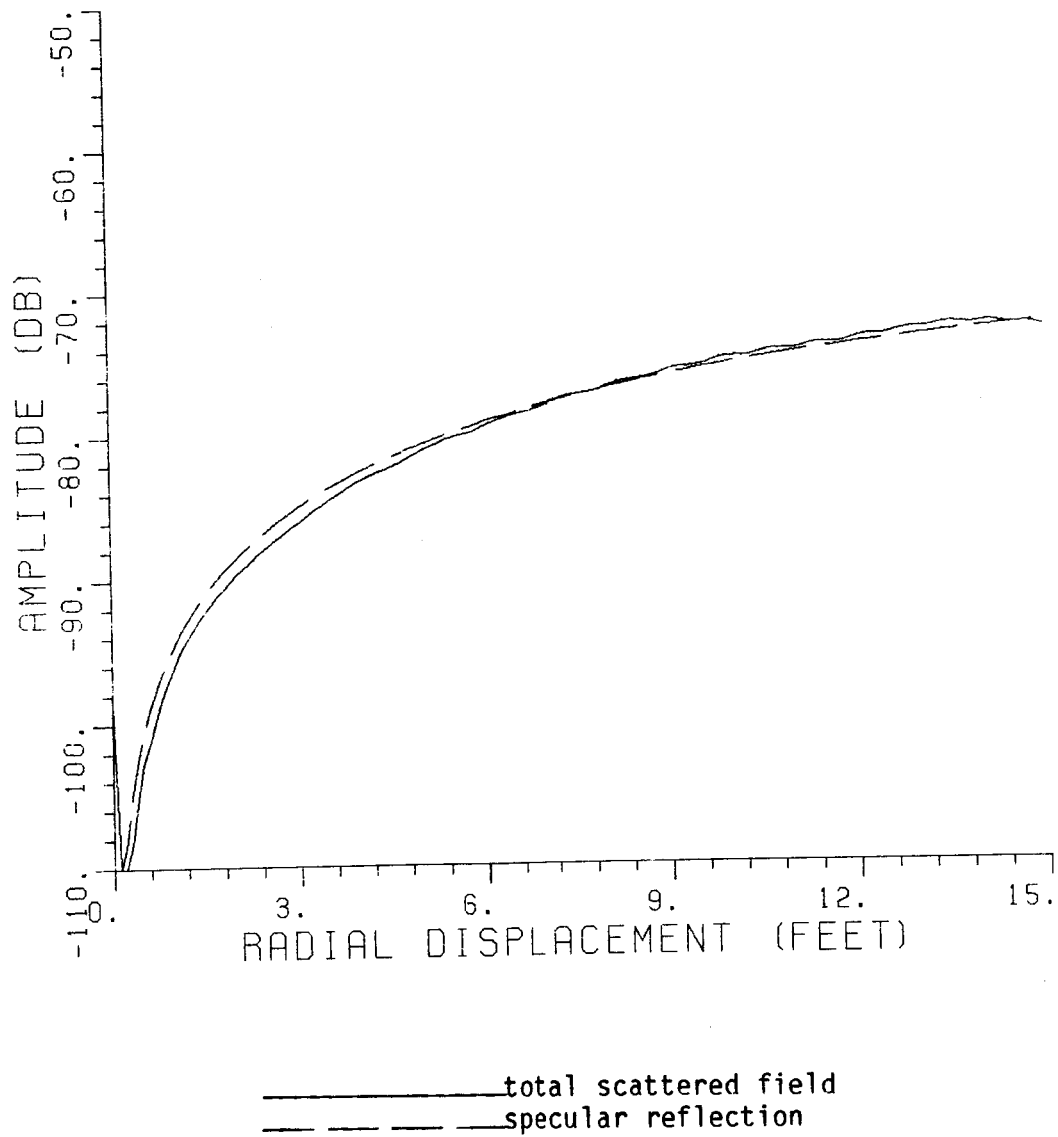


Figure 34. Cross-polarized (y) component of the scattered field versus radial displacement.  $\phi=75^\circ$ . Various mechanisms included in the field computation are:

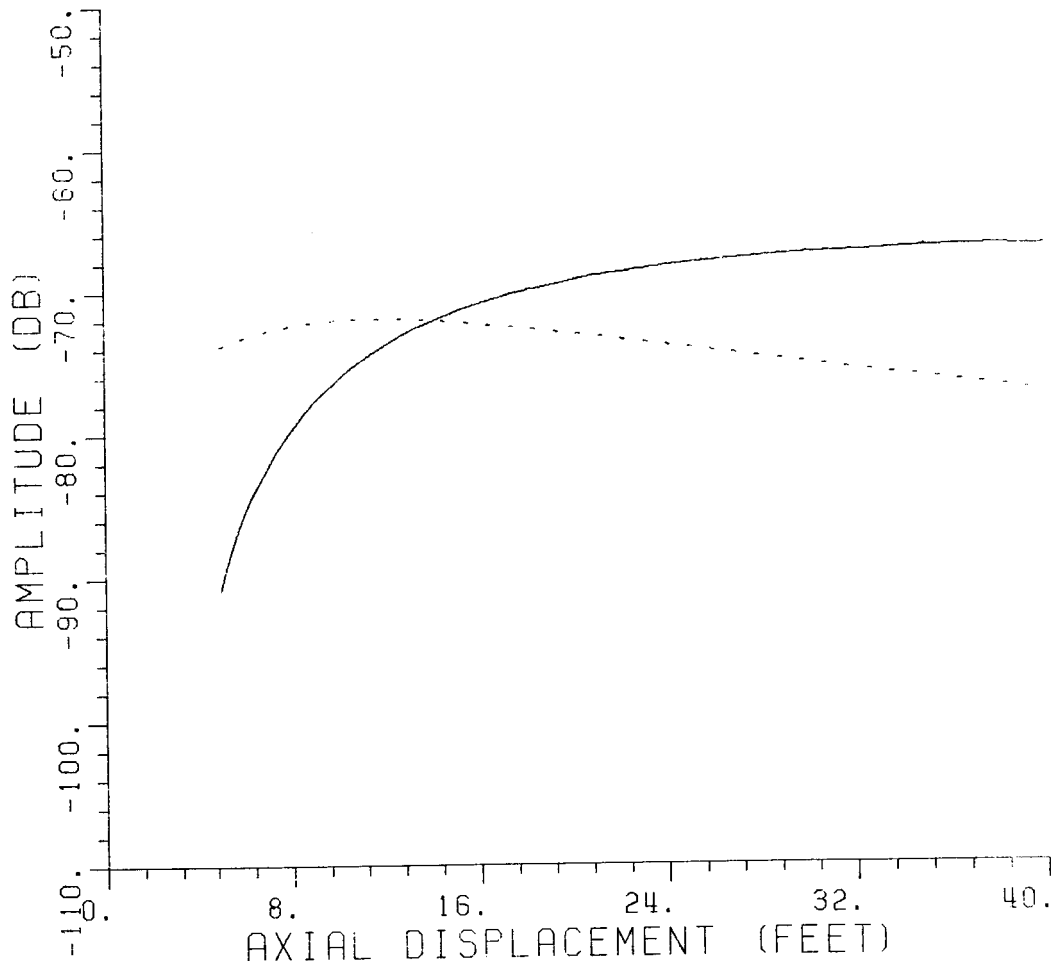
1. specular reflection
2. junction diffraction
3. skirt diffraction
4. feed blockage

Till now, our discussion has been limited to the scattered fields inside the sweet region. The code can also be used to compute scattered fields outside the sweet region. Outside the sweet region, one is interested in the scattered field intensity at the ceiling, walls and floor of the room housing the compact range. Thus, an axial cut is appropriate to compute the scattered fields. The scattered fields along various axial cuts is computed next. As pointed out before, the code computes only the specular reflection component along an axial cut. The radial distance of the axial cuts from the axis of the paraboloid is 30 feet.

Figure 35 shows x and z components of the scattered fields along 0° axial cut. The y component is zero in this cut. The feed is assumed to be a Huygen source tilted by 20°. For a radial displacement of 30 feet, the field point is outside the sweet region. Thus, the reflection point lies on the blended rolled edge. Note that the scattered fields are within 15-16 dB of the fields at the center of the target zone. Thus, the ceiling of the room is strongly illuminated by the reflector. The input data set used for computing the scattered field in the axial cut is as follows:

```
INPUT THE FREQUENCY OF OPERATION IN GHz
2.
INPUT THE FOCAL LENGTH OF THE REFLECTOR IN FEET
24.
INPUT THE RADIUS OF THE PARABOLIC SECTION IN FEET
15.
IS THERE A ROLLED EDGE ON TOP? IF YES, TYPE 1
1
IS THERE A SKIRT AT THE BOTTOM? IF YES, TYPE 1
1
```

IS THE FEED TO BE SIMULATED? IF YES, TYPE 1  
1  
INPUT THE MAGNITUDE OF THE MAGNETIC DIPOLES ALONG X AND Y AXES.  
0.,1.  
INPUT THE MAGNITUDE OF THE ELECTRIC DIPOLES ALONG X AND Y AXES.  
1.,0.  
INPUT THE FEED TILT ANGLE IN DEGREES  
20.  
INPUT THE TYPE OF CUT(IFCUT) ALONG WHICH PROBED NEAR FIELD DATA IS TO  
BE COMPUTED  
4  
INPUT PHI (degrees) FOR THE FIELD CUT  
0.  
INPUT THE DISTANCE OF THE FIELD CUT FROM THE VERTEX OF THE REFLECTOR IN  
FEET  
30.  
INPUT THE START POINT AND END POINT FOR FIELD PROBING  
5.,40.  
INPUT THE DISTANCE BETWEEN FIELD POINTS IN FEET  
0.2  
DO YOU WANT GO TERM? IF YES, TYPE 1  
1  
DO YOU WANT JUNCTION DIFFRACTION? IF YES, TYPE 1  
0  
DO YOU WANT SKIRT DIFFRACTION? IF YES, TYPE 1  
0  
DO YOU WANT FEED BLOCKAGE? IF YES, TYPE 1  
0  
DO YOU WANT FEED SPILLOVER? IF YES, TYPE 1  
0  
DO YOU WANT DIFFRACTION FROM THE MECHANICAL DISCONTINUITY? IF YES,  
TYPE 1  
0  
DO YOU WANT ELECTRIC FIELD AS THE OUTPUT? IF YES, TYPE 1  
1



\_\_\_\_\_ x component  
 - - - - - z component

Figure 35. Scattered field versus axial displacement.  $\phi=0^\circ$ , radial distance = 30 feet, feed tilt angle =  $20^\circ$ .

Figure 36 shows the scattered fields along a  $60^\circ$  axial cut. All the three components (x,y,z) of the scattered field are plotted. Again note that the scattered fields are within 15-16 dB of the fields at the center of the sweet region. Thus, the walls of the room are also strongly illuminated by the reflector. Next, the code's capability of computing diffraction from a mechanical discontinuity is demonstrated. As pointed out earlier, one needs to input the cross-sectional shape of the imperfect surface to compute this term. The computer code "SURFACE" given in Appendix A can be used to generate the imperfect surface.

Figure 37 shows the diffraction from a mechanical discontinuity at a radial distance of 16 feet. The wedge angle at the mechanical discontinuity is  $179.5^\circ$ . The scattered fields are computed along  $0^\circ$  radial cut at a distance of 36 feet from the vertex of the paraboloid. In this cut, there is no cross-polarized scattered field. Therefore, only the copolarized component is plotted. The input data set is as follows:

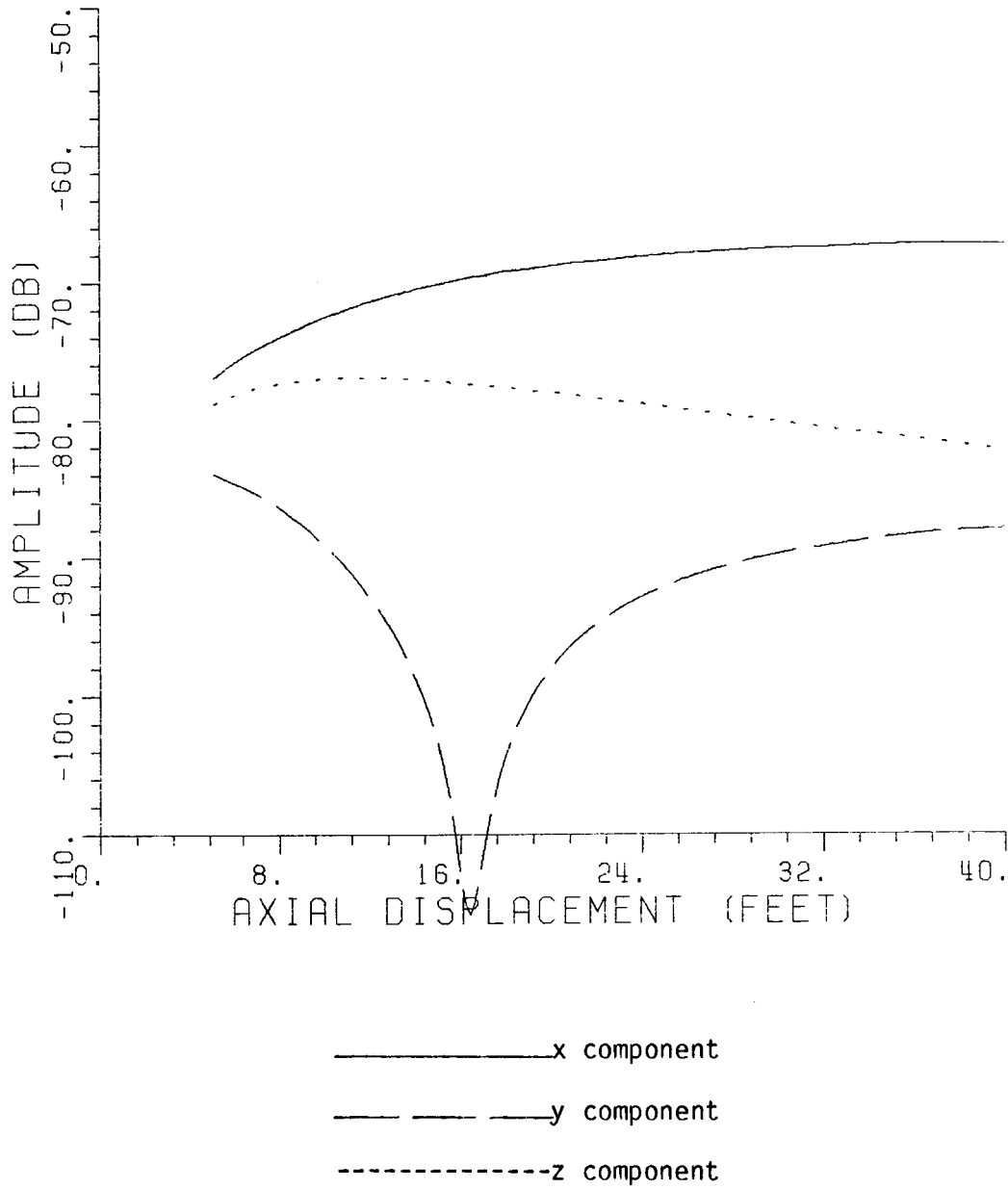
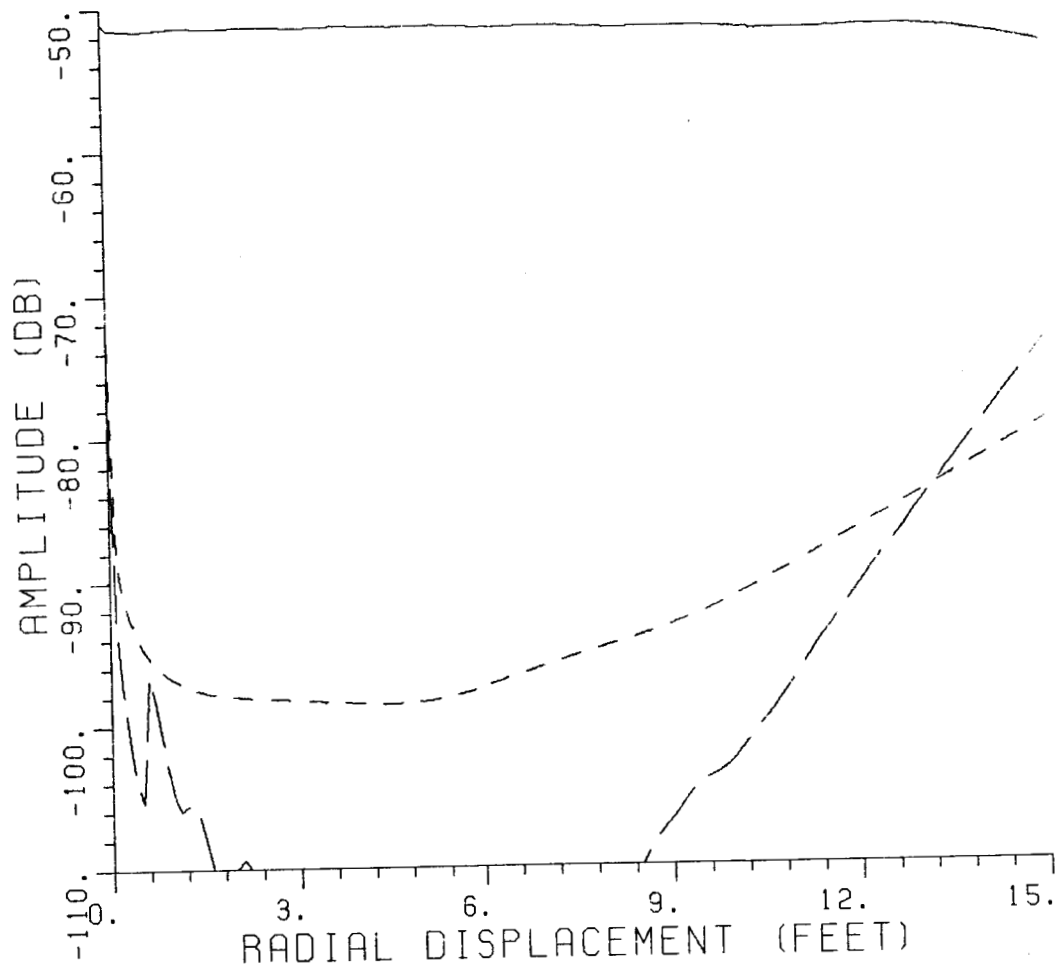


Figure 36. Scattered fields versus axial displacement.  $\phi=60^\circ$ , radial distance = 30 feet, feed tilt angle =  $20^\circ$ .



\_\_\_\_\_ total scattered field  
 - - - - - mechanical discontinuity scattering  
 - · - · - junction diffraction

Figure 37. Scattered field versus radial displacement.  $\phi=0^\circ$ , distance from vertex = 36 feet, mechanical discontinuity at 16 feet.

INPUT THE FREQUENCY OF OPERATION IN GHz  
 2.  
 INPUT THE FOCAL LENGTH OF THE REFLECTOR IN FEET  
 24.  
 INPUT THE RADIUS OF THE PARABOLIC SECTION IN FEET  
 15.  
 IS THERE A ROLLED EDGE ON TOP? IF YES, TYPE 1  
 1  
 IS THERE A SKIRT AT THE BOTTOM? IF YES, TYPE 1  
 1  
 IS THE FEED TO BE SIMULATED? IF YES, TYPE 1  
 1  
 INPUT THE MAGNITUDE OF THE MAGNETIC DIPOLES ALONG X AND Y AXES.  
 0.,1.  
 INPUT THE MAGNITUDE OF THE ELECTRIC DIPOLES ALONG X AND Y AXES.  
 1.,0.  
 INPUT THE FEED TILT ANGLE IN DEGREES  
 20.  
 INPUT THE TYPE OF CUT(IFCUT) ALONG WHICH PROBED NEAR FIELD DATA IS TO  
 BE COMPUTED  
 1  
 INPUT PHI (degrees) FOR THE FIELD CUT  
 0.  
 INPUT THE DISTANCE OF THE FIELD CUT FROM THE VERTEX OF THE REFLECTOR IN  
 FEET  
 36.  
 INPUT THE START POINT AND END POINT FOR FIELD PROBING  
 0.,15.  
 INPUT THE DISTANCE BETWEEN FIELD PINTS IN FEET  
 0.1  
 DO YOU WANT GO TERM? IF YES, TYPE 1  
 1  
 DO YOU WANT JUNCTION DIFFRACTION? IF YES, TYPE 1  
 1  
 WILL YOU BE STUDYING THE DIFFRACTION DUE TO MECHANICAL DISCONTINUITY?  
 IF YES, TYPE 1  
 1  
 DO YOU WANT SKIRT DIFFRACTION? IF YES, TYPE 1  
 0  
 DO YOU WANT FEED BLOCKAGE? IF YES, TYPE 1  
 0  
 DO YOU WANT FEED SPILLOVER? IF YES, TYPE 1  
 0  
 DO YOU WANT DIFFRACTION FROM THE MECHANICAL DISCONTINUITY? IF YES,  
 TYPE 1  
 1  
 TYPE THE RADIAL DISTANCE OF THE MECHANICAL DISCONTINUITY FROM THE AXIS  
 OF THE PARABOLOID IN FEET  
 16.  
 DO YOU WANT ELECTRIC FIELD AS THE OUTPUT? IF YES, TYPE 1  
 1

Note that the junction diffraction term is also computed. As pointed out in Section II, one needs the scattered fields from a perfect surface to isolate the diffraction from the mechanical discontinuity. The total scattered field (specular reflection + junction diffraction + mechanical discontinuity diffraction) and the junction diffraction alone is also plotted in Figure 37. Note that the diffraction from the mechanical discontinuity is of the order of the junction diffraction. Thus, the mechanical discontinuity will not cause a significant stray field in the target zone.

Finally, the code's capability of computing the feed spillover is demonstrated. As mentioned in the last section, one needs the measured feed pattern to compute the feed spillover. The measured feed data is read by the code from unit #19. The input data file assigned to unit #19 has the following information:

```
2
1
1
1,15
0.
0.,1.
10.,0.99
20.,0.965
30.,0.910
40.,0.785
50.,0.635
60.,0.485
70.,0.335
80.,0.185
90.,0.105
100.,0.025
110.,0.01
120.,0.01
150.,0.01
180.,0.01
```

Note that the input data is in volts/meter. The feed pattern is circularly symmetric and has vertical polarization. A plot of the feed pattern in  $x_f z_f$  plane is given in Figure 38. In the following example, the feed is tilted by  $20^\circ$ .

Figure 39 shows the feed spillover in  $0^\circ$  radial cut at a distance of 36 feet from the vertex of the reflector. The specular reflection in this cut is also shown in the figure. The copolarized (x) component of the scattered field is plotted. Note that the feed spillover is only 34 dB below the specular reflection. Thus, the feed spillover can cause undesirable oscillations in the scattered fields in the target zone. The same can be seen in the plots of Figure 40, where the total scattered field (specular reflection + feed spillover) is plotted. The specular reflection alone is also shown in the figure. Note that the ripple size of the oscillations is as large as 0.2 dB. Thus, the feed spillover can be a problem in RCS measurements if a pulse radar is not used to eliminate the feed spillover.

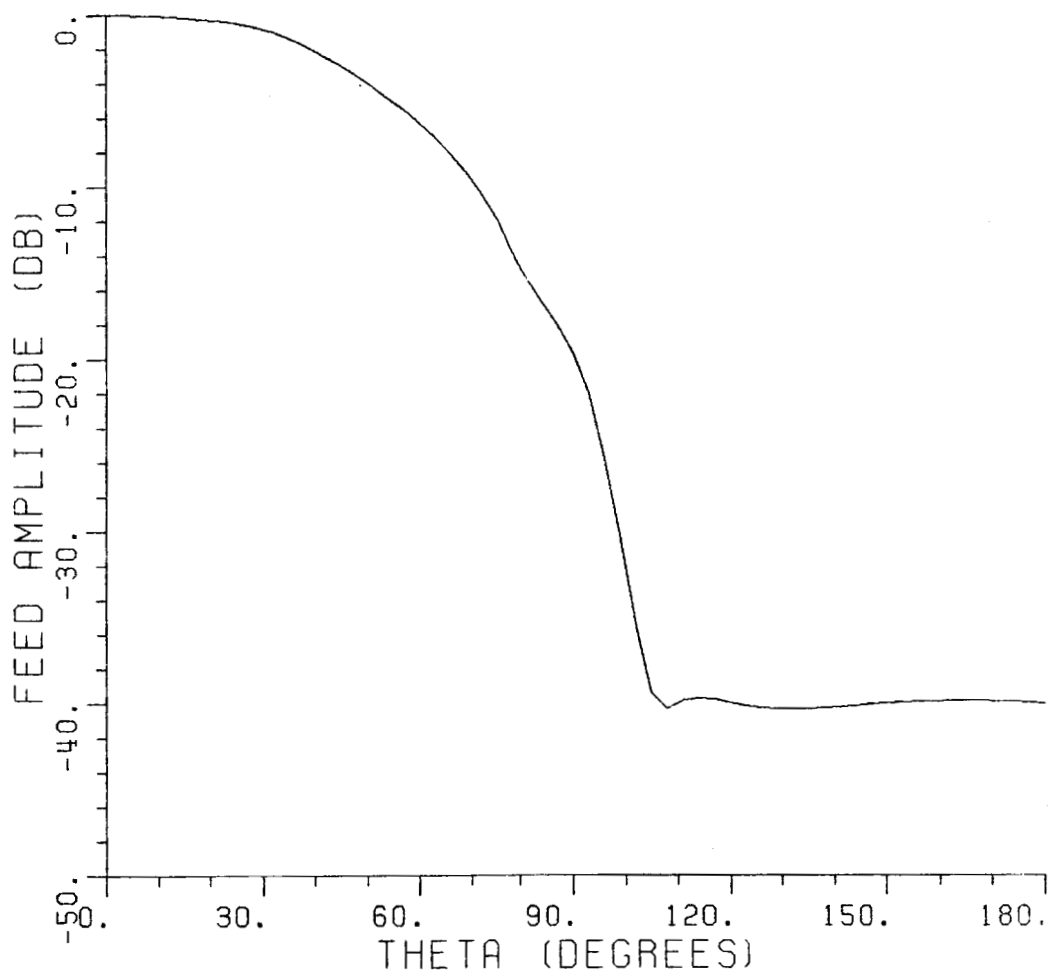
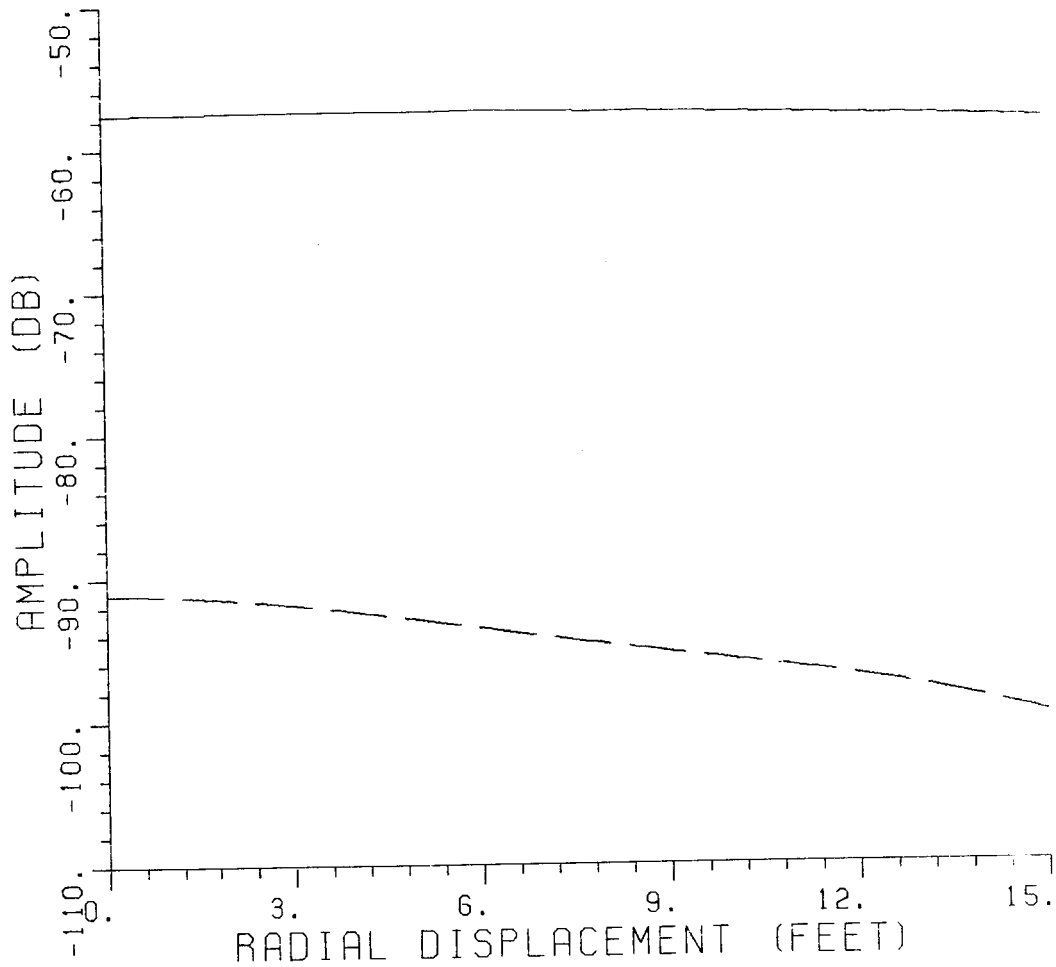


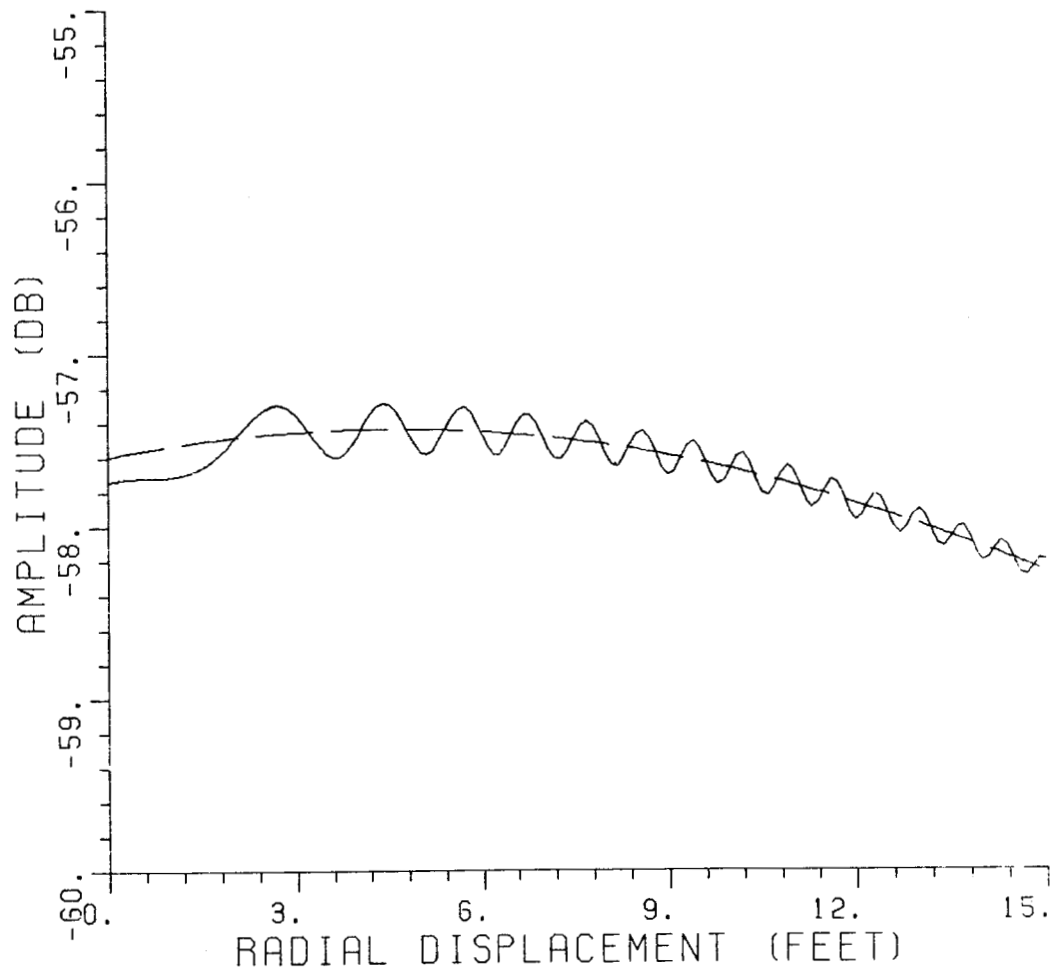
Figure 38. Feed pattern in  $x_f z_f$  plane.



———— specular reflection

- - - - - feed spillover

Figure 39. Feed spillover versus radial displacement.  $\phi=0^\circ$ , distance from vertex = 36 feet. Measurement feed pattern is used. Feed tilt angle= $20^\circ$ .



—————total scattered field  
 ————specular reflection

Figure 40. Scattered field versus radial displacement.  $\phi=0^\circ$ , distance from vertex = 36 feet. Measured feed pattern is used. Feed tilt angle= $20^\circ$ . Various mechanisms included are:  
 1. specular reflection  
 2. feed spillover

The input data set used in the above example is given below:

INPUT THE FREQUENCY OF OPERATION IN GHz  
2.  
INPUT THE FOCAL LENGTH OF THE REFLECTOR IN FEET  
24.  
INPUT THE RADIUS OF THE PARABOLIC SECTION IN FEET  
15.  
IS THERE A ROLLED EDGE ON TOP? IF YES, TYPE 1  
1  
IS THERE A SKIRT AT THE BOTTOM? IF YES, TYPE 1  
1  
IS THE FEED TO BE SIMULATED? IF YES, TYPE 1  
0  
MEASURED FEED PATTERN IS BEING READ FROM UNIT #19.  
THE FEED POLARIZATION IS VERTICAL.  
INPUT THE FEED TILT ANGLE IN DEGREES  
20.  
INPUT THE TYPE OF CUT(IFCUT) ALONG WHICH PROBED NEAR FIELD DATA IS TO  
BE COMPUTED  
1  
INPUT PHI (degrees) FOR THE FIELD CUT  
0.  
INPUT THE DISTANCE OF THE FIELD CUT FROM THE VERTEX OF THE REFLECTOR IN  
FEET  
36.  
INPUT THE START POINT AND END POINT FOR FIELD PROBING  
0.,15.  
INPUT THE DISTANCE BETWEEN FIELD POINTS IN FEET  
0.1  
DO YOU WANT GO TERM? IF YES, TYPE 1  
1  
DO YOU WANT JUNCTION DIFFRACTION? IF YES, TYPE 1  
0  
DO YOU WANT SKIRT DIFFRACTION? IF YES, TYPE 1  
0  
DO YOU WANT FEED BLOCKAGE? IF YES, TYPE 1  
0  
DO YOU WANT FEED SPILLOVER? IF YES, TYPE 1  
1  
DO YOU WANT DIFFRACTION FROM THE MECHANICAL DISCONTINUITY? IF YES,  
TYPE 1  
0  
DO YOU WANT ELECTRIC FIELD AS THE OUTPUT? IF YES, TYPE 1  
1

In this section various results obtained using the newly developed reflector code were presented to illustrate the code's capability and as samples of input/output sets. It was shown that the codes can be efficiently used to analyze semi-circular compact range reflector with or without a rolled edge. A summary of the work is given next.

## V. SUMMARY

A computer code has been developed at The Ohio State University ElectroScience Laboratory to analyze a semi-circular paraboloid reflector antenna with a rolled edge at the top and a skirt at the bottom. The operation of the code was described in this report. Various input and output statements were explained. Some results obtained using the computer code were presented to illustrate the code's capability as well as being samples of input/output sets. As it is true for most practical systems, the code has certain limitations. Various limitations of the code are:

1. The scattered fields are computed only for positive values of  $y$ . The structure is assumed to be symmetrical about  $x$  axis, therefore, scattered fields for negative values of  $y$  will be the same as for corresponding positive values of  $y$ .
2. Outside the sweet region, only specular reflection is computed.

3. Outside the sweet region, scattered fields are computed only for positive values of  $X$ .
4. Feed spillover can be computed only if the measured feed pattern is read as input data to the code.
5. To obtain a good approximation to the junction diffraction, one should compute scattered fields at least at 45 points in the sweet region.

## APPENDIX A

### CODE TO GENERATE THE CROSS-SECTIONAL SHAPE

Computer code "SURFACE" is used to generate the cross-sectional shape of the infinitely long cylinder. A listing of the computer code is given below:

```

PARAMETER (Ndim=10001)
DIMENSION X(Ndim),Y(Ndim)
REAL NUF,MAJT,MINT
COMMON /ONE/ FM,NUF,IBLEND
COMMON /TWO/ YIT,YFT,MAJT,MINT,THETAT,XELT,YELT
COMMON/THREE/ XWD,YWD,WAN,XDWD,YDWD,IFLAG,IMECH
C**
READ(70,*) FMC          ! frequency in GHz.
READ(70,*) FM           ! focal distance in feet
READ(70,*) YIT          ! y coordinate of the upper end of parabola
READ(70,*) YFB          ! y coordinate of the lower end of parabola
READ(70,*) IBLEND       ! type of blending (IBLEND = 1, 2, 3, 4 or 5)
READ(70,*) PSECT        ! length(feet) of the parabolic section blended
READ(70,*) NUF          ! section of the ellipse blended (degrees)
READ(70,*) MAJT,MINT    ! major and minor axis of ellipse in feet.
READ(70,*) DSSwl        ! spacing between samples in wavelength.
READ(70,*) IMECH        ! IMECH=1 for mechanical discontinuity.
READ(70,*) YWD          ! y coordinate of the mechanical discontinuity.
READ(70,*) WAN          ! wedge angle at the mechanical discontinuity.
READ(70,*) XDWD,YDWD   ! displacement (in inches) at the discontinuity.
C**
cdimin = 30.48006096 ! conversion constant from feet to centimeters
FM      = cdimin*FM
YFB     = cdimin*YFB
YIT     = cdimin*YIT
PSECT   = cdimin*PSECT
MAJT    = cdimin*MAJT
MINT    = cdimin*MINT
DSS     = DSSwl*29.97925/FMC ! DSS in centimeters
NUF     = NUF*3.141592654/180.
YWD     = cdimin*YWD
XDWD    = cdimin*XDWD/12.
YDWD    = cdimin*YDWD/12.
WAN     = 180.-WAN
XWD     = 0.25*YWD*YWD/FM
IFLAG   = 1
YFT     = YIT+PSECT
XATYIT  = YIT**2/(4.*FM)
XELT    = XATYIT-MINT/SQRT(1.+(YIT/(2.*FM))**2)
YELT    = YIT+MINT*YIT/(2.*FM)/SQRT(1.+(YIT/(2.*FM))**2)
THETAT  = ASIN((XATYIT-XELT)/MINT)
N=1

```

C PARABOLIC SECTION

```
C
  PY=YFB
  CALL XYCORM(PY,X(N),Y(N))
40  CONTINUE
  DXDY=Y(N)/(2.*FM)
  DY=DSS/SQRT(1.+DXDY**2)
  N=N+1
  PY=PY+DY
  IF(PY .GE. YIT) GOTO 50
  CALL XYCORM(PY,X(N),Y(N))
  GOTO 40
```

C
C UPPER ROLLED EDGE

```
C
50  FY=YIT
  CALL XYCORM(PY,X(N),Y(N))
60  DXDY=Y(N)*0.5/FM
  DY=DSS/SQRT(1.+DXDY**2)
  PY=PY+DY
  IF(PY .GT. YFT) GOTO 70
  N=N+1
  CALL XYCORM(PY,X(N),Y(N))
  GOTO 60
70  CONTINUE
  IOUT=17
  IF(IMECH .EQ. 1) IOUT=18
  WRITE(IOUT,*) N
  DO 100 I=1,N
100 WRITE(IOUT,*) X(I),Y(I)
  CALL EXIT
  END
```

C
C THIS SUBROUTINE CALCULATES THE X AND Y COORDINATES, GIVEN PY

```
C
  SUBROUTINE XYCORM(PY,X,Y)
  REAL NU,NUF,MAJT,MINT
  COMMON /ONE/ FM,NUF,IBLEND
  COMMON /TWO/ YIT,YFT,MAJT,MINT,THETAT,XELT,YELT
  COMMON /THREE/ XWD,YWD,WAN,XDWD,YDWD,IFLAG,IMECH
C
  IF (PY.GT.YIT) THEN
    NU=NUF*(PY-YIT)/(YFT-YIT)
    GOTO (12,14,16,18,19),IBLEND
12  BLEND=0.
    GOTO 20
14  BLEND=1.-NU/NUF
    GOTO 20
16  BLEND=1.-(NU/NUF)**2
    GOTO 20
18  BLEND=(1.+COS(3.141592654*NU/NUF))/2.
    GOTO 20
19  BLEND=(1.-COS(3.141592654*NU/NUF))/2.
    BLEND=1.-BLEND**2
20  X=PY**2/(4.*FM)*BLEND+(MAJT*SIN(NU)*
1  COS(THETAT)+MINT*COS(NU)*SIN(THETAT)+XELT)*(1.-BLEND)
  Y=PY*BLEND+(MAJT*SIN(NU)*SIN(THETAT)-MINT*COS(NU)
1  *COS(THETAT)+YELT)*(1.-BLEND)
  ELSE
    X=PY**2/(4.*FM)
    Y=PY
  ENDIF
  IF(IMECH .EQ. 1 .AND. Y .GE. YWD) THEN
  IF(IFLAG .NE. 1) GOTO 30
  YWD=Y
  XWD=X
  IFLAG=0
  TYPE *, ' MECHANICAL DISCONTINUITY IS AT ',XWD,YWD
30  X1=X
  Y1=Y
  X=XWD+(X1-XWD)*COSD(WAN)-(Y1-YWD)*SIND(WAN)+XDWD
  Y=YWD+(X1-XWD)*SIND(WAN)+(Y1-YWD)*COSD(WAN)+YDWD
  END IF
  RETURN
  END
```

The code reads the input data from unit #70. Various parameters read by the code are shown between dashed lines in the code and are self explanatory. To further help the user, various parameters are shown in Figures A.1, A.2, and A.3. IBLEND in the input data defines the blending between the parabolic and elliptical sections. IBLEND is equal to 1, 2, 3, 4 or 5 for no blending, linear blending, square blending, cosine blending, and cosine-squared blending, respectively. The blended section is defined as follows:

$$x = x_p(v)B(v) + x_e(v)(1-B(v))$$

and

$$y = y_p(v)B(v) + y_e(v)(1-B(v))$$

where  $(x_p, y_p)$  and  $(x_e, y_e)$  are the coordinates of the point on the parabola and ellipse, respectively, and B is the blending function which is defined by

$$B(v) = \begin{cases} 0 & \text{no blending} \\ 1-v/v_f & \text{linear blending} \\ 1-(v/v_f)^2 & \text{square blending} \\ \frac{1+\cos(\pi v/v_f)}{2} & \text{cosine blending} \\ 1 - \left[ \frac{1-\cos(\pi v/v_f)}{2} \right]^2 & \text{cosine-squared blending} \end{cases}$$

where  $\nu$  is the angular parameter of the ellipse and  $\nu_f(\text{NOF})$  is the section of the ellipse used in blending and is an input parameter.

$\text{DSS}\omega\lambda$  in the input data is the spacing between adjacent samples and should be of the order of 0.05 wavelengths. The code in its present form can store up to 2001 samples. If the number of samples on the cross-sectional shape exceeds 2001, the first statement should be adjusted accordingly.

The code can be used to generate a perfect (no mechanical discontinuity) as well as an imperfect surface with one mechanical discontinuity. For an imperfect surface, the input parameter (IMECH) should be set equal to unity. The code automatically assigns the cross-sectional shape of the perfect surface to unit #17 and that of the imperfect surface to unit #18.

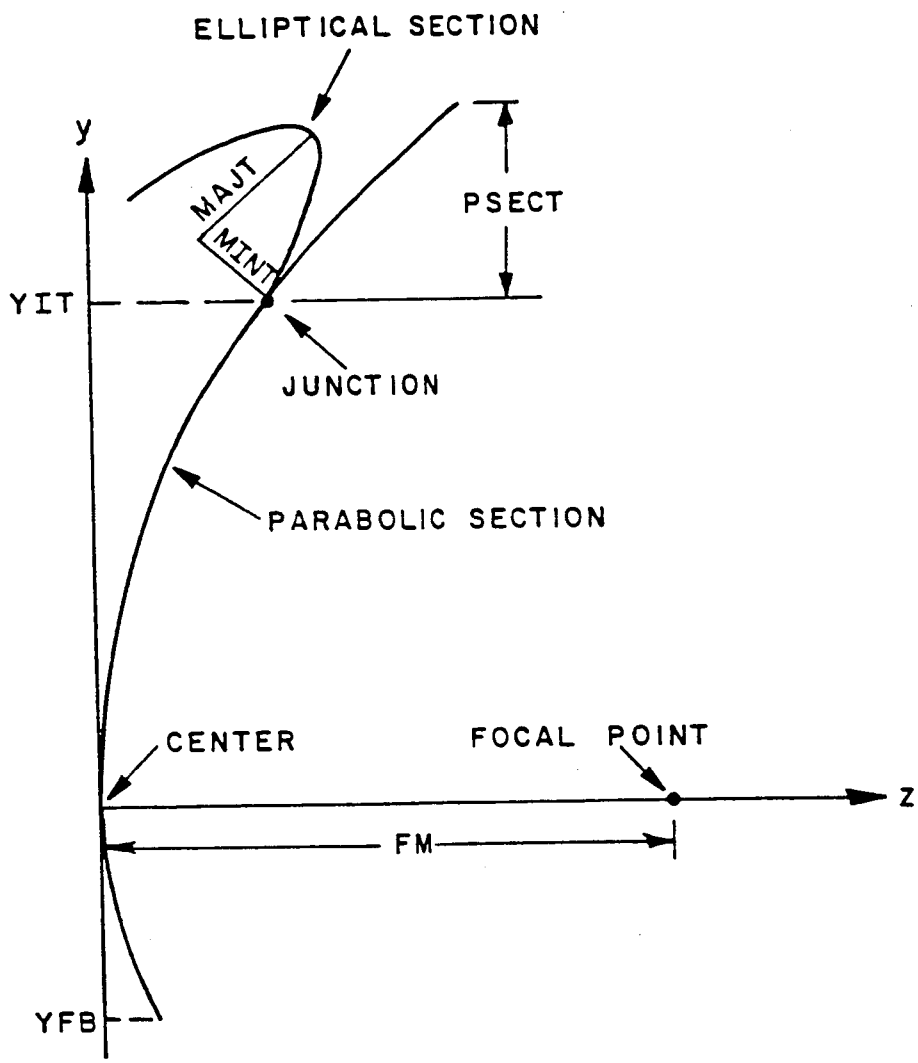


Figure A.1. Various parameters used in the code.

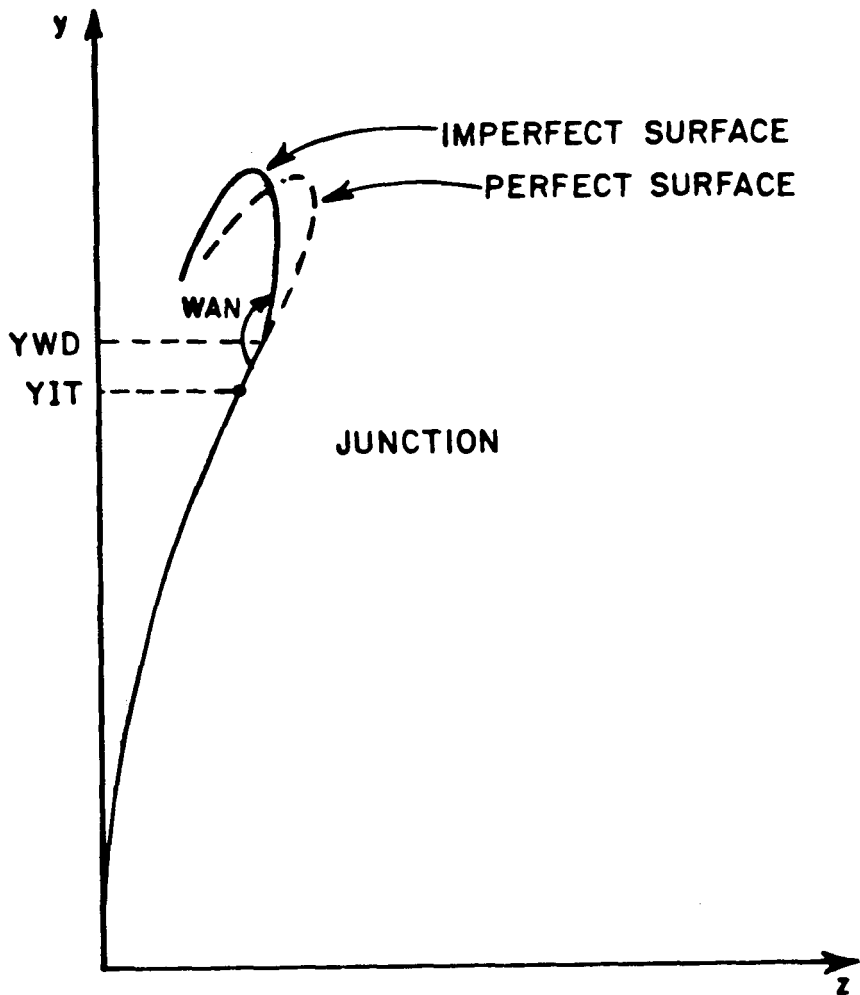


Figure A.2. Various parameters used in the code. Mechanical discontinuity due to tilt.

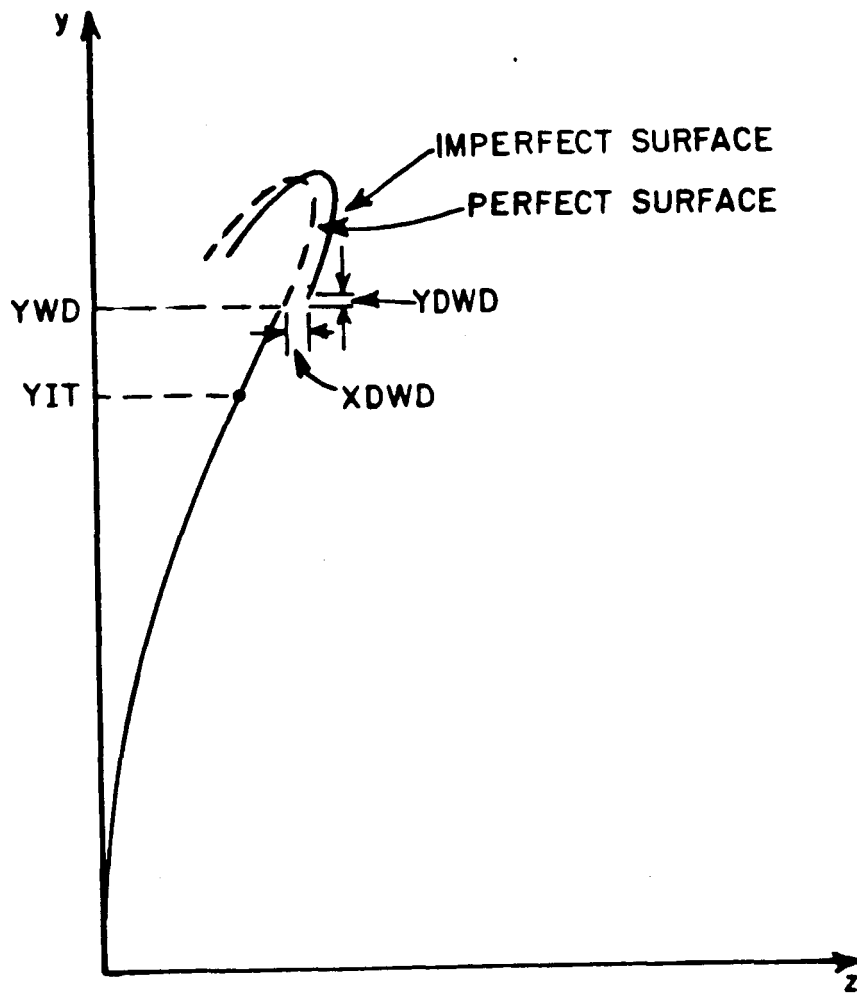


Figure A.3. Various parameters used in the code. Mechanical discontinuity due to displacement.

## REFERENCES

- [1] I.J. Gupta and W.D. Burnside, "A Numerical Method to Compute Diffraction from Blended Surfaces," to be presented at 1987 IEEE AP-S Symposium, Blacksburg, Virginia.
- [2] I.J. Gupta and W.D. Burnside, "A Physical Optics Correction for Backscattering from Curved Surfaces," accepted for publication in IEEE Trans. on Antennas and Propagation.
- [3] R.G. Kouyoumjian and P.H. Pathak, "A Uniform Geometrical Theory of Diffraction for an Edge in Perfectly Conducting Surfaces," Proc. of IEEE, pp. 1448-1461, November 1974.
- [4] Tai-Tseng Chu, "First Order Uniform Geometrical Theory of Diffraction Analysis of Scattering by Smooth Surfaces," Ph.D. Dissertation, The Ohio State University, Department of Electrical Engineering, Columbus, Ohio, March 1983.
- [5] W.B. Gordon, "Far-Field Approximations to the Kirchoff-Helmholtz Representations of Scattered Fields," IEEE Transactions on Antennas and Propagation, Vol. AP-28, No. 4, pp. 590-592, July 1975.
- [6] B.J.E. Taute and W.D. Burnside, "The Effects of Discontinuities in the Construction of a Compact Range Reflector," Technical Report 718331-4, The Ohio State University ElectroScience Laboratory, Department of Electrical Engineering, prepared under Grant GR9300 for Boeing Aerospace Company, Seattle, Washington, August 1986.